

A NOVEL MULTIFUNCTIONAL BINARY OXIDE TiO₂: MoO₃ THIN FILMS DEPOSITED BY SPRAY PYROLYSIS METHOD

Kothawade N B, Dhanwate S. V.,

Associate Professor and Head Department of Physics, Arts, Commerce and Science College, Kalwan (Manur) Dist. Nashik, India

Associate Professor and Head Department of Physics, Swami Muktanand College of Science, Yeola (Nashik), India

ABSTRACT

The sensitivity and selectivity of sensor is depends on dopants or additives which can change the gas sensing characteristics. A suitable catalyst or dopant is often added in small percentage in the pure material to enhance the sensitivity and selectivity. Nanocomposite term contain mixture of two or more nano oxide materials like binary oxide, ternary oxide, etc. Nanocomposite films consists of nanocrystalline or amorphous phase of a least two different materials TiO₂:MoO₃ binary oxide thin films were prepared by using spray pyrolysis technique on glass substrate at 400°C temperature. TiO₂ as dopant and MoO₃ as a functional material in film. The precursor TiCl₄ and MoCl₅ of concentrations 0.3N:0.3N. The characterization of deposited films were carried out for Electrical and structural characterization is one of the most important aids to XRD, surface morphology/specific surface area determine using SEM, and chemical composition determine using EDS and the results of the analysis are presented in the paper.

KEYWORDS :- XRD , SEM ,EDS. Gas sensor, spray pyrolysis technique , binary oxide thin films, TiO₂ , MoO₃ and Thin film,

INTRODUCTION

The TiO₂ and MoO₃ are metal oxide semiconductors (MOS). Has been one of the most important metal which has played significant role in material science. Gas sensors have a great incredible impact in numerous areas like environmental monitoring, domestic safety, public security, automotive applications, air conditioning in airplanes, space crafts and houses, sensors networks also solid state sensors are use for the detection of majority of harmful and toxic gases in many different area.

The parameters like sensitivity, selectivity, response time, grain size, surface area, and stability of the gas sensors are improved by addition of different dopants. In some cases dopants are added to a metal oxide to modify its properties by enhancing the desirable properties, while in other cases undesirable properties are reduced or eliminated.

EXPERIMENTAL METHODS

In this method the deposition of films modified spray pyrolysis setup has been developed, designed and assembled in laboratory to overcome limitations of conventionally designed setup; such as number of optimized parameters ,reliability and homogeneity of the deposited films. During the synthesis addition of impurity namely doping influence metal oxide properties which are important for gas sensing applications. Binary oxide TiO₂: MoO₃ thin films were prepared by

spray pyrolysis technique on glass substrate. The spray Pyrolysis process was carried out at substrate temperature 400°C. The precursor TiCl₄ and MoCl₅ of concentrations 0.1N, 0.2N and 0.3N were used. The thin films were prepared at concentration 0.3N:0.3N. The study of characteristics such as SEM, EDS, XRD, resistivity, activation energy, TCR and gas sensing property were done to study the changes due to dopant.

RESULTS AND DISCUSSION

The study of structural characteristics of Binary oxide TiO₂: MoO₃ thin films at 0.3N:0.3N was studied by techniques such as Surface Morphology using Scanning Electron Microscopy (SEM), Elemental analysis using Energy Dispersive X-Ray Analysis (EDAX), Structural characterization using X Ray Diffraction (XRD).

X-RAY DIFFRACTION ANALYSIS (XRD)

The XRD pattern of one of the represented composite is shown in figure. Which gives the structure and phases of binary oxide TiO₂: MoO₃ thin films on glass substrate fired at 400°C XRD study had been considered. X-ray diffraction analysis of TiO₂: MoO₃ thin films were carried out in 20-80° range using X powder 12(CuKα) Radiation.

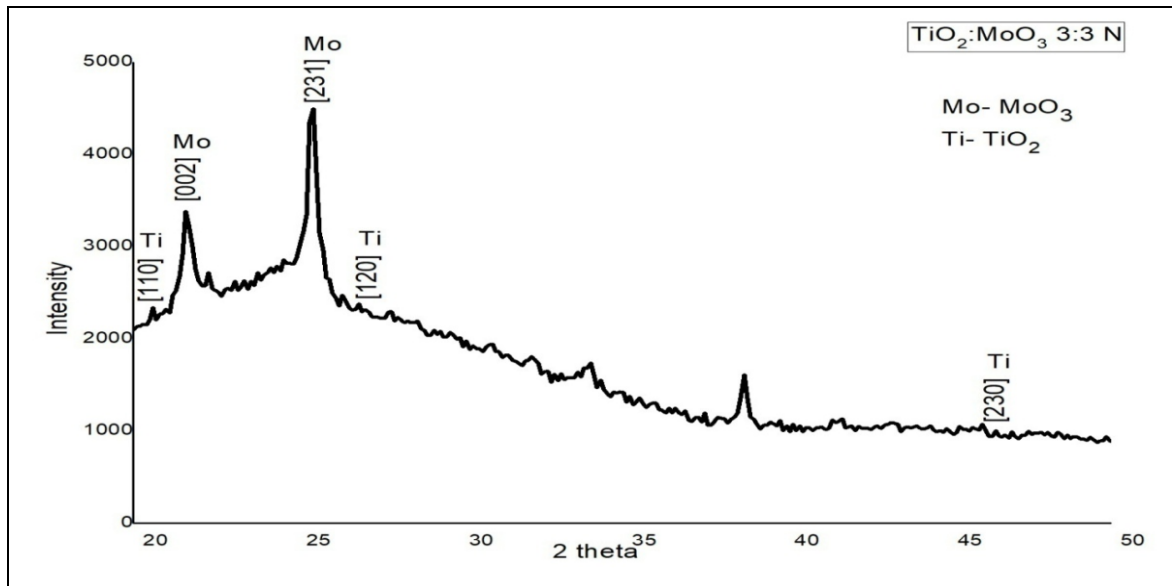


Figure: XRD of Binary oxide TiO₂: MoO₃ thin with conc. 0.3N:0.3N

XRD of Binary oxide TiO₂: MoO₃ thin film with concentration 0.3N:0.3N is found as below

Plane (hkl)	2θ	d-spacing	Intensity	I/I _o	FWHM
Ti- 110	20.59	4.11167	3386	75.3	2.310
Mo- 002	22.25	3.99089	2718	60.4	2.352
Mo- 231	25.47	3.49325	4499	100	4.202

Ti- 120	26.44	3.36722	2475	55	4.125
Ti- 230	46.08	1.96816	1075	23.9	24.657

The average grain size was determined by using Debye-Scherrer formula,

$$D = 0.9\lambda / \beta \cos\theta$$

β is full angular width of diffraction peak at half maximum peak intensity, λ is wavelength of X-radiation.

As per structural analysis the grain size were calculated by using Scherrer formula. The grain size of film at concentrations 0.3N:0.3N was found 2 nm.

SCANNING ELECTRON MICROSCOPY (SEM)

Scanning Electron Microscopy (SEM) is convenient technique to study Surface Morphology. Scanning Electron Microscopy (SEM) {Model JOEL 6300 LA GERMANY} was utilized to characterize the surface morphology. Figure shows the SEM of Binary oxide TiO₂: MoO₃ thin films of 0.3N:0.3N were deposited on glass substrate using a Spray Pyrolysis Technique and fired at 400°C. The magnifications of all SEM images are taken at 10000X.

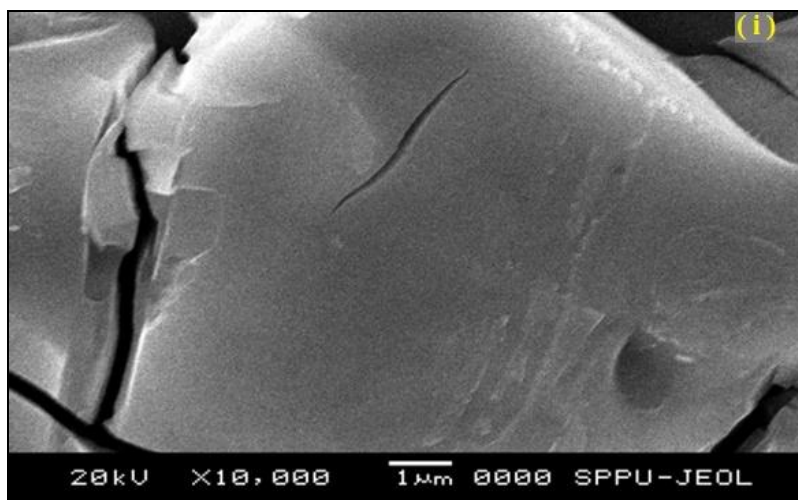


Figure: SEM of Binary oxide TiO₂: MoO₃ thin with conc. 0.3N:0.3N

Binary oxide TiO₂: MoO₃ Films prepared by Spray Pyrolysis were observed to be non porous as per SEM analysis. As per SEM analysis, the average particle size of film was calculated by using image j software. The average particle size of particle at concentrations 0.3N:0.3N were found 136 nm .

The specific surface area of Binary oxide TiO₂: MoO₃ thin film was calculated using BET method for spherical particles using the following equation .

$$S_w = \frac{6}{\rho d}$$

Where, d is the diameter of the particles, ρ is the density of the particles.

Specific Surface area with different concentrations of binary oxide is found as $\text{TiO}_2: \text{MoO}_3$ 10.253 m^2/g .

ENERGY DISPERSIVE X-RAY ANALYSIS (EDS)

The elemental analysis of Binary oxide $\text{TiO}_2: \text{MoO}_3$ thin films with normality 0.1N: 0.1N, on glass substrate and fired at 400°C was studied using EDAX (JOEL, JED Germany). The EDAX analysis shows presence of Ti, Mo and O as expected, no other impurity elements were present in the all samples. Figure shows count (along Y- axis) Verses KeV (along X-axis) EDS of 0.3N:0.3N concentrations of binary oxide $\text{TiO}_2: \text{MoO}_3$ thin films.

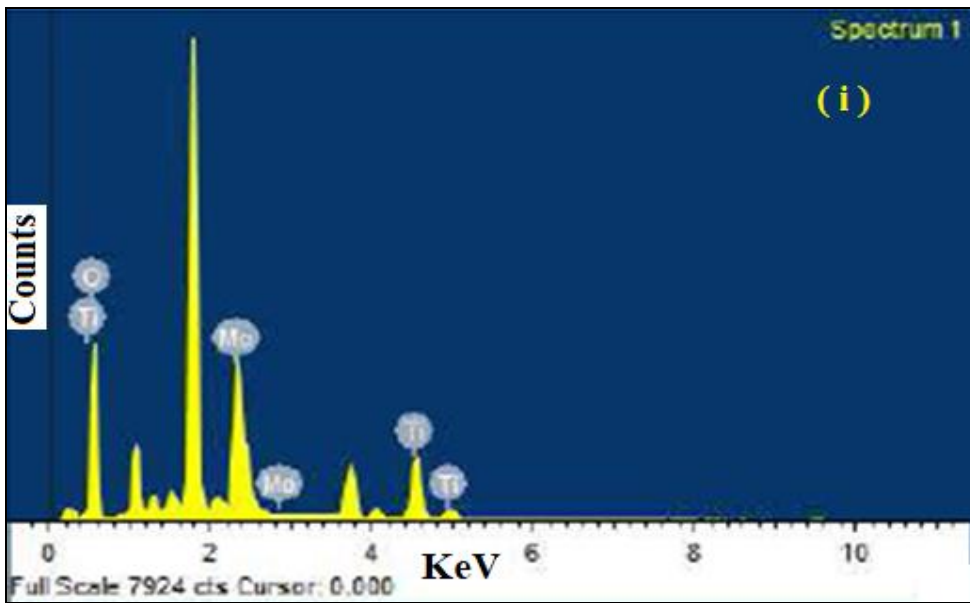


Figure: EDS of Binary oxide $\text{TiO}_2: \text{MoO}_3$ thin with conc. 0.3N:0.3N

EDS of Binary oxide $\text{TiO}_2: \text{MoO}_3$ thin film with Concentration 0.3N:0.3N is shown in table

From the EDAX spectra, it is found that mass% and at. wt.% of In, Mo and O is nearly matched.

Element	Atomic %
O	92.62
Ti	2.85
Mo	4.53

ELECTRICAL CHARACTERIZATION

RESISTIVITY

The DC resistance of TiO₂:MoO₃ thin films with normality 0.1N:0.3N on glass substrate and fired at 400°C was measured by using half bridge method as a function of temperature. Figure shows resistance variation of TiO₂:MoO₃ thin films with normality 0.3N:0.3N temperature variation in an atmosphere. There is decrease in resistance with increase in temperature indicating semiconductor behavior, obeying $R = R_0 e^{-AE/KT}$ in the temperature range of 40-350°C.

The resistance TiO₂:MoO₃ thin films with normality 0.3N:0.3N falls rapidly, decreases linearly up to certain transition temperature and after resistance decreases exponentially with increase in temperature and lastly saturates to steady level.

The resistivity of TiO₂:MoO₃ thin films at constant temperature is calculated using the relation,

$$\rho = (R \times A) / l$$

$$\rho = (R \times b \times t) / l \quad \text{ohm-m}$$

Where, R = Resistance of TiO₂:MoO₃ thin film at constant temperature

t = thickness of the film sample

l = length of the thin film

b = breadth of the thin film

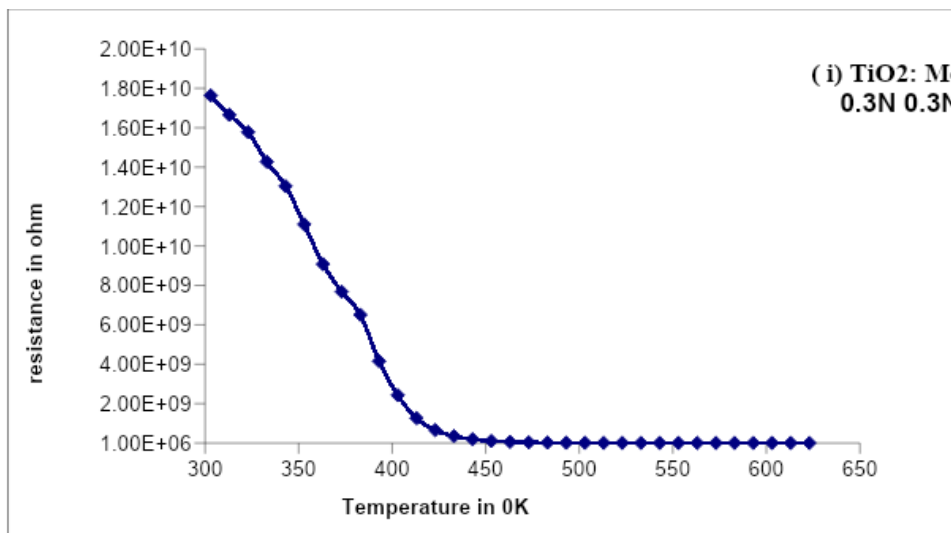


Figure: Resistance of Binary oxide TiO₂: MoO₃ thin with conc. 0.3N:0.3N

The resistivity of binary oxide TiO₂: MoO₃ samples with concentrations 0.3N:0.3N, of MoO₃ as additives in TiO₂ film was calculated 0.616 x10⁴ Ω-m.

ACTIVATION ENERGY

Figure shows plot of log(R) versus reciprocal of temperature, ($1/T$) for TiO₂:MoO₃ thin films with normality 0.3N: 0.3N.

This plot is reversible in both heating and cooling cycles obeying the Arrhenius equation

$$R=R_0.e^{-\Delta E/KT}$$

Where, R_0 = the constant = Resistance at room temperature

ΔE = The activation energy of the electron transport in the conduction band,

K = Boltzman constant and

T = Absolute temperature

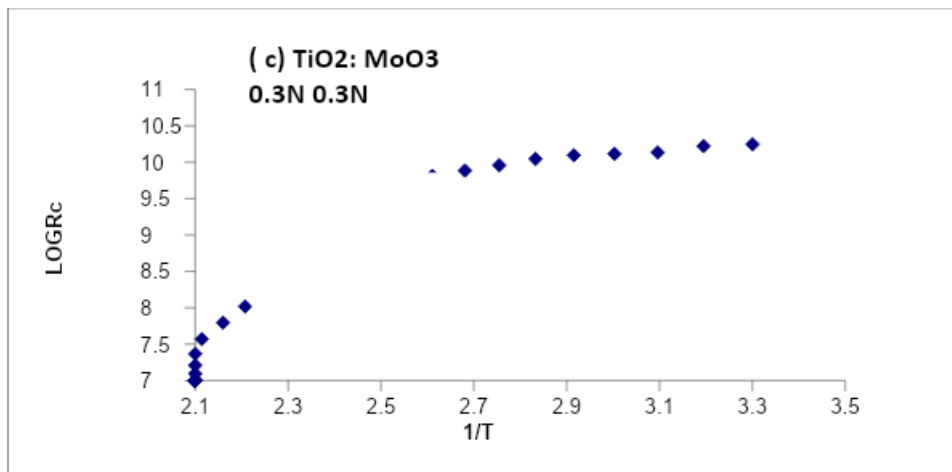


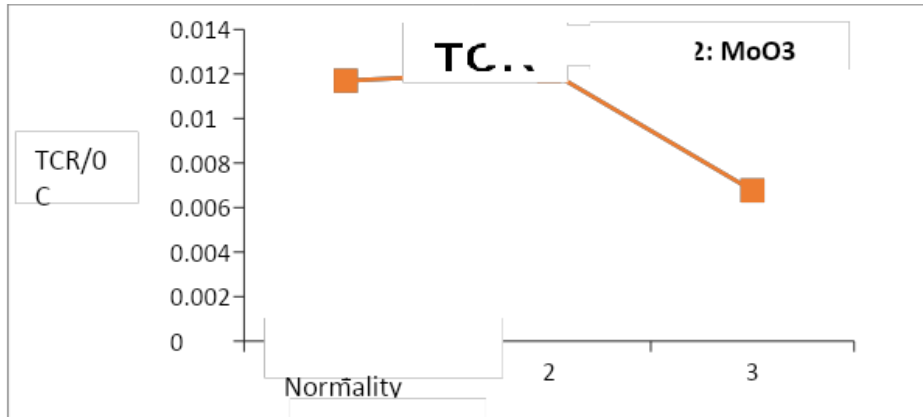
Figure: Activation energy of Binary oxide TiO₂:MoO₃ thin film with conc. 0.3N:0.3N

The Activation energy at high temperature and at low temperature were found 0.1017 eV and 0.8324 eV respectively at 0.3N:0.3N .

TEMPERATURE COEFFICIENT OF RESISTANCE (TCR)

Temperature coefficient of resistance (TCR) of TiO₂: MoO₃ thin films prepared at 400°C is calculated by using the following relation,

$$TCR = \frac{1}{R_0} \left(\frac{\Delta R}{\Delta T} \right) / ^\circ K$$



: TCR graph of Binary oxide $\text{TiO}_2:\text{MoO}_3$ thin film with conc. 0.3N:0.3N

The temperature coefficient of resistance were found was $0.009854/^\circ\text{C}$.

GAS SENSING PROPERTIES

The main characterization is the optimization of operating temperature of film sample for test gases. On the basis of measured data, the sensitivity and selectivity of thin film sensor for a fixed gas concentration of 1000 ppm in air surrounding condition are estimated.

The variation in sensitivity of binary oxide $\text{TiO}_2:\text{MoO}_3$ thin films as a function of temperature and for LPG, Ethanol, NH_3 , CO and NO_2 gases [1000 ppm concentration]. The operating temperature was varied at the interval of 50°C . From the measured resistance in air as well as in gas atmosphere, the sensitivity of gas was determined at particular operating temperature using the following equation

$$\text{Sensitivity}(S) = \left| \frac{R_a - R_g}{R_a} \right| \times 100$$

Where,

R_a – resistance of thin film in air atmosphere,

R_g – resistance of thin film in gaseous atmosphere.

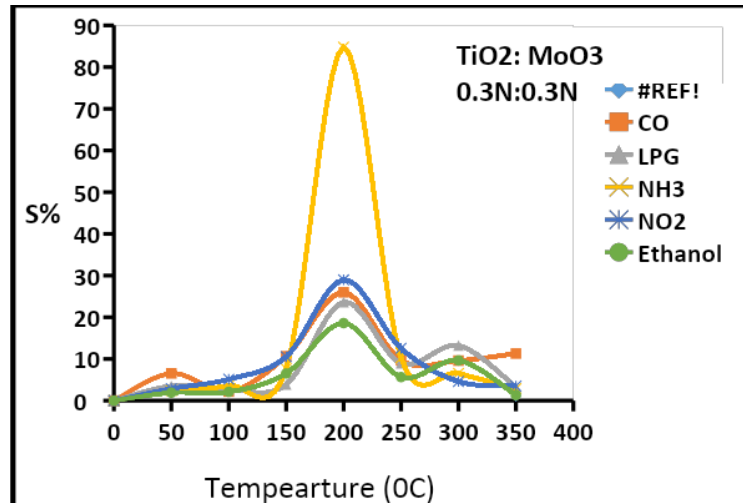


Figure: Gas sensitivity response of Binary oxide $\text{TiO}_2 : \text{MoO}_3$ thin film with concentration 0.3N:0.3N

The film of binary oxide $\text{TiO}_2:\text{MoO}_3$ was exposed to various gases. The film of $\text{TiO}_2:\text{MoO}_3$ at 0.3N:0.3N showed 84.80 % sensitivity for NH_3 gas at operating temperature 200°C and NH_3 gas concentration was at 200 ppm.

CONCLUSION

The Binary oxide $\text{TiO}_2: \text{MoO}_3$ thin films with normality 0.3N:0.3N on glass substrate and fired at 400°C to change the characteristic properties of thin film . The average particle size of film at concentrations 0.3N:0.3N were found 136 nm. Specific Surface area with different concentrations of binary oxide $\text{TiO}_2:\text{MoO}_3$ was found as $10.253 \text{ m}^2/\text{g}$. The atomic % of O, Ti, Mo were found as 92.62% ,2.85% and 4.53% respectively. XRD gives the grain size of film 2 nm. The resistivity of sample was calculated $0.616 \times 10^4 \Omega\text{-m}$. The Activation energy at high temperature and at low temperature were found 0.1017 eV and 0.8324eV respectively .The temperature coefficient of resistance were found was $0.009854 / ^\circ \text{C}$. The film of $\text{TiO}_2:\text{MoO}_3$ at 0.3N:0.3N showed 84.80% sensitivity for NH_3 gas at operating temperature 200°C and NH_3 gas concentration was at 200 ppm.

REFERENCES

1. N. Barsan, D. Koziej, U. Weimar, Metal oxide–based gas sensor research: how to? Sens. Actuators B 121 (2007) 18–35.
2. X. Chen, S.S. Mao, Chem. Rev. 107 (2007) 2891–2959.
3. A. Ruiz, J. Arbiol, A. Cirera, A. Cornet, J.R. Morante, Mater. Sci. Eng. C 19 (2002) 105–109.
4. Manavalan, S., Jose Ananth Vino, V., V-116, I-19 Special Issue, PP-401-404, 2017
5. Manavalan, S., Rakesh, N.L., International Journal of Pure and Applied Mathematics, V-116, I-17 Special Issue, PP-405-407, 2017
6. Manikandan, J., Hussain, J.H., International Journal of Mechanical Engineering and Technology, V-8, I-8, PP-1588-1593, 2017
7. Manikandan, J., Sabarish, R., International Journal of Pure and Applied Mathematics, V116, I-17 Special Issue, PP-85-88, 2017

8. T. Brezesnski, J. Wang, S. H. Tolbert and B. Dunn, *Nat. Mater.*, 9 (2010) 146.
9. Y.F. Sun, S.B. Liu, F.L. Meng, J.Y. Liu, L.T. Kong, J.H. Liu, *Sensors* 12 (2012) 2610–2631.
10. AnanyaDey, *Semiconductor metal oxide gas sensors: A review*, Elsevier *Materials Science & Engineering B* 229 (2018) 206–217.
11. N. Jayadev Dayan, S. R. Sainkar, R. N. Karekar, R. C. Aiyer, *Meas. Sci. Technol.* 9 (1998) 360-364
13. Linsebigler, Amy L., Guangquan Lu, and John T. Yates Jr., *Chemical reviews* 95.3 (1995): 735-758.
14. G. A. Tompsett, G. A. Bowmaker, R. P. Cooney, J. B. Metson, K. A. Rodgers, J. M. Seakins, *J. Raman Spectrosc.* 26, 57 (1985).
15. D. V. Ahire, S. D. Shinde, G. E. Patil, K. K. Thakur, V. B. Gaikwad, V. G. Wagh1 and G. H. Jain, Vol. 5, No. 3, September 2012, Issn 1178-5608.
16. E. B. Santos, F. A. Sigoli, I. O. Mazali, *J. Solid State Chem.* 190 (2012) 80-84.
17. A.K. Prasad, P.I. Gouma, D.J. Kubinski, J.H. Visser, R.E. Soltis, P.J. Schmitz, *Thin Solid Films*, Vol. 436, No. 1, 2003 pp. 46–51.
18. A.K. Prasad, D.J. Kubinski, P.I. Gouma, *Sens. Actuators B: Chem.*, Vol. 93, No. 1, 2003, pp. 25–30.
19. Sian.T.S and Reddy.G.B, *Appl.Surf.Sci.*, 2004,236, 1-5.
20. T. Sahm, L. Madler, A. Gularo, N. Barsan, S.E. Patsinis, U. Weimar, *Sens. Actuators B* 98 (2004) 148–153.
21. L. Shiwai, D. Li, J. Wu, X. Li, S.A. Akbar, *Sens. Actuators B* 156 (2011) 505–509.
22. R.A. Slepety, P.A. Vaughan, *J. Phys. Chem.* 73 (1969) 2157–2162.
23. D.M. Smyth, *Solid State* 129 (2000) 5–12.
24. Manavalan, S., Golden Renjith Nimal, R.J., *International Journal of Pure and Applied Mathematics*, V-116, I-19 Special Issue, PP-407-411, 2017
25. Titkov.IE, Delimova.LA, Zubrilov.AS, Seredova.NV, Liniichuk.IA and Grekhov.IV: ZnO/GaN hetero structure for LED applications, *J Mod Opt.*, 2009, 56, 653–660.
26. Dinesh C.Sharma1, SubodhSrivastava, Y.K.Vijay, Y.K.Sharma, *International Journal of Recent Research and Review*, 2012, Vol. II, 16- 20.
27. T. Brezesnski, J. Wang, S. H. Tolbert and B. Dunn, *Nat. Mater.*, 9 (2010) 146.

Thermo Study of Commercial Samples of *Lohabhasma*

Dr Rupali Ajesh Gulalkari

Dept of Chemistry

BJS'S ASC College Wagholi Pune

Abstract

Ayurved firstly introduced the concept of '*bhasma*' in its medicinal system but, it is difficult to trace out the origin of this concept, although references regarding the term '*bhasma*' are found in ancient *sanskrit* literature. From the citations related to '*bhasma*' in original *sanskrit* texts, it seems that *bhasma* obtained from calcination of (i) living as well as non-living matters (ii) vegetable as well as non-vegetable materials, possessed some special significance and importance in various religions functions, yoga and meditations.

In this research article I have done the comparative study of thermogravimetric analysis of two commercial samples of *lohabhasma*. Traditional method of preparation of *lohabhasma* is also important. Originally, *ayurvedic* system of medicine was mostly restricted to medicinal plants (*vanaushdi*) and to some extent to animal products such as cow-urine, cow-dung, cow-milk, honey etc. Later on metal-based *bhasmas* were introduced and subsequently they constituted the most important class of drugs of mineral origin. *ayurved* and *ayurvedic* medicines will receive more and more appreciation and importance all over the world. Metal-based *ayurvedic* drugs being the superior drugs as compared to all other classes of drugs, there is an excellent opportunity to rejuvenate this original art with the help of modern scientific development.

Keywords: *lohabhasma*, *ayurved*, *vanaushdi*, *drugs*, *cowurine*

Introduction

Iron, being an element of vital importance, in life process, possesses equal importance in all medical systems, eastern or western. Therefore, iron based medicinal preparations are pharmaceutical products of common interest of all pharmacies. *Lohabhasma* is one of such product for which there is large scale demand both for clinical purpose as well as for other *ayurvedic* formulations of which *lolabhasma* is an important constituent. Accordingly, the number of *ayurvedic* pharmacies and modern pharmacies, preparing *lohabhasma* on small or large scale is tremendous and, in every state, *lohabhasma* is prepared by traditional methods. The selection of particular method depends on the location of the pharmacy and availability of the raw materials required for synthesis.

All the commercial samples sold in the market in India may be broadly divided into two or three categories as Ordinary *lohabhasma* prepared from metallic iron, which is synthesized by some traditional process, the details of which are not specified. Since cheaper or waste iron powder or sheets are used as starting materials and readily available media are used such as cow-urine or medicinal plant materials are used for *bhasmikanana*, these are much cheaper and therefore they are commonly used for clinical purpose. *Anta lohabhasma* prepared by using magnetite or other type of magnetic iron as the starting material. This is more costly and prepared by some *ayurvedic* physicians for their treatment. Here also the method of synthesis is neither specified nor literature reference is given..

From medicinal point of view, no significant difference in the properties of *lohabhasma* belonging to any category is reported along with experimental supports. Therefore, all the commercial samples are more or less similar in their quality and utility. Due to this reason, and

because the number of pharmacies is very large, only representative pharmacies from different states are listed in Table 1 For *lohabhasma* some work has been carried out by us previously,

But the present work is the first attempt to carry out a systematic work on comparative study of two commercial samples using modern techniques such as **thermogravimetric analysis**. Comparative study of the commercial samples of metal-based *ayurvedic bhasmas* is one of our main activity during past few years.

Experimental Procedure.

In this method firstly the iron powder (500g) was subjected to general method of purification in which the powder was heated to red heat and then dipped successively in *til* oil, butter milk, cow urine and aqueous extract of dolichos (*kulith*) and rice (*kanji*). For special purification, the above processed iron powder (500g) was heated and dipped in freshly collected cow-urine. This operation of heating and dipping the hot iron powder in cow urine was repeated seven times.

After special purification, the iron powder was taken in a mortar and mixed with cow-urine and the mixture was triturated for six hours. This mixture was kept overnight for interaction to complete the destruction of metallic state (*marana*).

SOME REPRESENTATIVE AYURVEDIC PHARMACIES MANUFACTURING LOHABHASMA

Table 01

Representative ayurvedic pharmacies, which manufacture *lohabhasma*

No.	Name of the pharmacy	Place	State
1	Kalpataru Ayurvedic works Ltd.	Kolkatta	West Bengal
2	Dhanwantari	Mumbai	Maharastra
3	Deendayal Ayurved Pharmacy		Madya Pradesh
4	Unza Pharmacy	Unza	Gujrat
5	Dabur pharmaceutical works	Sahidabad	Uttarpradesh
6	Krishna Gopal Ayurved Bhavan	Ajmer	Rajasthan
7	Dootpapeshwar	Panvel	Maharastra
8	Ayurved Seva Sangh	Pune	Maharastra

In the present work about two such pharmacies are selected and their names and places are given in Table 02 . Selection of ayurvedic pharmacies for comparative study.

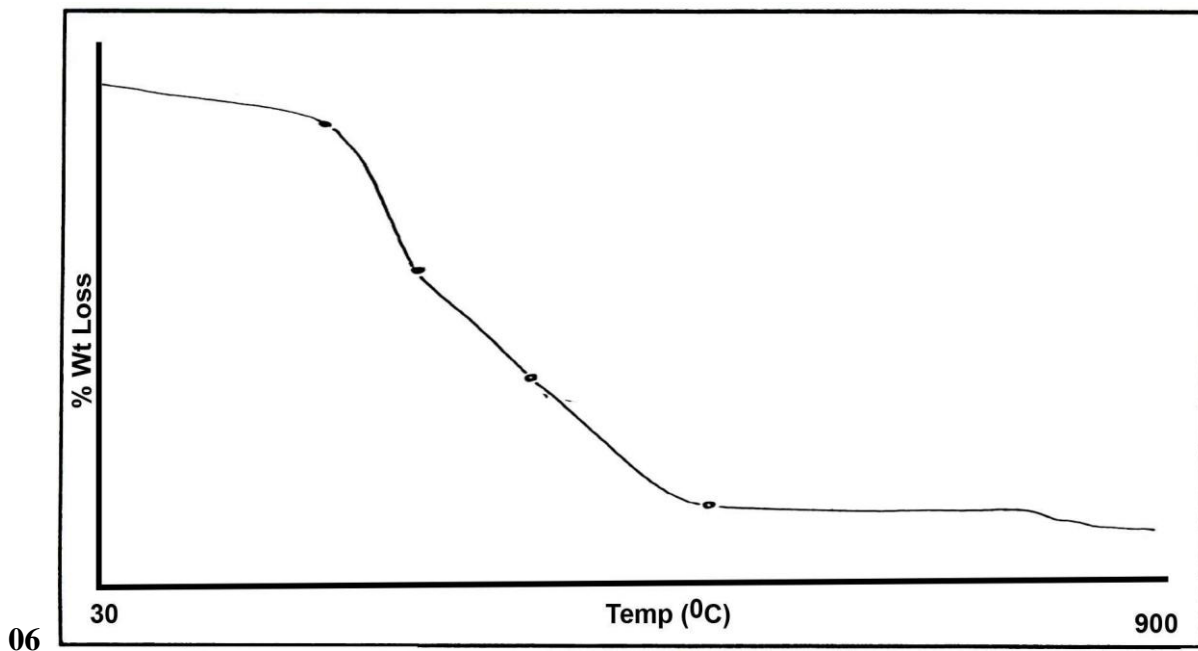
Table-02

Sr No	Code Name and Name of Pharmacy	Name and Place of Pharmacy
1	LB-01 Dootpapeshwar	Dootpapeshwar Panvel
3	LB-02 Ayurved Seva Sangh	Ayurved Seva Sangh Pune

THERMOGRAVIMETRIC PATTERNS OF *LOHABHASm*

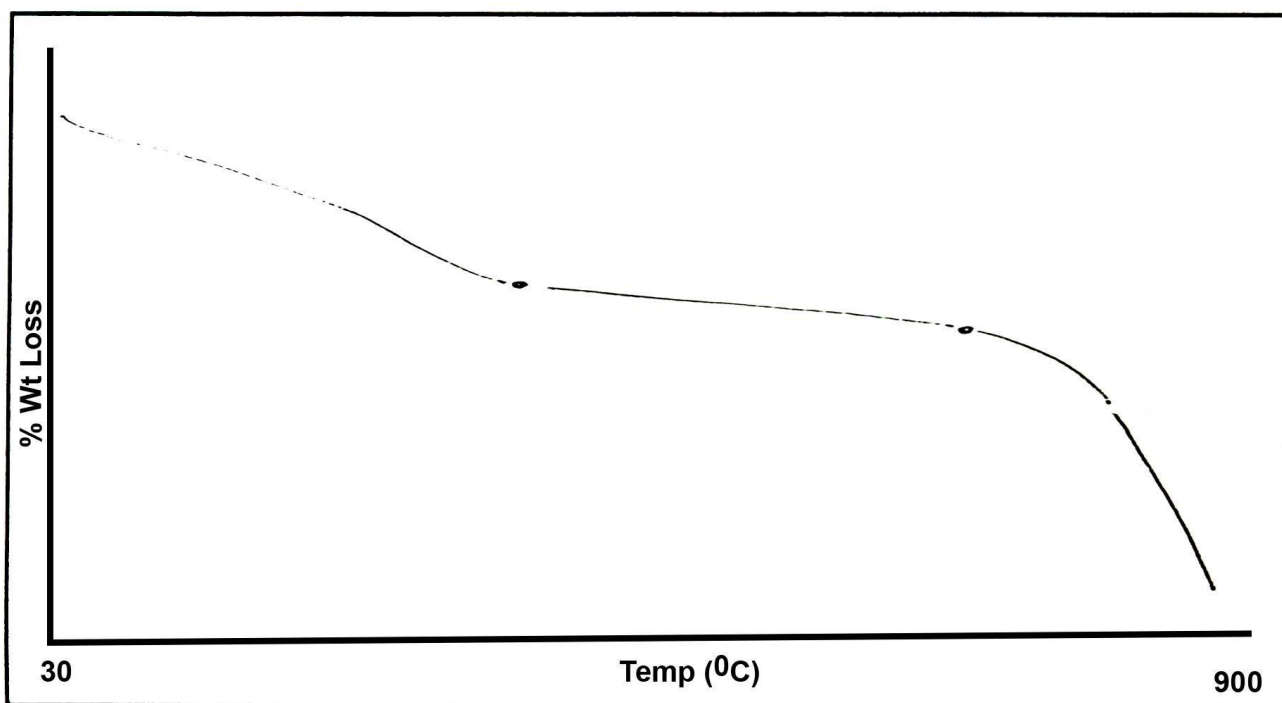
Figure No. : 1

LB- 01 Dhootpapeshwar



Ayurved Seva Sangh

Figure No. : 2
LB-02



Result

Most of the metallic *bhasmas* are synthesized by applying higher temperatures (upto 800 or 1000°C). Therefore, they are not expected to show any significant thermal decomposition behavior in the temperature range (25-600)°C, if they are purely metal oxides as assumed by some modern scientists. But still their thermogravimetric study may be found to be useful in certain aspects such as

- a. Presence or absence of adhered, or absorbed water or moisture.
- b. Indications of any decomposable organic matter associated with these *bhasmas*, if any and
- c. Similarities or differences in thermal decomposition behavior among different commercial samples which might be reflected in their TG curves.

Therefore, study of some commercial samples LB-01, and LB-02 was carried out to examine their thermal decomposition behavior.

For this purpose, the thermograms of these samples of *lohabhasma* were recorded in air atmosphere on a NATZSCH simultaneous thermo analyzer STA.40 a model provided with platinum thermo cups and Pt/Pt/ 10% Rh thermocouples. For each run about 20-25 mg of a well ground sample was taken and the heating rate was maintained at 10°C per minute. The nature of the TG curves is shown in Figure 1 to 2

On the basis of T.G. patterns samples of *Lohabhasma* may be classified into two groups.

One group consisting of Fe-BAI and Fe-R. This shows thermal stability of the samples over the entire range R.T. to 900°C

. This shows different behavior. These samples show two to three stage decomposition patterns indicating that they consist of decomposable organic matter.

From this it may be concluded that the methods of preparation of *Lohabhasma* are different from one another, due to which end products are not identical.

REFERENCES

- 1 S.H. Bhosale, G.S. Jagtap, B.A. Kulkarni and S.S. Kadam. Study of Some Commercial Samples of Moutik bhasma.
79th Indian Science Congress, Baroda (1992).
- 2 S.S. Kadam, S.H. Bhosale, S.D. Gaikwad, P.T. Bhadve, and B.A. Kulkarni.
Comparative study of Commercial samples of Kapardik bhasma.
81st Indian Science Congress, Jaipur (India) 1994 .
- 3 Comparative study of some commercial samples of Naga bhasma
Mrudula Wadekar, Vishwas Gogte, Prasad Khandagale and Ashmita Prabhune.
Ancient Science of Life Vol.XXIII, 48-58 (2004).
- 4 S.H. Bhosale, G.S. Jagtap and B.A. Kulkarni.
Comparative Study of Commercial Samples of Jasad bhasma.
29th Annual Convention of Chemists. Rewa (M.P) (1992).
- 5 S.H. Bhosale, G.S. Jagtap, S.S. Kadam and B.A. Kulkarni
Comparative Study of Commercial Samples of Praval bhasma .
Proe. of 80th Indian Science Congress Goa (1993).
- 6 S.H. Bhosale, G.S. Jagtap, B.A. Kulkarni and S.S. Kadam
Analytical studies in some commercial samples of praval bhasma
28th Indian chemical society's convention Calcutta (1991)
- 7 R.W. Jawale, Vividha Dhapte, P.S. Khandagale, **Rupali Lad**, R.D. Kankariya and S.T. Takale.
Comparative Study of Commercial Samples of Hiraka bhasma.
97th Indian Science Congress Vishakhapatnam (2009).
- 8 Mrudula Wadekar, G.T. Panse, B.A. Kulkarni, P.S. Khandagale, and P.K. Khanna.
Chemical and Structural Characterization of Commercial Samples of Naga bhasma.
39th Indian Chemical Society Convention Nagarjunnagar A. P. (2002).
- 9 L.V. Krishnamurthy and R.T. Sane.
Studies on Aurvedic bhasma on the basis of modern analytical instrumental techniques.
Research Journal of chemistry and Environment 5, 65-67 (2001).
- 10 S.M. Sondhi and G.K. Janani.
Determination of mineral elements in some Ayurvedic Bhasmas used for the cure of various ailments.

- Indian Drugs 32, 152-157 (1995).
- 11 H.P. Kalug and L.E. Alexander.
X-ray diffraction procedures for polycrystalline and amorphous metaterials.
John Wiley and Sons New Yark (1974).
 - 12 T.K. Bhowmick, A. K. Suresh, S.G. Kane, A.C.Joshi and J.R. Bellare.
Physicochemical Characterization of an Indian traditional medicine jasad bhasmas;
detection of nano particles containing non-stotiometric zinc oxide.
J.Nanopart. Res.11, 655-664 (2009).
 - 13 S.Pandit,T.K. Bhiswas, D.K Debnath, A.V.Saha U.Chowdhary.
Chemical and Pharmacological evaluation of different ayurvedic preparation of iron.
J.Ethnopharmacol. 65, 149-156 (1999).
 - 14 K.K. Asundhi and R.M.Dixit.
Spectragraphic and X-ray fluorecence analysis of a class of ayurvedic medicines-
Calcium bhasmas.
J.Res.Ind.Med.Yoga.Homeopat.13, 1 (1978).
 - 15 F.Vratny, M.Dilling, F.Gugliotta and C.N.R. Rao.
Infrared Spectra of Metallic oxides, Phosphates & Chromates.
J.Sci..Industr.Res.20B.590-593 (1963).
 - 16 Mrudula Wadekar, Shivaji Takale, **Rupali Lad**, R.D Kankaria, Y.N. Bendale and B.A.
Kulkarni
Characterization of Zinc-based ayurvedic drug synthesized by using plant materials.
International conference of ‘ Drug Analysis’ Namur (Belgium) (2006).
 - 17 Mrudula Wadekar, **Rupali Lad**, Rajendra Kankaria and
Ashmita Prabhune.
XRD Investigations of Lohabhasma
93rd Indian Science Congress, Hyderabad (2006).
 - 18 Shivaji Takale, D.G. Kanase, B.A. Kulkarni and Mrudula Wadekar.
Comparative study of Naga bhasma and lead oxides.
93rd Indian Science Congress Hyderabad (2006).
 - 19 Mrudula Wadekar, Yogesh Bendale, P.S. Khandagale and
Ashmita Prabhune.
Preparation and Chemical Study of Vanaspati marita, Swarna bhasma.
24th Indian Council of Chemists.
Annual conference Ranchi, Bihar (2005).
 - 20 Mrudula Wadekar, **Rupali Lad**, R.D Kankariya and R.G.
Sarawadekar.
Synthesis and Analytical Study of Loha bhasma
24th Annual Conference of Indian Council of Chemists Ranchi, Bihar (2005)

Development of an Extractive and Spectrophotometric determination of Strontium(II) with N,N''-bis(O-hydroxy-acetophenone) ethylenediimine (HAPED) derivative as an analytical reagent

Jayashree S. Patil¹

¹Department of Chemistry, J.S.M. College, Alibag, Raigad, Maharashtra, India

ABSTRACT

The Spectrophotometric method is coupled with solvent extraction technique and used for the determination of Sr(II) using N,N''-bis(O-hydroxy -acetophenone) ethylene diimine(HAPED) as an analytical reagent. This reagent is synthesised in the laboratory and characterised by NMR, IR, mass and elemental analysis for its purity. The reagent forms a light yellow-coloured stable complex with manganese metal, which can be quantitatively extracted into chloroform at pH 5.2. This Sr(II)-HAPED complex in Chloroform exhibit intense absorption peak at 585nm. Beer's law is obeyed in the range of 1-10 ppm of Strontium solution giving linear and reproducible graph. The stoichiometric ratio of complex studied by Job's continuous variation method, Mole ratio and Slope ratio method. The Molar absorptivity and Sandell's sensitivity are also calculated. The Molar absorptivity is 1,265.65 L/mol/cm and Sandell sensitivity is 0.0572 µg/cm². The proposed method is rapid, sensitive, reproducible, accurate and has been satisfactory applied for determination and separation of Sr(II) in commercial mixtures, pharmaceutical samples and alloys.

Keywords: HAPED reagent, Strontium(II), Sandell'Sensitivity, Molar Absorptivity, Spectrophotometric determination.

INTRODUCTION

Spectrophotometry is essentially a trace- analytical technique and is one of the most powerful tools in chemical analysis¹⁻³. A wide variety of reagents have been proposed for the spectrophotometric determination of Strontium. The extractive spectrophotometric analysis enables to separate desired metal ion, which is to be estimated in presence of other metal from samples. In the present study, solvent extraction methods are proposed for the metals like Sr(II), Ni(II), Fe(II), Co(II), Cu(II), Mn(II), Cr(III)etc⁴. These metals have proved to be of immense importance in various chemicals, biochemical, pharmaceuticals and industrial applications⁵⁻⁷. It provides good separation and determination methods. Optimum extraction conditions are evaluated to study several experimental parameters like effect of reagent concentration, different diluents, effect of temperature etc⁸. Diverse ion studies are carried out to study the selectivity for the method. This method is used for the analysis of real sample like various alloys, pharmaceutical samples. Extractive methods are highly sensitive but generally lacks in simplicity. In the present work a novel analytical reagent N,N'bis''(O-hydroxyacetophenone)

ethylenediimine (HAPED), was used for the extractive spectrophotometric determination of Strontium. The developed method can be employed for efficient determination of Strontium at microgram level. The results of analysis obtained were compared with those obtained by known methods⁹⁻¹¹.

EXPERIMENTAL WORK

1. Instruments :- Shimadzu 2100 UV-Visible spectrophotometer with 1.0 cm quartz cell was used for absorbance studies. An Elico LI-120 digital pH-meter was used for pH adjustment.

2. Synthesis of Reagent:- The HAPED reagent was synthesised by O-hydroxyacetophenone and ethylene diamine in methanol in 2:1 molar proportions are mixed in round bottom flask. Shake the flask for 10 to 15 min. immediately light-yellow-colour solid is obtained which is poured in ice-cold water. The solid obtained is separated by filtration and washed with cold water and the product is recrystallised from ethanol. The yield was about 96%. It is then characterised and used for extractive spectrophotometric determination of Sr(II). A stock solution of HAPED reagent with concentration 0.1% was prepared in methanol. The scheme of reaction is shown in Figure 1.

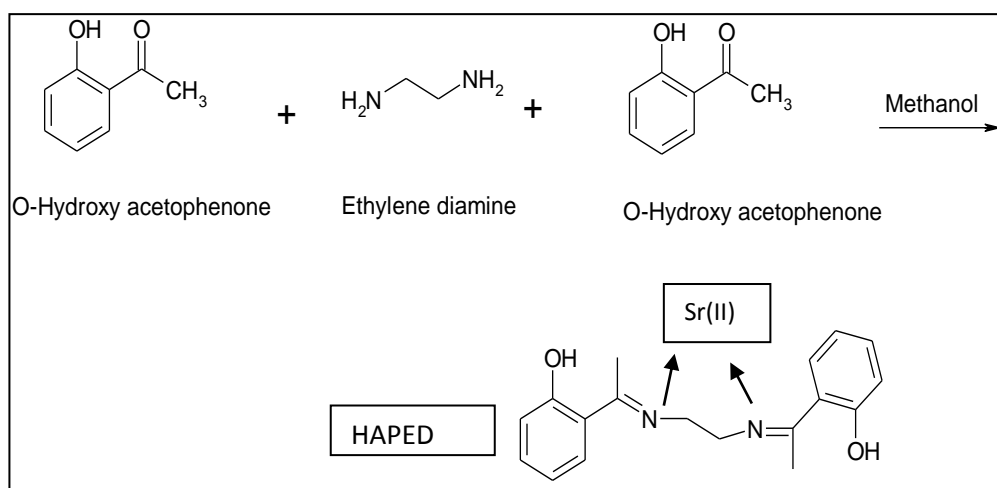
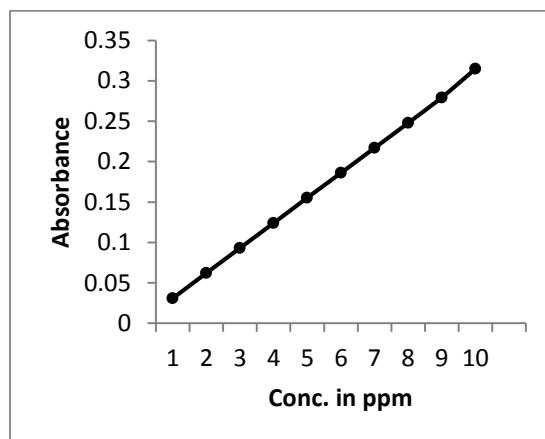


Figure-1:-Synthesis of reagent N,N'-bis (O-hydroxy-acetophenone) ethylene diimine (HAPED)

3. Preparation of stock solution:- A weighed quantity of Strontium Chloride was dissolved in double distilled water containing dilute hydrochloric acid and then diluted to desired volume by double distilled water. The solution was then Standardised by titrimetric Method.

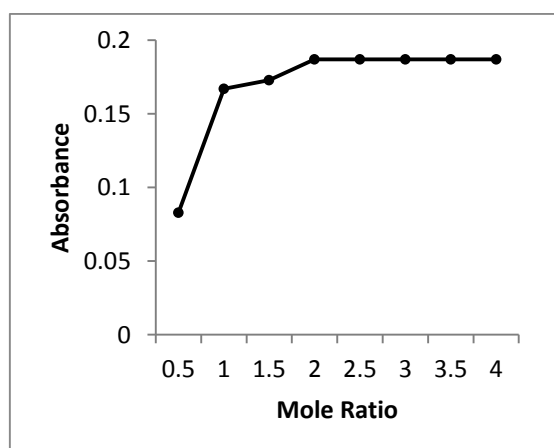
4. Recommended procedure:- Mix 1-cm³ aqueous solution containing 1-100mg of Strontium and 2 cm³ of 0.1% methanolic solution of HAPED reagent in 25 cm³ beaker. Adjust the pH of the solution to required value with buffer solution Make the final volume 10cm³. Transfer the solution into 125 cm³ separate funnel and equilibrate for 1min. with 10cm³ Chloroform. Allow the two phases to separate and measure the absorbance of organic phase containing the complex at 585 nm against reagent blank.

5. Preparation of calibration plot:- The calibration curve is prepared by taking known amount of Strontium which is described in the procedure. A graph of absorbance against concentration is shown in Figure 2. The concentration of the unknown Strontium solutions is determined from the calibration plot.



Figure,2: Calibration plot for extractive spectrophotometric determination of Strontium(II) with Chloroform.

6. Composition of the extracted species :- The Composition of the extracted species was determined by using the Job's continuous variation method and verified by Mole ratio method and Slope ratio method. These methods show that the composition of Strontium(II)- HAPED reagent is 1: 2 which is represented in Figure 3.



Figure,3: Composition of the Extracted Strontium(II) - HAPED species by Mole ratio method

7. Effect of foreign ions:- Various cations and anions were investigated to find the tolerance limit of these foreign ions in the extraction of Strontium (II) presented in Table 2. The effect of diverse ions on the Strontium(II) determination was studied, in presence of a definite amount of a foreign ion. The tolerance limit of the foreign ion was taken as the amount required causing an error of not more than 2% in recovery of Strontium(II). The ions which interfere in the spectrophotometric determination of Strontium were masked by using appropriate masking agents presented in Table 3.

Table:1

Sr.No	Different parameters Studied	Observation
1	Solvent	Chloroform
2	pH	5.2
3	Equilibrium time	1 min.
4	Stoichiometry M:L	1:2
5	95% confidence limit	± 0.2752
6	Reagent Concentration	0.1%
7	Volume of Reagent	2cm ³
8	Average of 7 determination	9.60
9	Stability of the complex	35 h.
10	Sandell sensitivity	0.0572- $\mu\text{g}/\text{cm}^2$
11	Molar absorptivity	1,265.65 L/mol/cm

Table :2 Effect of foreign ions

Sr. No.	Interfering ions	Tolerance limit
1	Tartrate, acetate, BrO ₃ ⁻ , Br ⁻ , NO ₃ ⁻ , IO ₃ ⁻ , SO ₄ ⁻ , SO ₃ ⁻ , CN ⁻ ,	08
2	Co(II), Fe(II), Cu(II), Ni(II), Mn(II) EDTA	Interfere strongly
3	Oxalate , Phosphate,	07
4	Al(III), Mg(II), Mo(VI), Cd(II), W(VI),	06
5	Al(III), Bi(III), Ce(IV),Ca(II),	10
6	Na ⁺ , Ag ⁺ ,K ⁺	05

Table-3: Effect of masking agent

Sr. No.	Interfering Ions	Masking Agents
1	Pd(II)	Thiourea
2	Ce(IV), Fe(III), Co(II)	Sodium Fluoride
3	Cr(III)	Ammonium acetate
4	Ni(II)	DMG
5	EDTA, Cyanide ion	Boiled with conc.HNO ₃

8. Comparison between reagents

Various reagents were investigated by the earlier researchers for removal of Sr(II). The proposed reagent (HAPED) is found more superior as that of reported reagents and are presented in Table 4.

Table 4: Comparison between reagents

Sr./ No.	Reagent	Remark
1	Diantipryl-(p-chloro)-phenylmethane	Beer's range 0-400 $\mu\text{g}/25\text{ cm}^3$
2	Hydroxamic acid	Sandell Sensitivity is poor
2	Piconaldehyde nicotinoylhydrazone	Beer's Range 0.02-1.5ppm yellow-coloured complex with M:L ratio as 1:2
3	N,N'-diethylaniline	Require heating At 100°C
4	Methylene green	Beer's range 0.2-30 cm^3
5	Ethylenebis(triphenyl Phosphonium cation	Mn ²⁺ interferes

9. Applications

The present method was applied for determination of amount of Strontium(II) in various samples of alloys, commercial mixtures, Honey sample, water sample etc. The results obtained were in well agreement with the standard methods shown in Table -5. Every result is the average of independent determinations.

Table 5: Applications

Sr. No.	Sample	Amount of Sr(II) predicted from Standard method	Amount of Sr(II) predicted from Present method
1	Celestite ore	43.88%	43.86%
2	Strontianite	27.00%	26.94%
4	Sr(5) + Zn(5)	4.95ppm	4.93ppm
5	Sr(50) + Cd(50) + Ni(50)	50ppm	49.98ppm

RESULT AND DISCUSSION:

In this section, experimental results of solvent extraction for removal of Sr(II) by using HAPED as organic reagent are presented. The stability of Strontium complex is 35h. Represented as in figure:3. It is observed from this figure that a linear calibration curve was obtained in the range of 1-10 ppm Strontium. Effect of various parameters like pH, absorbance, wavelength and validity of Beer's and Lambert's law. The absorption is observed maximum at wavelength 585 nm. The equilibrium is attained within 1 min. The best results of solvent extraction were obtained in aqueous phase at pH 5.2 whereas organic phase containing Chloroform as solvent.

1. Effect of pH and absorbance

Chloroform is found to be the most suitable solvent which is carried maximum extraction which is shown in figure 5. 1 cm³ aqueous solution contain 100 ppm Sr(II) at different pH shaking with 2 cm³ of 0.1% HAPED in chloroform, after separated a two layers measure the absorbance of organic phase at wavelength of 535nm and pH of 5.2 respectively which is represented in figure: 6.

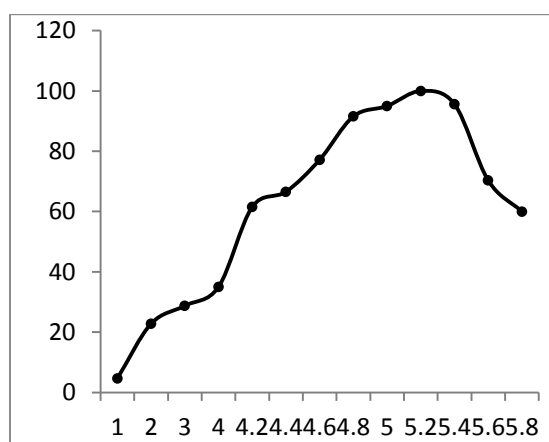


Figure :6- Effect of pH on the extraction of Sr(II):HAPED complex

2 Selection of the Solvent

Various solvents were tried to determine the maximum extraction of Chromium. Chloroform was found to be most suitable solvent as it showed the maximum extraction. The extraction of Strontium varied from maximum to minimum for the solvent in the order of chloroform > ethyl Acetate > n-butanol > xylene > cyclohexanone > diethyl ether > toluene > carbon Tetrachloride > n-Hexane > nitrobenzene which is shown in figure:7.

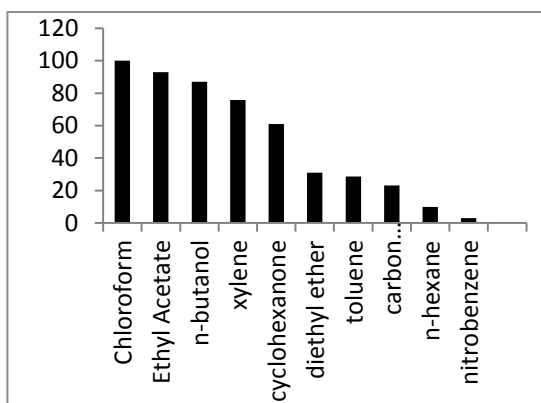


Figure :7 Effect of various solvents on Strontium(II) : HAPED complex

3. Shaking time effect

1-cm³ aqueous solution contain 100 ppm Sr(III) at pH 5.2 after added 2 cm³ of 0.1% HAPED in Chloroform, shaking for different times (0-60) min. after separating

the layers, measuring the absorbance of organic phase at wavelength of 585nm.

4 Mole ratio method

Solution of 0.01M HAPED in Chloroform used to extract 0.01M Sr(II) from aqueous solution at optimum conditions, also determine absorbance of organic phase at wavelength of 585nm against chloroform, figure : 3 indicates that the ratio of Sr(II) to complex was 1:2[Sr⁺²:(HAPED)].

4. CONCLUSION

The proposed novel reagent is found to be more effective over reagents reported by earlier investigators. The proposed method is simple, more highly sensitive and selective than the reported methods for the extractive Spectrophotometric determination of microgram amounts of Strontium. It has been successfully applied to the determination of Strontium at trace level in synthetic mixtures and ores. It offers advantages like reliability and reproducibility in addition to its simplicity, instant colour development and suffers from less interference. This method is easily employed anywhere as does not require sophisticated instruments.

REFERENCES

1. Ahluwalia, V.K., Bhagat, P., Agarwal, R. and Chandra R., 2005 Intermediates for organic synthesis, I.K. International Pvt. Ltd. Vogel, A.I. Textbook of organic synthesis, 3rd edition ; ELBS, London, 1957.
2. Cheng C.Y., "purification of synthetic laterite leach solution by solvent extraction using D2EHPA," hydrometallurgy, Vol.56, 369-386(2000).
3. Devi N.B., Nathsarma K.C., Chakravorty V., "Extraction and separation of Mn(II) and Zn(II) from Sulphate solution by sodium salt of Cyanex 272".
4. Pellerano R. G., Romero C. H., Acevedo H.A., and Vazquez F.A., Determination of Strontium in the Parana river by solid phase spectrophotometry, J. Argen, Chem., Soc, 49(416), 83-90(2006).

5. Sonawale S., Ghalasasi Y., and Argekar A., Extraction of Strontium(II) and Copper(II) from Salicylate media by tributyl phosphine oxide, *Anal. Sci.*, 17(2), 285-289(2001).
6. Singh P., Goel R.L., and Singh B.P., "Synthesis, Characterization and biological activity of Schiff Bases", *J. Ind. Chem. Soc.*, 52, 958(1975).
7. Skoog D.A., West D.M., Holler F.J., "Fundamentals of Analytical Chem.", 5th Ed. Saudeer, New York, 1988.
8. Vogel A.I., "Text Book of qualitative Inorganic Analysis, Longmann Green and Co. Ltd. London (1961).
9. Kostenko E.E, solid phase spectrophotometric determination of Strontium using Chromazurol, *J. Anal. Chem.*, 65(4), 366-370(2010).
10. Deep A., Gupta B.,Malik., and Tandon, S.N., "Extraction and Separation of some 3d transition metal ions using Cynex 923," *Solvent Extraction. Ion Exchange*, **20**, pp. 81-96(2002).
11. Holler F.J., Skoog D.A., West D.M., "Fundamentals of Analytical Chem.", 5th Ed. Saudeer, New York, (1988).

Study of Human Body Response for the Classical Ragas used for Releasing Tension, Played on Wind Instrument Shehnai using Psycho-Physiological Method

R. N. Wadalkar¹ S. P. Bakale²

Department of Physics, Swami Mukatanand College of Science, Yeola. (Nasik)

Abstract:

The raga-based approach broadly involves application of music pieces with specific emphasis on swara pattern, embellishment & appropriate rhythms. This approach being both melodic and rhythm depends on the intended music function & therapeutic objective identified. Raga with swaras having short and long intervals and different embellishment could be chosen with appropriate slow, medium or fast tempo, with or without virtuosity. The application would vary for different music function identified.

a) Audio, analgesic, anxiolytic sedative, b) to be stimulatory and energizing and C) to be an active focus of attention etc. This music therapy is based on long empirical tradition but not proven by the conventional western experimental methods. It is unique and cultural and throws a great scope for further studies.

Keyword: Music therapy, Classical Raga, Psycho-physiological, etc.

Introduction:

There are several studies conducted on physical and psychological influence of music and sound on human body parameters like GSR, HRV, blood pressure etc. Vibration of human skull, as produced by loud vocalization, exerts a massaging effect on brain and facilitates elution of metabolic product from the brain into cerebrospinal fluid (CSF). Music has been known to have direct effect on the people's moods. By just listening to music people's mood can be altered. Several tests were conducted to test people's mood changes after listening to certain kind of music (Schoen 89-99)^[3]. A study conducted by Zimny and Whitefeller (1963)^[7] looked at the effects of the music on galvanic skin response (GSR) in children. They find evidence that stimulating and calming music would have different effects on children. They postulated from their results that a decrease in skin resistance indicates an increase of emotional excitement in response to exciting music and an increase in skin resistance indicates a decrease in emotional excitement in response to calming music. A study by Landreth (1974)^[8] noted changes in heart rates of 22 subjects. They concluded that music did not cause any consistently reliable effect on listeners' heart rate, particularly the participant's heart rates habituated in response the more time they listened to the music. Music therapy has been used since ancient days. Kenneth Bruscia (1984)^[4] defined music therapy as "a systematic process of intervention where the therapist helps the client to achieve health, using musical experiences and the relationship that develop through them as dynamic forces of changes". Maranto (1933b)^[5] has outlined instances where the use of music may be regarded as music therapy. By using background music to mask the aversive sound level of a neo-natal isolate, music therapists have helped facilitate homeostatic and increased the neurological development of pre-term infants

(Stanley 1991b)^[6]. The equipment was first used as an aid for physical stimulation of children with multiple physical and mental handicaps. Olav Skille wrote several articles in Norwegian and Nordic journals. Dr. Med W. Trankle^[10] has done some preliminary experiments on changes in reflector muscle-tonous and musical experiences. Music as sleep therapy is described by H. Wendt^[9] who says that “The connection between sleep therapy and music is indirect. Music is harmonizing the cortical regulations which create improved readiness for sleep”.

We are daily subjected to stress which we cannot let loose in Natural way. The human body prepare for danger when it is subject to stress. This means that stress hormones are pumped into the blood stream, and the body prepare for physical activity: Fight or Flee! The blood is filled with substances which make it possible to exert a powerful burst of energy^[1]. In Most situation this burst will be suppressed it does not suit a civilized being to react in this way and our body is left with unused and caged reserves of energy. These traces of stress will be stored as waste product in cells and blood vessels. These May in time, lead to serious consequences for our health. If we consider the image of body being a skin sack receiving sound waves, each and every cell in the body receives a massage by being exposed to sound vibration from music. The Cell membrane is not completely tight, however the mild internal massage which music therapy is giving, make it possible for metabolic waste products to the expelled from the cell. The escape of this waste product from the cell would ordinarily take very long time. The extra cellular fluid carries the waste product onward through the lymphatic system, the blood system for normal excretion from body. The objective of the study is to study the psycho-physiological response to the classical raga played on shehnai

Methodology:

The method for obtaining the psycho-physiological response can be adopted with the following procedure. The subject will be asked to listen the classical ragas Ahir Bhiarav recorded on CD. In the 30to60 minute’s session, the subject will keep to eye closed. They will also breathe slowly and rhythmically by electronic digital blood pressure meter. The reading will be taken when the subject is listening the classical ragas, which are used to reduce the mental tension, played on wind instrument shehnai. The data will be further analyzed using statistical technique. Ahir Bhairav raga is an ancient raga that is considered to be extremely old and originated many centuries ago. The origin of Bhairav raga is disputed. According to some musicians, Bhairav raga was the first raga that originated from the mouth of Lord Shiva. While some musicians argue that Bhairav raga originated from the mouth of Lord Surya. Bhairav is grave in mood and suggests seriousness, introversion as well as devotional attitude.

Experimental:

Table-1: First week session

Sr. No	Name	Age	BP Before Listening Raga		BP After Listening Raga	
			Diastolic	Systolic	Diastolic	Systolic
1	Manisha Bhagwat Pansare	21	79	120	80	118
2	Dipali Sunil Bhise	21	78	122	79	120
3	Santosh Vasant Somase	30	80	120	80	120

4	Babasaheb Bhagwat Pansare	26	85	115	82	115
5	Dnyaneshwar Laxman Pansare	39	78	125	80	123
6	Bhagwat Namdev Pansare	50	85	130	84	128
7	Janabai Namdev Pansare	62	90	135	90	130
8	Chandrabhaga Rambhau Pansare	58	82	125	80	130
9	Laxman Dagdu Pansare	68	90	140	90	138
10	Vasant Karbhari Somase	56	75	130	75	135
11	Bhikaji Sakharam Kudale	55	85	140	82	138
12	Dilip Rangunath Kudale	45	80	115	80	110
13	Ganesh Ramnath Jagtap	51	82	124	80	120
14	Rushikesh Kantilal Dusane	35	70	110	75	115
15	Manoj Narayan Patil	42	80	130	85	125

Table-2: Second week session

Sr. No	Name	Age	BP Before Listening Raga		BP After Listening Raga	
			Diastolic	Systolic	Diastolic	Systolic
1	Manisha Bhagwat Pansare	21	80	120	80	120
2	Dipali Sunil Bhise	21	80	122	80	120
3	Santosh Vasant Somase	30	82	120	80	118
4	Babasaheb Bhagwat Pansare	26	90	120	85	120
5	Dnyaneshwar Laxman Pansare	39	80	125	78	120
6	Bhagwat Namdev Pansare	50	82	132	82	130
7	Janabai Namdev Pansare	62	90	135	90	130
8	Chandrabhaga Rambhau Pansare	58	80	128	80	125
9	Laxman Dagdu Pansare	68	90	140	85	132
10	Vasant Karbhari Somase	56	78	130	78	127
11	Bhikaji Sakharam Kudale	55	90	140	90	137
12	Dilip Rangunath Kudale	45	80	118	80	120
13	Ganesh Ramnath Jagtap	51	85	125	80	122
14	Rushikesh Kantilal Dusane	35	75	115	75	115
15	Manoj Narayan Patil	42	80	130	82	126

Table-3: Third week session

Sr. No	Name	Age	BP Before Listening Raga		BP After Listening Raga	
			Diastolic	Systolic	Diastolic	Systolic
1	Manisha Bhagwat Pansare	21	80	120	80	120
2	Dipali Sunil Bhise	21	80	122	80	120
3	Santosh Vasant Somase	30	82	120	80	120
4	Babasaheb Bhagwat Pansare	26	80	122	80	120
5	Dnyaneshwar Laxman Pansare	39	80	125	80	118
6	Bhagwat Namdev Pansare	50	85	130	82	125
7	Janabai Namdev Pansare	62	85	130	85	125
8	Chandrabhaga Rambhau Pansare	58	80	125	80	125
9	Laxman Dagdu Pansare	68	90	135	86	132

10	Vasant Karbhari Somase	56	82	128	80	125
11	Bhikaji Sakharam Kudale	55	85	135	85	130
12	Dilip Ragnath Kudale	45	80	120	80	117
13	Ganesh Ramnath Jagtap	51	85	125	80	122
14	Rushikesh Kantilal Dusane	35	78	120	80	120
15	Manoj Narayan Patil	42	80	125	82	122

Table-4: Fourth week session

Sr. No	Name	Age	BP Before Listening Raga		BP After Listening Raga	
			Diastolic	Systolic	Diastolic	Systolic
1	Manisha Bhagwat Pansare	21	80	120	80	120
2	Dipali Sunil Bhise	21	80	122	80	120
3	Santosh Vasant Somase	30	82	120	80	120
4	Babasaheb Bhagwat Pansare	26	80	122	80	120
5	Dnyaneshwar Laxman Pansare	39	80	125	80	118
6	Bhagwat Namdev Pansare	50	85	130	82	125
7	Janabai Namdev Pansare	62	85	128	85	125
8	Chandrabhaga Rambhau Pansare	58	82	125	80	124
9	Laxman Dagdu Pansare	68	90	135	86	130
10	Vasant Karbhari Somase	56	80	128	80	126
11	Bhikaji Sakharam Kudale	55	85	132	82	130
12	Dilip Ragnath Kudale	45	80	120	80	120
13	Ganesh Ramnath Jagtap	51	82	123	80	118
14	Rushikesh Kantilal Dusane	35	75	120	80	120
15	Manoj Narayan Patil	42	80	125	80	122

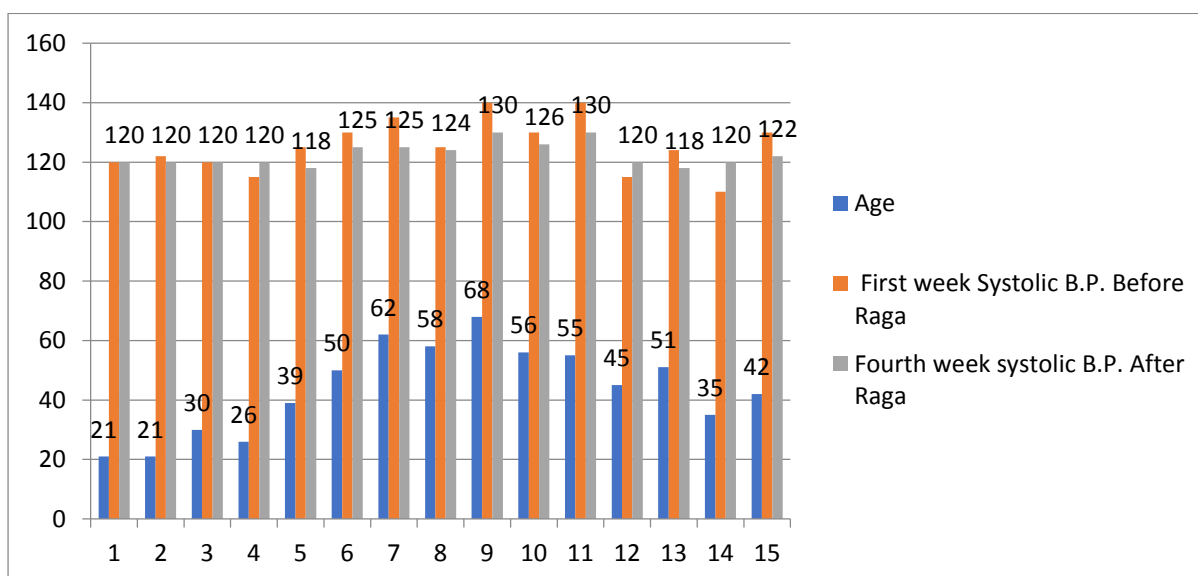


Fig.-1: Graph of systolic Blood Pressure (BP) of first week and fourth week of group under experiment

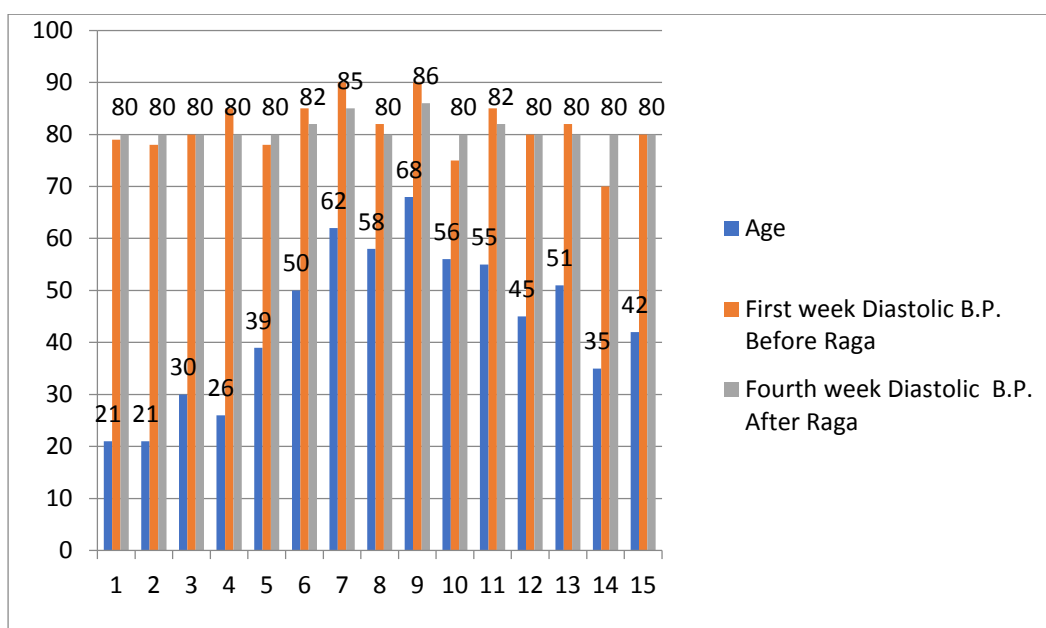


Fig.-2: Graph of Diastolic Blood Pressure (BP) of first week and fourth week of group under experiment

Result:

The complete study of the group under experiment has been represented in table-1 to table-2. It has been seen that majority of participant within age group 50 plus. The Blood pressure (BP) before and after classical raga Ahir Bhairav are in experimental group. In table First to fourth weekly changes in Blood Pressure (BP) should be recorded. It should be observed that the overall Blood pressure (BP) of hyper tension participant should be stable within expected range.

Conclusion:

Present study was only of 28 days (Fourth week). No much measures were taken to prevent monetary. Thus music has positive impact on the B.P. It may be expected that special and systematically designed music therapy intervention by altering the vigil tone may beneficially affect cardiovascular and respiratory regulation (Brandes et. al. 2008) [11], there by promoting healthy living. The finding of present study may be considered significant since it indicated that listening raga Ahir Bhairavi of Hindustani classical music may acts as a preventive measure to restrain the rise of Blood pressure (BP) in symptomatic subjects.

References:

1. Music and sound in healing art, John Beaulieu, Station Hill Press, Barry town, NY.
2. API: Textbook of medicine, 4th edition 1986, pp460.
3. Schoen, Max. The Psychology of Music: A Survey for Teacher and Musician. New York: The Ronald Press Company, 1940.
4. Bruscia K., Defining music therapy. Spring City, PA; Spring House Books, (1989).

5. Maranto, C.D., Application of music in medicine in M. Heal, T. Wigram (eds) Music therapy in health and education. London; Jessica Kinsley publications, 1993B.
6. Stanley, J.M., The role of music in pacification/stimulation of premature infants with low birth weight. Music therapy perspectives, 9, pp19-25.
7. Zimny. G.H. and Whitefeller, E.W., The effect of music on GSR and Heart rate. American Journal of psychology, 1963, 73, pp311-314.
8. Landrenth J. E. and Landrenth H.F., Effect of music on physiological response. Journal research in music education, 1974, 22, pp4-12.
9. http://quadrillo.tripod.com/e_manual.html
10. http://www.misha-artist.de/en/artists_roster/orchestra/the-national-philharmonic.
11. Brandes V., Thayer J.F, Columbus O.H, Joachim, Fischer: effect of respective music therapy on heart rate variability in hypertensive patents psychomatic medicine, 2008, 70 (3) A-18-19.

Role of Heavy Metal Oxide on Vanadium Doped Lithium Borate based Quaternary Glasses

By

Dr. B. Kalyani,

Assistant Professor, Department of Physics,
University College for Women, Koti, Hyderabad.

Abstract

Electron paramagnetic resonance studies of the $x\text{PbO}-(30-x)\text{Li}_2\text{O}-10\text{AS}_2\text{O}_3-58\text{B}_2\text{O}_3$ (where $x=5, 10, 15, 20$ and 25 mol %) containing 2 mol% V_2O_5 as the paramagnetic probe were carried out at room temperature. These glasses were prepared using conventional melt quenching. The amorphous nature of the prepared glass samples was confirmed by x-ray diffraction studies. The EPR spectra were recorded at X-band frequencies with 100 kHz frequency modulation at room temperature. The spin-Hamiltonian parameters (SHP) of VO^{2+} ions, dipolar hyperfine parameter (P) and Fermi contact interaction parameter (K), molecular orbital coefficients (α^2 and γ^2), the number of spins participating in the resonance (N), and susceptibility (χ) have been evaluated. From the spin-Hamiltonian parameters it was observed that $g_{\parallel} < g_{\perp} < g_e$ ($g_e=2.0023$) and $A_{\parallel} > A_{\perp}$. From these results it was concluded that the vanadyl ions exist as VO^{2+} ions in octahedral coordination with tetragonal compression with C_{4v} symmetry and the ground state is d_{xy} . Tetragonality ($\Delta g_{\parallel}/\Delta g_{\perp}$) of V^{4+} ion sites exhibited nonlinear variation with glass composition in all the glasses studied. This nonlinear variation might be due to changes in the ligand field at the site of V^{4+} ion, indicating variation in octahedral symmetry. It is observed that the SHPs depend slightly on the relative concentration of PbO.

Introduction

Electron paramagnetic resonance (EPR) spectroscopy of transition metal (TM) ions in glasses is an attractive and one of the most widely used research subject and affords a method to investigate glass structure. It provides information concerning the valence state of TM ions, local environment and the nature of interactions between them. The transition metal ions can be used to probe the glass structure because their outer d-electron orbital functions have rather broad radial distributions and their responses to surrounding cations are very sensitive [1]. Vanadyl ion (VO^{2+}) has been used as a spectroscopic probe for characterization of glasses because their EPR spectra are rich in hyperfine structure due to ^{51}V nucleus and is easily observable at room temperature [2,3]. Thus, the doping of vanadium into glass introduces vanadyl

ion (VO^{2+}) causing change in the local structure of glasses. The bond length between vanadium and the vanadyl oxygen is very small as compared with its bond length with other ligands. Vanadyl ion in glass matrix generally acquires threefold or fourfold symmetry.[4-6]. Alkali borate glasses are well known due to their high transparency, low melting point and high thermal stability. B_2O_3 is established as glass forming oxide whereas PbO is a glass former or modifier. The addition of PbO to alkali borate glasses improves the optical quality with a tendency to devitrify during cooling because of their strong ionic bonding. Alkali lead borate glasses are familiar due to their infrared transmission and this glass network offers a highly suitable environment for hosting TM ions. Lithium vanadate glasses have successfully been used as cathode active materials in lithium ions batteries. Glasses containing heavy metal oxides (HMO) are of interest due to their wide range of applications in the area of glass ceramics. Borate glasses containing unconventional PbO as network former possess high refractive index, high optical basicity, extended far IR transmission [7-11]. The large polarizability and small field strength of Bi_2O_3 in oxide glasses make them suitable for optical devices such as ultra fast all-optical switches, optical isolators, optical Kerr shutter (OKS) and environmental guidelines. The addition of PbO to the traditional glass former (i.e. B_2O_3) improves the chemical durability and thermal stability of the glasses [12,13]. B_2O_3 is one of the most common glass formers. According to Krogh-Moe [14] the structure of vitreous B_2O_3 consists of a random network of boroxol rings and BO_3 triangles connected by B-O-B linkages. Mozzi and Warren [15] found that the addition of other oxides such as PbO causes a progressive change of the boron atom coordination from 3 to 4 and results in the formation of various units like diborate, triborate, or tetraborate groups.

Experimental

Glass samples with composition $58\text{B}_2\text{O}_3-10\text{As}_2\text{O}_3-x\text{PbO}-(30-x)\text{Li}_2\text{O}-2\text{V}_2\text{O}_5$ ($x=5,10,15,20,25$) has been prepared by melt quenching method using appropriate amounts of reagent grade $\text{Li}_2\text{CO}_3, \text{As}_2\text{O}_3, \text{H}_3\text{BO}_3$ and $\text{PbO}, \text{V}_2\text{O}_5$ were well mixed and melted in porcelain crucibles in the temperature range of $1150-1200^\circ\text{C}$, depending on the glass composition, in an electrical muffle furnace for about 60 minutes. The porcelain crucibles containing glass melt was stirred frequently to ensure the homogeneity. The clear liquid (free of bubbles) was quickly cast in a stainless steel mold kept at 200°C and pressed with another steel disc maintained at the same temperature. Later, the samples were annealed 200°C below their respective glass transition temperature for about 24 hours and slowly cooled to laboratory temperature. The room temperature EPR spectra of present glass samples were recorded using a BRUKER, EPR spectrometer in the range $2200\text{G}-4200\text{G}$ operating in the X-band and employing a field modulation of 100 kHz. DPPH was used as the standard g marker for the determination of the magnetic field.

Results and Discussions:

EPR spectra:

Neutral vanadium has an atomic number (Z) equal to 23 and its electronic configuration is $[\text{Ar}]3d^34s^2$. Vanadium forms V^{4+} ion after losing two electrons each from 4s and 3d leaving a single unpaired electron in 3d shell. V^{4+} exists as VO^{2+} with single unpaired electron bound to oxygen atom by a strong double covalent bond. The natural abundance of ^{51}V isotopes is 99.76% with an electron spin $S = -\frac{1}{2}$ and nuclear spin $I = \frac{7}{2}$. In a vanadium complex containing oxygen, the force of attraction between vanadium ion and oxygen atoms is so high that they become inseparable and form a molecular ion VO^{2+} . Thus, in its tetravalent state vanadium ion (V^{4+}) exists as VO^{2+} ion with single unpaired d electron bound to an oxygen by a strong double bond. The hyperfine structure of VO^{2+} consists of eight lines ($I=\frac{7}{2}, S=\frac{1}{2}$) in agreement with $(2I+1)$ levels. No EPR signals were observed in the un doped glasses (without V_2O_5) confirming that the starting material used in the present investigation were free from the paramagnetic impurities. The EPR spectra of $x\text{PbO}-(30-x)\text{Li}_2\text{O}-10\text{As}_2\text{O}_3-58\text{B}_2\text{O}_3-2\text{V}_2\text{O}_5$ are shown in Fig.1 The spectra are characteristic of hyperfine interaction of a single unpaired electron with the ^{51}V nucleus whose nuclear spin is $I = \frac{7}{2}$. The spectra consisted of two sets of hyperfine lines corresponding to the parallel and perpendicular components and showed a pattern similar to those found for various other borate glasses containing VO^{2+} [25-35].

The EPR spectra were analyzed by using the spin-Hamiltonian[36] given below

$$H = \beta [g_{\parallel} H_z S_z + g_{\perp} (S_x H_x + S_y H_y) + A_{\parallel} I_z S_z + A_{\perp} (I_x S_x + I_y S_y)] \quad (1)$$

where β is the Bohr magneton, g_{\parallel} and g_{\perp} are the parallel and perpendicular principal components of the g tensor, A_{\parallel} and A_{\perp} are the parallel and perpendicular principal components of the hyperfine coupling tensors, H_x , H_y and H_z are the components of the magnetic field, S_x , S_y and S_z and I_x , I_y and I_z are the components of the spin operators of the electron and nucleus, respectively.

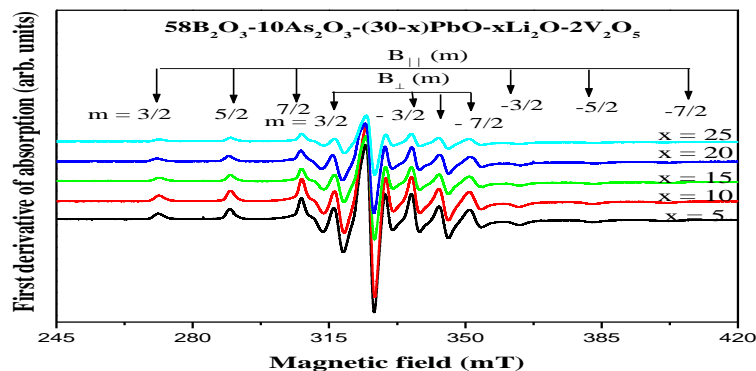


Figure 1. EPR spectra of $x\text{PbO}-(30-x)\text{Li}_2\text{O}-10\text{As}_2\text{O}_3-(58-x)\text{B}_2\text{O}_3-2\text{V}_2\text{O}_5$ glass system (where $x=5, 10, 15, 20$ and 25 mole%)

The solutions of the spin-Hamiltonian, for the parallel and perpendicular orientations are given by the following equations, respectively,

$$H_{\parallel}(m) = H_{\parallel}(O) - mA_{\parallel} - \left\{ \frac{63}{4} - m^2 \right\} \frac{A_{\perp}^2}{2H_{\parallel}(O)} \quad (2)$$

$$H_{\perp}(m) = H_{\perp}(O) - mA_{\perp} - \left\{ \frac{63}{4} - m^2 \right\} \frac{A_{\parallel}^2 + A_{\perp}^2}{2H_{\perp}(O)} \quad (3)$$

The A_{\parallel} and A_{\perp} values were evaluated using the following equations

$$A_{\parallel} = \frac{1}{7} \left[H_{\parallel} \left(-\frac{7}{2} \right) - H_{\parallel} \left(\frac{7}{2} \right) \right] \quad (4)$$

$$A_{\perp} = \frac{1}{7} \left[H_{\perp} \left(-\frac{7}{2} \right) - H_{\perp} \left(\frac{7}{2} \right) \right] \quad (5)$$

where m is the magnetic quantum number of the vanadium nucleus which has values $\pm 7/2, \pm 5/2, \pm 3/2$ and $\pm 1/2$, $H_{\parallel} = h\nu/g_{\parallel}\beta$ and $H_{\perp} = h\nu/g_{\perp}\beta$ where h is Planck's constant, ν is the microwave frequency and β is the Bohr magneton. Measurements for the H_{\parallel} position were taken which correspond to a maximum in the first derivative curve of the parallel hyperfine structure (hfs) component for a given m value, whereas the H_{\perp} position is enclosed between the first derivative perpendicular peak and its 'zero' [37,38].

The spin-Hamiltonian parameters g_{\parallel} , g_{\perp} , A_{\parallel} and A_{\perp} of VO^{2+} ions were determined and are given in Table 1. Since the EPR spectra were not simulated, the values of g_{\perp} and A_{\perp} are approximated values. Hecht & Johnston[39] who studied the EPR and optical spectra of V^{4+} ions in soda-boric glasses observed that the vanadyl existed in the glasses with one of the two possible symmetries, either three-fold or fourfold symmetries. They concluded that the V^{4+} ions in the glasses studied must exist in octahedral coordination with a tetragonal compression. An octahedral site with tetragonal compression would give $g_{\parallel} < g_{\perp} < g_e$ ($g_e = g$ value for a free electron) and $A_{\parallel} > A_{\perp}$. From the values of the spin-Hamiltonian parameters obtained in present investigation, it can be concluded that V^{4+} ions exist as VO^{2+} ions in octahedral coordination with a tetragonal compression with a C_{4v} symmetry and that the ground state is d_{xy} orbital. The values of $\Delta g_{\parallel}/\Delta g_{\perp}$ which measure the tetragonality of the V^{4+} sites, are given in Table 2. It is observed that $\Delta g_{\parallel}/\Delta g_{\perp}$ varies in a nonlinear fashion with Bi_2O_3 content. The variation of $\Delta g_{\parallel}/\Delta g_{\perp}$ with PbO content is shown in Figure 2. The nonlinear variation may be due to changes in the ligand field strength around the V^{4+} ion. The tetragonal distortion in the present glass system at ($x=25$ mol%) is a minimum compared to the other compositions studied.

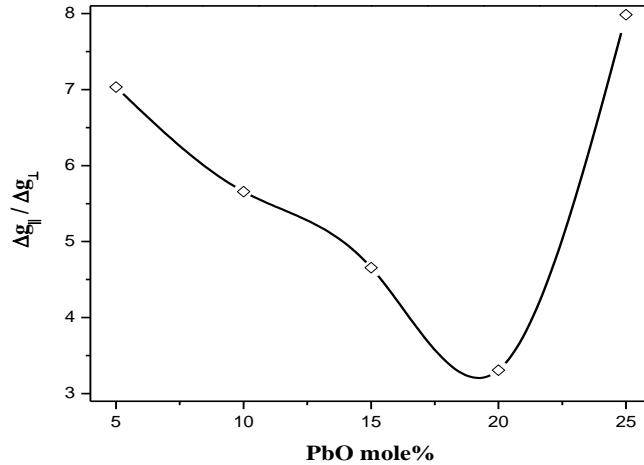


Figure 2. Variation of $\Delta g_{||} / \Delta g_{\perp}$ with PbO content in the present glass system

The $g_{||}$ and g_{\perp} values are related to the bonding parameters by [40]

$$\Delta g_{||} = g_e - g_{||} = \frac{4\lambda\alpha^2\beta'^2 g_e}{\Delta E_2} \quad (6)$$

$$\Delta g_{\perp} = g_e - g_{\perp} = \frac{\lambda\nu^2\beta'^2 g_e}{\Delta E_1} \quad (7)$$

$$A_{||} = -P \left[\beta'^2 \left(\frac{4}{7} + K \right) + \Delta g_{||} + \left(\frac{3}{7} \right) \Delta g_{\perp} \right] \quad (8)$$

$$A_{\perp} = P \left[\beta'^2 \left(\frac{2}{7} - K \right) - \left(\frac{11}{14} \right) \Delta g_{\perp} \right] \quad (9)$$

Where ΔE_1 and ΔE_2 represent the energies of transitions (${}^2B_{2g} \rightarrow {}^2E_g$) and (${}^2B_{2g} \rightarrow {}^2B_{1g}$) respectively. β'^2 is a measure of the out-of-plane π -bonding with equatorial ligands and is assumed to be equal to 1 [30] λ is the spin-orbit coupling constant and is equal to 249 cm^{-1} . The values of $(1-\alpha^2)$ and $(1-\gamma^2)$ represent the covalency rates. $(1-\alpha^2)$ indicates the influence of the σ -bonding with the equatorial ligands while $(1-\gamma^2)$ gives the indication of the π -bonding between the V^{4+} ion and the vanadyl oxygen. Since no optical absorption peaks were observed in the present glass system, the covalency rates $(1-\alpha^2)$ and $(1-\gamma^2)$ were calculated using Equations (4) and (5) by taking the values of $\Delta E_1 = 12500 \text{ cm}^{-1}$ and $\Delta E_2 = 16000 \text{ cm}^{-1}$ and are given in Table 2.

The values of the covalency rates indicate moderate covalency for the σ - and π -bonds. These values indicate only trends in the variation of magnitude of molecular orbital parameters. From the spin-Hamiltonian values the dipolar hyperfine coupling parameter P and the Fermi interaction parameter K were evaluated using [41] The term $-PK$ in Eqs.(8) and (9) is due to the s -character of the magnetic spin of the vanadium. This s -

character arises due to partial unpairing or polarization of the s-electrons because of an interaction with the unpaired d electrons [41]. The effect of polarization on the hyperfine coupling was determined by Heine [41] and is included as $-PK$ term in the expression for hyperfine coupling, K is found to be positive [42, 38].

$$A_{\parallel} = -P \left[\beta'^2 \left(\frac{4}{7} \right) + \Delta g_{\parallel} + \left(\frac{3}{7} \right) \Delta g_{\perp} \right] - p\beta'^2 K \quad (10)$$

$$= A_{\parallel}' - P\beta'^2 K$$

$$A_{\perp} = P \left[\beta'^2 \left(\frac{2}{7} \right) - \left(\frac{11}{14} \right) \Delta g_{\perp} \right] - P\beta'^2 K \quad (11)$$

$$= A_{\perp}' - P\beta'^2 K$$

The values of β'^2 is taken as unity. Using Equations (10) and (11) the values of P and K were evaluated and are given in Table 2.

In the present glass system a large value of K at $x=10$ mole %, compared to other glasses indicate a large contribution to the hyperfine constant by the unpaired s- electrons. This high value suggests an increase in the tetragonal nature of the $V^{+4}O_6$ complex because of strongly bonded oxygen atom at V^{+4} ion in the site opposite to the vanadyl oxygen atom [38]. For the same system, low value of P indicates that the $3d_{xy}$ orbit of unpaired electron in vanadium expands and so its interaction with the nucleus decreases [38].

However low value of $\Delta g_{\parallel}/\Delta g_{\perp}$ values suggest the less tetragonal distortion around vanadyl ion for the composition at $x=25$ mole % it is in accordance with the given optical basicity values in table 2.

The hyperfine components A_{\parallel} and A_{\perp} consist of the contributions from A_{\parallel}' and A_{\perp}' of the $3d_{xy}$ electron to the hyperfine structure and PK term arises due to the anomalous contribution of the s-electrons. The equations can be rewritten as [17].

The values of A_{\parallel}' and A_{\perp}' were calculated using Equations (10) and (11) and are given in Table. The decrease of the anisotropic contribution (i.e. $|A_{\parallel}'|$ and $|A_{\perp}'|$) of the $3d_{xy}$ electron to the hyperfine splitting is brought about by increasing [38, 17] screening of the $3d_{xy}$ orbital from its nucleus through overlap of the electron orbits of the surrounding oxygen ligands. This screening

produces an expansion of the $3d_{xy}$ orbital, resulting in a decreased interaction between these magnetic electrons with the vanadium nucleus.

For the present glass samples at $x=15$ mole % $|A_{||}|'=63.48$ and $|A_{\perp}|'=43.97$ low values compared to all glass samples. This is also supported by low value of $P=120$ and high value of $K (=0.969)$ suggests the site symmetry around vanadium ion is octahedral coordination with a tetragonal compression with a C_{4v} symmetry.

The theoretical optical basicity (Λ_{th}) serves, in the first approximation, as a measure [44] of the ability of oxygen to donate a negative charge in the glass. In other words, the optical basicity reflects the Lewis basicity of the oxide glasses. As the ability of the equatorial ligands to donate the electron (i.e. Lewis basicity) decreases, σ -bondings between V^{4+} and the ligands reduce [45,46]. This reduction, in turn, increases the positive charge on V^{4+} and increases the π -bonding between V^{4+} and vanadyl oxygen. This increase decreases the bond length of V^{4+} -vanadyl oxygen. Consequently, the tetragonal nature of the $V^{4+}O_6$ complex is enhanced. Calculated values of Λ_{th} is included in Tables 2. Value of Λ_{th} decreases with increase in the mol% of PbO. This behavior suggests that the tetragonal nature of the $V^{4+}O_6$ complex should decrease with increase in the concentration of PbO in the glass systems under study. Therefore, in PbO-Li₂O-As₂O₃-B₂O₃ glasses the experimental findings are in accordance with the variation in Λ_{th} ; whereas in case of PbO-As₂O₃-Li₂O-B₂O₃ glasses the SHP are independent of Λ_{th} . $(1-\alpha^2)$ gives an indication of the effect of σ bonding among the vanadium atom and the equatorial ligands, while $(1-\gamma^2)$ indicates the effect of the π bonding with the vanadyl oxygen. In this system these two bonding's are moderately covalent in nature.

Conclusions:

- In all the glass systems studied the vanadium V^{4+} ions exist as VO^{2+} vanadyl ions in octahedral coordination with tetragonal compression and belong to C_{4v} symmetry, with d_{xy} ground state.
- The values of $\Delta g_{||}/\Delta g_{\perp}$ that measure the tetragonality of the V^{4+} sites vary in a nonlinear manner with the glass composition. This nonlinear variation indicates that the variation in tetragonal distortion of the $V^{4+}-O_6$ complex is nonlinear.

- For the glass system 58B₂O₃-10As₂O₃-15PbO-5Li₂O-2V₂O₅ the $\Delta g_{\parallel}/\Delta g_{\perp}$ value is lower compared to other glasses, indicating less tetragonal distortion. The octahedral symmetry is improved in this composition, In remaining complexes moderate tetragonal distortion was observed. For x=20 mol%,
- Octahedral symmetry is reduced at V⁺⁴ion and the tetragonality of the V⁺⁴-O₆ complex increases.
- The covalency rates (1- α^2) and (1- γ^2) indicated moderate covalency for the σ and π bonds in all the complexes.
- The high $\Delta g_{\parallel}/\Delta g_{\perp}$ values for the present glass system suggest the vanadyl ions in the glass are more tetragonally distorted.

Table 1. Spin-Hamiltonian parameters of VO²⁺ion in xPbO-(30-x)Li₂O-10As₂O₃-58B₂O₃-2V₂O₅ glass system

GLASS SYSTEM	g_{\parallel}	g_{\perp}	Δg_{\parallel}	Δg_{\perp}	A_{\parallel} $\times 10^{-4}$ cm^{-1}	A_{\perp} $\times 10^{-4}$ cm^{-1}	$ A_{\parallel} '$ $\times 10^{-4}$ cm^{-1}	$ A_{\perp} '$ $\times 10^{-4}$ cm^{-1}
5PbO-25Li ₂ O- 10As ₂ O ₃ -58B ₂ O ₃ - 2V ₂ O ₅	1.958	1.996	0.0443	6.3×10 ⁻³	184	71	66.34	47.14
10PbO-20Li ₂ O- 10As ₂ O ₃ -58B ₂ O ₃ - 2V ₂ O ₅	1.961	1.995	0.0413	7.3×10 ⁻³	185	72	67.91	46.45
15PbO-15Li ₂ O- 10As ₂ O ₃ -58B ₂ O ₃ - 2V ₂ O ₅	1.959	1.993	0.0433	9.3×10 ⁻³	186	79	63.48	43.97
20PbO-10Li ₂ O- 10As ₂ O ₃ -58B ₂ O ₃ - 2V ₂ O ₅	1.972	1.993	0.0303	9.3×10 ⁻³	188	73	70.32	44.37
25PbO-5Li ₂ O- 10As ₂ O ₃ -58B ₂ O ₃ - 2V ₂ O ₅	1.952	1.996	0.0503	6.3×10 ⁻³	196	74	70.72	51.66

Table 2. Tetragonality and covalency rates of VO²⁺ ions in the xPbO-(30-x)Li₂O-10As₂O₃-58B₂O₃-2V₂O₅ glass system

Glass system	$\Delta g_{ }/\Delta g_{\perp}$	$1 - \alpha^2$	$1 - \gamma^2$	K	P	Λ_{th}
5PbO-25Li ₂ O-10As ₂ O ₃ -58B ₂ O ₃ -2V ₂ O ₅	7.032	0.645	0.842	0.937	126	0.640
10PbO-20Li ₂ O-10As ₂ O ₃ -58B ₂ O ₃ -2V ₂ O ₅	5.657	0.669	0.817	0.929	127	0.631
15PbO-15Li ₂ O-10As ₂ O ₃ -58B ₂ O ₃ -2V ₂ O ₅	4.656	0.653	0.767	0.969	120	0.629
20PbO-20Li ₂ O-10As ₂ O ₃ -58B ₂ O ₃ -2V ₂ O ₅	23.308	0.757	0.767	0.914	129	0.626
25PbO-5Li ₂ O-10As ₂ O ₃ -58B ₂ O ₃ -2V ₂ O ₅	7.984	0.596	0.842	0.928	135	0.624

References

1. J. Wong, C.A. Angell, Glass Structure by Spectroscopy, Marcell Dekker Inc., New York, 1976.
2. A. Agarwal, V.P. Seth, P.S. Gahlot, S. Khasa, P. Chand, J. Phys. Chem. Solids 64 (2003) 2281–2288.
3. H. Toyuki, S. Akagi, Phys. Chem. Glasses 15 (1974) 1–5.
4. Moulton, P.F. Spectroscopic and Laser Characteristics of Ti: Al₂O₃. *J. Opt. Soc. Am. B* 1986, 3, 125.
5. Aronne, A.; Depero, L.E.; Sigaev, V.N.; Pernice, P.; Bontempi, E.; Akimova, O.V.; Fanelli, E. Structure and Crystallization of Potassium Titanium Phosphate Glasses Containing B₂O₃ and SiO₂. *J. Non. Cryst. Solids* 2003, 324, 208–219. Page 17 of 33
6. Osipov, A.A.; Korinevskaya, G.G.; Osipova, L.M.; Muftakhov, V.A. Titanium Coordination in TiO₂-Na₂O-SiO₂ Glasses of xTiO₂ · (100 - x) [2Na₂O · 3SiO₂] (0 ≤ x ≤ 30) Composition Based on Raman Spectroscopy. *Glass Phys. Chem.* 2012, 38, 357–360.
7. V. Dimitrov, Y. Dimitriev, A. Montenero, J. Non-Cryst. Solids 180 (1994) 51.
8. J.C. Lapp, W.H. Dumbaugh, M.L. Powley, Riv. Staz. Sper. Vetro 1 (1989) 91
9. D.W. Hall, M.A. Newhouse, N.F. Borrelli, W.H. Dumbaugh, L.A. Weidman, Phys. Lett. 54 (1989) 1293.
10. B.V.R. Chowdari, Zhou Rong, Solid State Ionics 90 (1996) 151.

11. W.H. Dumbaugh, *Phys. Chem. Glasses* 27 (3) (1986) 119.
12. A. Agarwal, V.P. Seth, P.S. Gahlot, S. Khasa, P. Chand, *J. Phys. Chem. Solids* 64 (2003) 2281-2288.
13. M.H. Shaaban, A.A. Ali, *J. Electron. Mater.* 43 (2014) 4023-4032.
14. J. Krogh-Moe, *Phys. Chem. Glasses* 3 (1962) 101.
15. R.L. Mozzi, B.E. Waren, *J. Appl. Crystallogr.* 3 (1970) 251.
16. J. Ballhausen, H.B. Gray, *Inorg. Chem.* 1 (1962) 111.
17. A.K. Bandopadhyay, *J. Mater. Sci.* 16 (1981) 189.
18. J.A. Duffy, M.D. Ingram, *J. Inorg. Nucl. Chem.* 37 (1975)
19. R. Muncaster, S. Parke, *J. Non-Cryst. Solids* 24 (1977) 399.
20. Shaik Kareem Ahmmad, M.A. Samee, A. Edukondalu and Syed Rahman, *Results in Physics*,175–181 (2012)
21. A. Edukondalu, B. Kavitha, M. A. Samee, Shaik Kareem Ahmmad, Syed Rahman, K. Siva Kumar, *J. Alloys Compd.*552, 157-165 (2013).
22. Avula Edukondalu, T. Sripathi, ShaikKareem Ahmmad, S Rahman and K. Sivakumar, *J. Elect. Mater.* 46(2)808 –816 (2017).
23. M. A. Samee, Shaikh Kareem Ahmmad, A. Edukondalu and Syed Rahman, *J. Elect. Mater.* 42, 2516 (2013).
24. A. Edukondalu, Syed Rahman, V. Sathe, and K. Siva Kumar *Physica B: Condensed Matter.*438, 120-126 (2014).
25. S.Khasa, V.P.Seth, S.K.Gupta and R.Murali Krishna, *Phys.Chem.Glasses* 40(5) (1999) 269.
26. Neena Chopra, Abhai Man Singh and Pawan Mathur, *J.Non- Cryst.Solids* 146 (1992) 261.
27. I.Chand, V.P.Seth, D.Prakash and S.K.Gupta, *Phys.Chem.Glasses*, 40(3) (1999) 153.
28. Md.Shareefuddin, Md.Jamal, K.Vanaja, Ambuja Iyengar and M.Narasimha Chary, *J.Mat.Sci.Letts.* 14 (1995) 646.
29. [29]. B.Sreedhar, P.Indira, A.K.Bhatnagar and K.Kojima, *J.Non-Cryst.Solids* 167 (1994) 106.
30. [30]. V.P.Seth, S.Gupta, A.Jindal and S.K.Gupta, *J.Non-Cryst. Solids* 162 (1993) 263.
31. [31]. D.Suresh Babu, M.V.Ramana, S.G.Satyanarayan and G.S.Sastry, *Phys. and Chem. of Glasses*, 31(2) (1990) 80.

32. M.V.Ramana, K.Siva Kumar, Syed Rahman, D.Suresh Babu, S.G.Satyanarayan and G.S.Sastry, *J.Mat.Sci.Letts*, 8 (1989) 1221.
33. B.Sreedhar, J.L.Rao and S.V.J.Lakshman, *J.Non-Cryst.Solids* 116 (1990) 111.
34. Md.Shareefuddin, Md.Jamal, G.Rama Devudu, M.L.Rao, M.Narasimha Chary, *J.Non-Cryst.Solids* 255 (1999) 228.
35. Abragam, A. & Bleaney, B. *Electron Paramagnetic Resonance of Transition ions*, Clarendon Press, Oxford, 1970, 175.
36. Seema Gupta, N.Khanijo and A.Mansingh, *J.Non-Cryst.Solids* 181(1995) 58.
37. H.G. Hecht, T.S. Johnston, *J. Chem. Phys.* 46 (1967) 23.
38. Effect of Bi₂O₃ on EPR, optical transmission and DC conductivity of vanadyl doped alkali bismuth borate glasses A.Agarwal, V.P. Seth, P.S. Gahlota, S. Khasa, P. Chand *Journal of Physics and Chemistry of Solids* 64 (2003) 2281–2288
39. Hecht, H. G. & Johnston, T. S. *J. Chem. Phys.*, 1967, 46, 23.
40. Kivelson, D. & Lee, S. K. *J. Chem. Phys.*, 1964, 41, 1896.
41. V. Heine, *Phys. Rev.* 107 (1957) 1002
42. B.R. Mcgarvey, in: R.L. Carlin (Ed.), *Transition Metal Chemistry*, vol. 3, Dekker, NY, (1966) p. 115.
43. Weil, J. A., Bolton, J. R. & Wertz J. E. *Electron Paramagnetic Resonance Elementary Theory and Practical Applications*, John Wiley, New York, 1994, 498.
44. A. Klonkowski, *Phys. Chem. Glasses* 26 (1985) 11.
45. H. Hosono, H. Kawazoe, T. Kanazawa, *J. Non-cryst. Solids* 26 (1979) 125.
46. Role of PbO in EPR, optical properties and DC conductivity of vanadyl-doped alkali lead borate glasses P.S. Gahlota, V.P. SETHA, A. Agarwal, S. Sanghib, P. Chand, D.R. Goyal, *physica B* 355(2005)44-53.

Nanoparticles and Their Applications in Agriculture: A Review

Quadri F B¹ Naseem Deshpande² Sangeeta Shinde³

¹Dr. Rafiq Zakaria College for Women, Aurangabad

²Abeda Inamdar Senior College of Arts, Science and Commerce, Pune

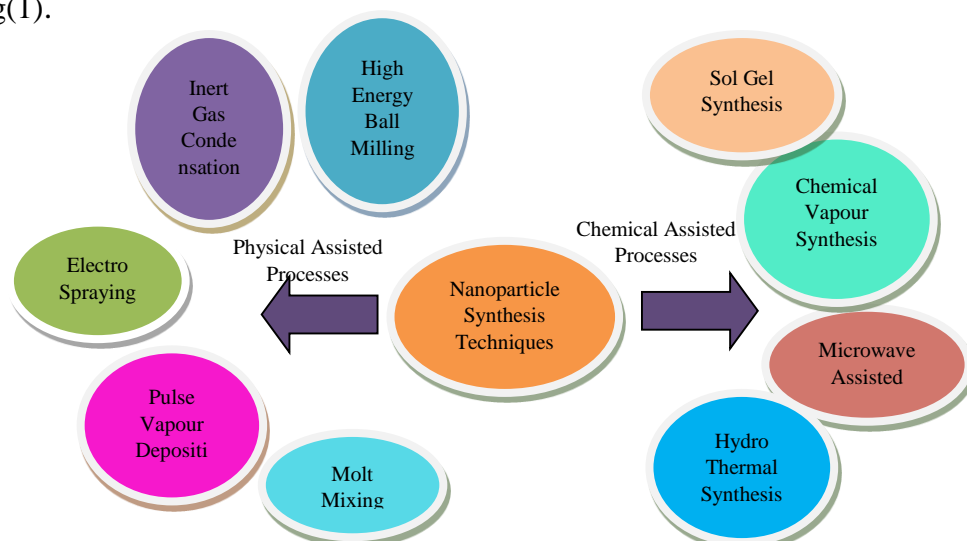
³Pratishthan Mahavidyalaya Paithan, Auragabad

Abstract: Reduced size of ENPs has advanced physical and chemical properties which make them an edge above their counterpart bulk materials. These particles find applicability in every walk of life right from the ancient activity of agriculture to advanced fields like IOT (Internet of Things) and space explorations. Present paper summarizes different types of NPs and reviews the various aspects of agriculture that uses NPs to combat the challenges to changing environmental conditions while keeping the pace of yield with the increasing population. NPs, in a way are also proving helpful in minimizing the concentration of pollutant thereby preventing the contamination of the soil and maintaining its fertility. Lastly, on field application has yet to be monitored with NPs, supplemented by the formulation of guidelines for the assessment of the risk factors for the betterment of mankind and the environment.

I. Introduction: Owing to the unique features and properties, engineered nanoparticles (ENP) have attracted the research community all over the world. Innovative and advanced techniques have been developed to make commercial use of them for the benefit, comfort and luxurious life of the mankind. Rapid development and wide applications of nanotechnology brought about a significant increment on the number of engineered nanoparticles (ENs) inevitably entering our living system. Globally, industries are in the production and commercialization of ENP so as to develop sophisticated and smart devices that can be encashed. ENPs have been incorporated in almost every field of life because of their advanced characteristics as compared to their bulk counterparts. Nanoparticles of different shapes and sizes can be engineered and fabricated according to the need and make them applicable thereby revolutionizing many aspects of our lives. Even in ancient period nanomaterials were used in sculptures and architecture for their beauty and enhanced features. This is very much apparent from the architectural work of that era. The study of nanomaterials gained momentum only after the discovery of higher resolving power instruments like atomic force microscope (AFM) and Scanning Tunneling Microscope (STM).

At nanoscale, quantum effects are apparent and they play a vital role in defining the parameters of the materials. At nanoscale, it becomes easier to control and manipulate the formation and movement of atoms and molecules and mould them as per our requirement. With such structures the ENPs exhibit advanced physiochemical properties as compared their bulk counterparts. ENPs show greater chemical reactivity, higher tensile strength, more sensitive to light spectrum, quantum confinement, higher surface to volume ratio, etc. Production techniques vary from very simple to complex materials in the form of granular particles, thin films, nanotubes, etc. Nanoparticles has been used in various commodities in the past decades but, recent merger of various branches of science have revolutionized the production methods and, multiplied their applications in the sectors like drug delivery, space missions, agricultural and food industry, cosmetic, textile, sustainable energy, green environment, etc. to name a few. The NPs can be used in sensing [1 2], chemical and biological sensing [3], for drug delivery [4], and other various applications [5]. Desalination is yet another field where nanoparticles find their application [6]. Thus nanotechnology has a wide impact on the life style of the society and has also contributed a large towards the economy of the nation.

Nanoparticles of diverse materials like ceramics, polymers, semiconductors, etc in solid, liquid or sol-gel form are synthesized. These materials exhibit unique structural, physical, chemical and morphological properties that make them applicable in domestics as well as commercial fields like electronics, food and preservatives, biomedical, green environment, clean energy production, catalysis, imaging, space missions, etc. Their optical properties are dependent on their size making them useful in different sensors. Various physical and chemical assisted methods are adopted for the synthesis of nano materials of different size and structure as shown in fig(1).



1.1 Different methods of nanoparticles Synthesis

The preparation of nanomaterial basically involves a direct and synthetic process that gives particles in the nanosize range, this is followed by the physical assisted processes like grinding or milling, high pressure homogenization, and sonication to reduce its size [7].

Physical and chemical methods for Metal oxide NP synthesis have many disadvantages like, it requires many expensive instruments along with high heat generation, high energy consumption and also the yield of the final product is low [8 &9]. The chemicals that are used remain in the surroundings for longer periods and pose danger for the environment [9, 10]. Hence, the current aim of the researchers is the green synthesis of metaloxide NPs from biological means such as microorganisms, plants, microbial enzymes, polysaccharides and degradable polymers [11]. A safer, energy efficient and minimal wastage production technique called Green nanotechnology is adopted for the synthesis of NPs that has less emission of harmful gases. This technique uses renewable raw materials and has low impact on the environment[12-14]. Green synthesis methods are advantageous over traditional physical and chemical methods as they are simple, free of toxic chemicals, cost-effective and, has therefore gained considerable importance in recent years [10].

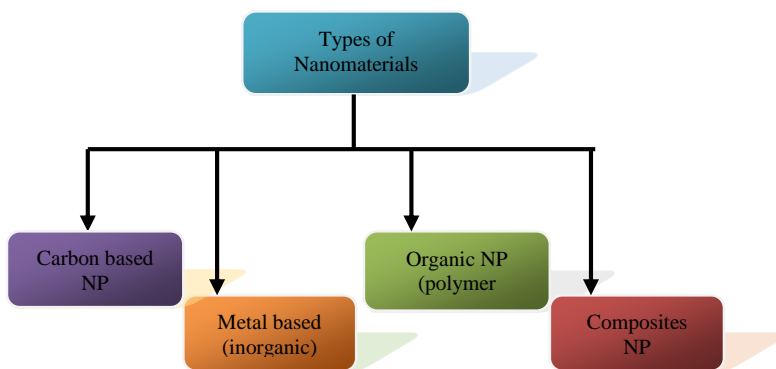
Bionanoparticles are synthesized by micro organisms assisted biogenetic techniques and template techniques. Physiological factors along with microbial source, reaction temperature, pH, pressure, proportion of the metal within the salt and incubation time affect the synthesis of various metaloxide NPs. NPs of definite shape, size and composition is achieved by biosynthesis techniques[8,15&16]. [43] Using green chemistry techniques, Shebl et al produced zinc, manganese and iron nanooxide, with the help of a microwave-assisted hydrothermal method. The nanoparticles were with an average size of 20-60 nanometers Eco-friendly and inexpensive synthesis of various metal oxide NPs with metals like nickel, silver, gold, copper, zinc and palladium is achieved by the use of different microorganisms. In this process, the required metal ion is captured from the environment and is treated enzymatically converting it into elemental form, following a reduction mechanism.

Some of the materials show existence of natural CNTs as well as fullerenes [17,18]. The compound mixture of coal-petroleum showed presence of CTNs [17]. Researchers used hot lava containing metal oxides as substrate and catalyst for synthesis of single walled CNTs and, with the positive results doubted the formation of carbon nanotubes at such high temperature as that of volcanic eruptions [19 20]. Fullerenes, the other carbon based NP were

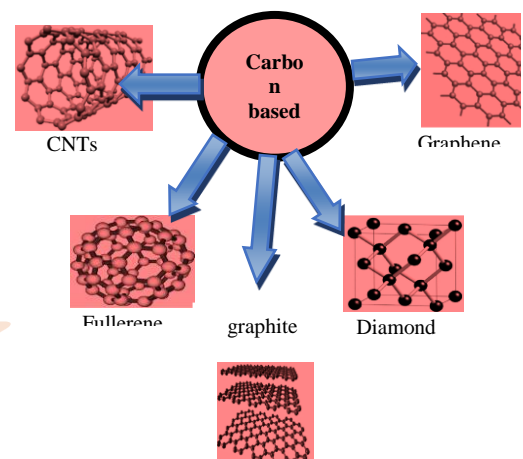
see in some geological rock and meteorite samples of cosmos[21-25]. Fullerenes like spherical structured pollen grains were reported in the Chinese hibiscus flowers. These pollen grains possess the properties that make them highly adaptable for pollination[26].

II. Classification of Nanoparticles:

Nanoparticles are categorized into different types, depending on their shapes, sizes, morphology and physiochemical properties as shown in fig(2).



Fig(2)Types of Nanoparticles



Fig(3)Carbon based NP

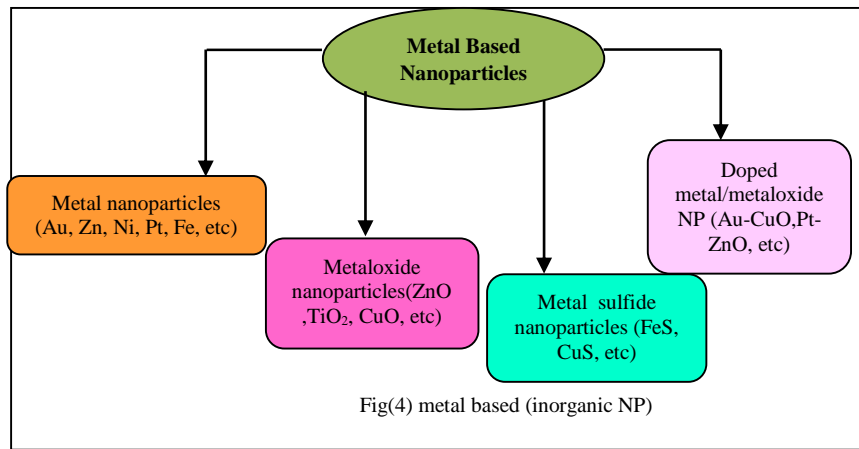
1. Carbon based NP

Carbon based nanoparticles are diamonds, carbon nanotubes, fullerene, graphene and graphite, shown in fig(3) that are engineered for fabrication in different products to have a final commodity with advanced features. Depending on their shape, CNT are of three types i.e. armchair CNTs, zigzag CNTs and chiral CNTs and, depending on the number of layers they are single walled (SWCNT) and multi walled (MWCNT). For synthesis of such CNT catalyst is required more often. Scanning electron microscopy (SEM) is used to observe the interaction of carbon nano tubes on the surface and within the plant cell. It provides vital information about the internal mechanism, transportation of the nutrients and other developments that are taking place within the plant tissue that help in its development and growth[27, 28].

2. Inorganic (Metal Based) NP

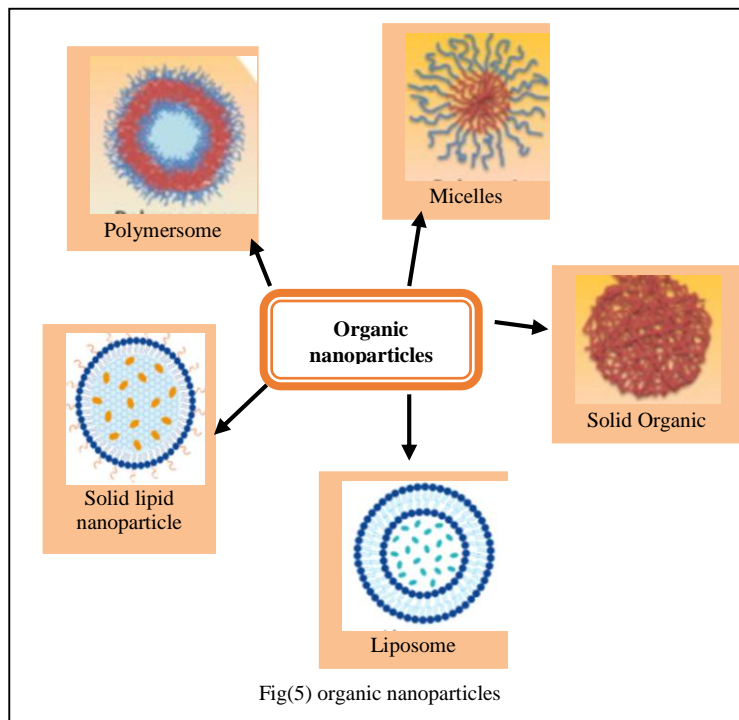
These class of nanoparticles are made up of metal, metal oxides, metal sulfides and doped metal and metal oxides, fig.(4). Some of their examples are quantum dots, polystyrene, ceramics, magnetic, etc. Their central core is madeup of inorganic matter that gives them

the unique electrical, magnetic, optical and thermal properties. They find wide applications in food, cosmetics and drug related industries.



3. Organic (Polymer based) NP

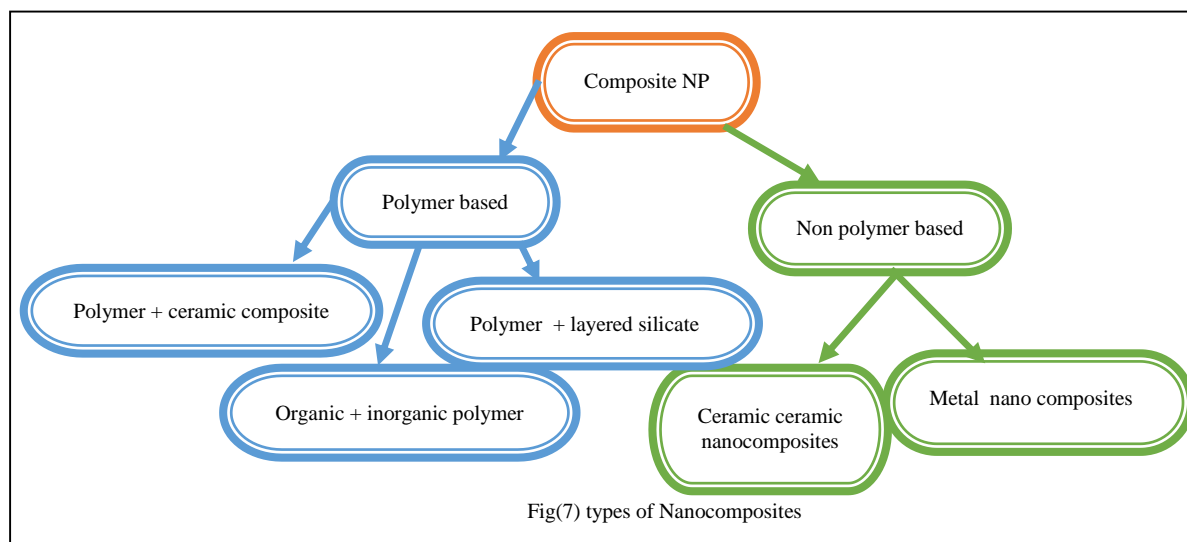
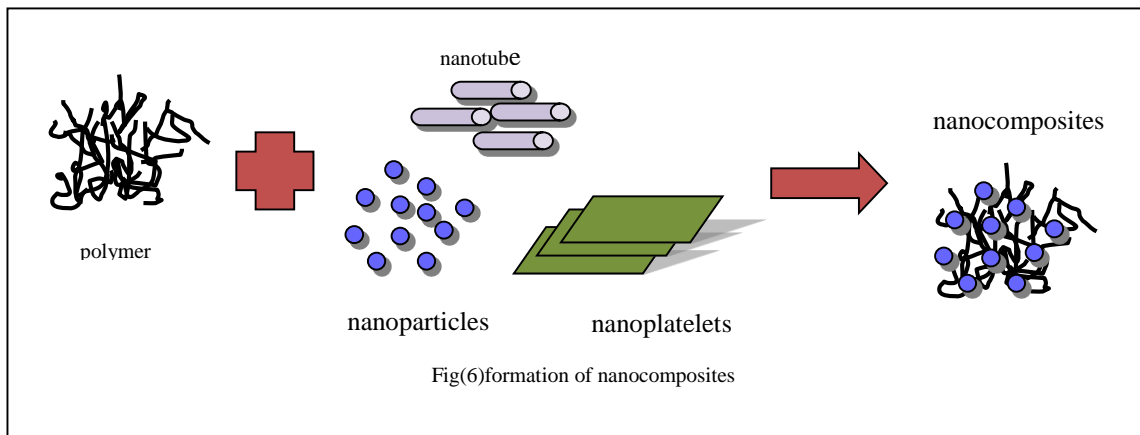
They are made up of organic materials excluding carbon atoms and find their application in drug delivery and biosensors. Some of their examples are dendrimers, cyclodextrin, micelles, Ferritin, liposomes, etc. as shown in fig(5).



4. Composite NP

They are the complicated structures like a metal organic framework formed by the combination of metal, metal oxide or carbons based NP as shown in fig(6), and exhibit advanced properties as compared to their constituent NPs. In such composites, one of the constituent material has

dimensions of nanoscale. Polymer based nanocomposites are widely studied because of its film forming ability, activated functionalities, diversified applications and dimensional variability. Different types of nanocomposites are as given in fig(7).



III. Applications in Agriculture

Agriculture is the main occupation of many of the developing countries and their economy rely on the produce of it. Presently, agricultural sector is facing a global crisis due to unfavorable climatic conditions that have brought a drastic change in the factors that are essential for nutritional and healthy farming. Unpredictable rainfalls, contaminated soil due to excessive use of pesticides and fertilizers, polluted water bodies due to the waste dumped from the nearby industries, labor shortage, decreasing concentration of organic matter in soil has contributed to lower the produce of the agricultural field [29]., Urbanization is yet another factor that has reduced the percentage of land available for cultivation, hence With the aim to minimize the ill effect of changing climatic conditions and to increase the yields to meet the demand of increasing population, nanotechnology has been used extensively in the agricultural sector.

Innovative techniques has been adopted to develop novel tools that can be used for the sustainable intensification of the yield and also reduce the expenditure incurred [30 31]. It is a practice of increasing the product of the same agricultural land by using the best practices involving NPs without harming the environment. New age agricultural practices have been transformed into precision agriculture with the use of numerous nanoparticles based pesticides, fertilizers, pesticides, that improves the diseases resistance property, enhance the nutritional value and also increase the yield of the crop.

1. Physiochemical Effects:

Physiochemical properties, size, shape, surface charge of the NP play a prominent role in the uptake and interaction of NP with the plant [32]. Intake of NPs changes the physiology of the plants to an extent. Nanoparticles have the dimensions that are very small in comparisons with the different barriers or openings in the plant structure, that gives them an advantage for easy entry [33]. Difference in the morphological and physiological nature of the plants gives rise to variation in the NPs uptake capability of the plants[34]. Diverse uptake mechanisms are seen in different root and shoot system inside the plant tissue[35].The size of cuticle layer of the epidermis is also an another example for the uptake of the NPs by the plants [36-37]. Interaction of nanosized particles with the cell wall further increases the pore size that facilitates the entry of them within the premises of the cell [38]. NPs have great degree of mobility that helps them in uptake, absorption and trespassing within the plant cell. The surface charge property of NPs shows an impact on the aggregation and surface interaction. The transport of charged NPs from roots as well as shoots, through the cell membrane can be varied by the surface charge modification [39-44] Use of NPs in the form of multiwalled carbon nano tubes (MWCNTs) showed a great impact on the growth of tobacco, soyabean, corn and barely crops [45 46]. Fluorescent nanoparticles (NPs) or quantum dots (QDs) are developed for labeling the plant proteins [47 48]. NP are fruitful in the penetration of the hard coat of the seeds and allow water importation that increases the growth. Seeds are treated specially, before sowing using nanotechnology to increase their sustainability [49]. Research papers have reported that semiconductor SWCNTs show high electrical conductivity and are also able to absorb those solar radiations that are weakly absorbed by the chloroplast of the leaves [50]. Mesoporous silica based NPs enhance the photosynthesis process by interacting with chlorophyll, this affects the metabolism and hence the growth rate of the plant. By diffusion process nanoparticles penetrate through the chloroplast membrane and supply the electrons required for the photosynthesis electron chain hence influencing photosynthesis process[51]. Silica based NPs have greater impact on different functioning of the various parts of the plants [52

53]. Another NP that was studied extensively to see its effect on plant, right from germination of seeds to plant growth promoting processes is TiO₂ NPs [54-56]. Carbon nanotubes along with NPK fertilizers were applied on French bean plant by foliar method to see the impact on its growth and they reported that it improved the growth and yield and antioxidant system of the plant. Foliar application of nanofertilizers has many positive points than soil application.

2. NPs as Abiotic Stress Reliever

Green vegetation is found everywhere, in places where the conditions are favourable for their growth and also at places where climatic conditions are not on their side. Different NPs assist the growth of the plants and also found to be helpful to protect them from abiotic stress conditions. Abiotic stress includes, salinity, alkalinity, temperature fluctuations, drought and mineral and metal toxicity. Owing to their large surface area, toxic metal binds to them and thus reduce their availability. Researchers have shown that NPs of different metal, metaloxide and carbon based are able to reduce or minimize various abiotic stress factors and encipitate in the growth and development of plants even in crop unfriendly landfields. Tafadar et al. showed that foliar application of nano fertilizers can lessen the stress in plants [57]. Dimpka et al noted that draught like stress was mitigated in soyabeans by use of composite nanofertilizer [58]. Nanofertilizers incorporated with microorganisms, called as nanobiofertilizers helps the plants in overcoming the abiotic stress conditions and also prove beneficial in other aspects. Use of biofertilizers in combination with nanosilicon dioxide found to increase the productivity of the crop. In the case of fertilizer delivery, several investigations confirmed that the application of nano-silicon dioxide with biofertilizer was useful to increase the crop yield [59]. Plant hormones assist them in adapting to the conditions of the surroundings and make them sustainable according the climatic situations [60 61]. These hormones are produced intrinsically for better adaptation against adverse situations like drought, temperature fluctuations, incessant rainfalls that hider the development of the plant. These hormones can also be supplemented externally in the form of nanoparticles to for better growth against the odd conditions. Many metal based NPs have found applicable in overcoming abiotic stress factors that act as a hurdle in the development of the plants [62-66].

3. Nanofertilizers:

Plants require macronutrients like N, P, K, S, Ca, Mg as well as micronutrients like B, Fe, Mn, Cu, Zn, Mo, etc. for their proper growth and nourishment. Macronutrients are required in larger proportions and micronutrients, though required in smaller quantity are very much essential like that of macronutrients [67 - 69]. Both nutrients play vital roles in the developmental stages of the plant, stimulate enzyme activation and helpful in building the defensive mechanism

against odd conditions and diseases [70]. Studies suggest that animals and humans depend on plants of their need of nutrients and any discrepancy in it will hamper the growth of the plant and also lessen its nutritional value [71]. Naturally, under favorable conditions plants extract these nutrients from the soil but when the conditions are not favorable the nutrient precipitates and remains unavailable for the plant. Usability of available plant nutrient by the plants is measured by Nutrient use efficiency (NUE). Conventional methods of spraying fertilizers has some drawbacks like overdoses, loss of nutrients by evaporation, time delay in functioning, hence to overcome this soil limiting factors, a new target orientated method called smart delivery systems and nanoencapsulation with greater potential is used. It causes gradual and controlled release of nutrients, increases its efficiency, and prevents the adverse affects of excessive use [72 73]. It reduces nutrient loss and stimulates plant development in agrochemical industry[74]. Composite of FeO_x and MnO_x nanoparticles showed good response to germination and plant development claiming as a potential micro nutrient fertilizer[75]. Abd El-Azeim et al showed that foliar application of macronutrients NPK is more beneficial in terms of production, quality and economy as compared to soil application[76]. Carbon nano particles are mostly applicable in this regard as they increase the plant nutrient availability. They have the ability to penetrate the cell membrane and cell walls, this ability of CNTs make them applicable as nanofertilizers in agro industry[77]. Number of research papers have reported that nano fertilizers are beneficial in every stage of plant development, right from the formation and growth of the seedling to the development of healthy and enhanced seed weight and finally the yield is increased[78 79].

Encapsulation of nanofertilizers by nanomaterials is another technique to provide nutrients to the crops. Depending on the size of the capsule i.e. micro and nanocapsule, different technologies have developed[80]This technique enables the slow and controlled release of nutrients into the soil, thereby increasing the efficiency of the fertilizers and preventing the contamination of the soil and water resources. This method also minimizes the extend of fertilizers used [81-83]. Besides mass production of encapsulated nanofertilizer is highly economical. Encapsulation of potassium nitrate by graphene oxide delays the process of release of the fertilizer[84].

4. Nanopesticides

At the developmental stage, the crop has to be protected against many ill factors like pests, fungus and bacteria. Care should be taken even after the harvesting to protect the final

products from the insect pests and pathogens to increase the life[85].NPs are incorporated with the aim for better plant protection as they increase bioavailability ad decrease the harmful effect on the nanotarget organisms[86]. They can also be used for the degradation of the remnant or slowly degrading harmful pesticides that can enter the food chain and prove fatal. In this way NPs prove to be environmental friendly[87].

Carbon based nanoparticles show good antifungal and antibacterial properties, this character of CNTs, graphene oxide and fullerenes make them highly applicable in this field of agriculture against pathogenic fungi. Although, all of them are equally beneficial in this regard, SWCNTs showed greatest antifungal activity. Graphene oxide exhibits antibacterial property and its peculiar size and structure make it advantageous in combating the bacterial activity in various species[88-92]

Nanoencapsulation process has the benefits of slow and controlled release which makes this technique very much helpful in the agricultural sector. It exhibits much better solubility, stability and specificity as compared to other methods of application[93]. The pesticide is wrapped in a protective cover to avoid premature degradation and preserve its anti-pesticide efficiency for longer duration. This method reduces the excess use of pesticide and gives minimum human exposure to it proving to be environmental friendly [94]. Encapsulation is a non-toxic and promising pesticide delivery systems for increasing global food production while taking care of the negative impacts on the environmental and ecosystem [93 95-97]. Even nanoemulsions of active ingredients are available in the market[98].

Synthesized halloysite or claynanotubes acts as carrier for pesticides for good contact and delayed release thereby reducing the actual cost of the pesticides and its impact on the water bodies [99].

Even metal based NPs like titanium, copper, silica are used as fungicide and pesticides.Silica based pesticides show good results in comparison with their bulk counterpart [100]. Bacterial spot diseases was reduced to a greater extend by using NPs of TiO₂ along with other active ingredients [101]. Lower concentration of Cu based nanopesticide was able to suppress the bacteria growth on pomegranate crop [102]. Numerous metal based NPs exhibit the antibacterial and antifungal property. They manipulate the structure of the cells, destroy the protein and lipid layer surrounding the bacteria and fungi Some metal NPs cause dehydration in pests and finally leads to their death[103].

5. Polymer nanopesticides

In these type of pesticides, a nano polymer of polyesters and polysaccharides encapsulates the active ingredient as a protective case. This covering enhances their dispersion property in aqueous medium, improving their slow and controlled release activity. They are in great demand and are manufactured commercially because of their versatile design and degradability.

6. Nanoemulsions

It is an oil in water emulsion with active ingredient in the form of nano sized droplets with water. Anjali et al reported that the nanoemulsion of neem oil with smaller sized of droplets were readily absorbed by the plants[104]. Similar results were noted by other researchers with different nanoemulsion used on various species of the plants[105 106]. Hence nanoemulsion have an advantage of higher solubility and uptake mechanism in comparison with other methods of application. Slow and controlled release of nanoemulsion is also an indicator for the sustained and prolonged existence of these materials in the soil, a possible factor for soil contamination.

7. Photocatalysis

Transition metal oxide materials exhibit visible light photocatalysis, using this property several nanofoams, nanoporous fibers and nanoparticles are developed for microbial and fungal disinfectants. Such materials, in the tubular form destroys the cell resulting to the death of the microorganisms and also removes organic pollutants[107].

8. Nanoherbicides

Herbs or weeds are the unwanted plants that compete with the crop plant for the nutrients resulting in the declination of its growth. They also affect the fertility of the soil and hinder their development finally decreasing its yield. They are the biggest threat to the economy of the agricultural sector. Removal of them manually is very tedious and time consuming task hence target specific herbicides with minimal damage to the crop, and quality of the soil are required. Many pest management or herbicides have been developed for efficient functioning with minimum exposure to human beings[108]. Nanoherbicides serve the required purpose. They are good at controlling the growth of the weeds and also maintaining the fertility of the soil in ecofriendly manner[109].

9. NP Sensors used in Agriculture

Environmental degradation and accumulation of pollutants in the surroundings is the matter of concern today. Climatic changes, noted all over the world are showing its

adverse effects on the various components of the ecosystem and also on the wellbeing of the society. In the present scenario, wise and admissible use of nanotechnology can prove a boon to the mankind and the environment. Unique features of NPs are employed in each and every field for the betterment of the community.

Nanosensors

Advanced physical and chemical properties of NPs are explored in the fabrication of sensors that are very much helpful in monitoring the crop growth and development. The sensing capacity and performance of the sensors has enhanced by use of nanosensors. With the invention of high precision instruments and development in the transduction technologies, advanced nanosensors that are ruling the agricultural world have been developed. With the rapid development in fabrication industry nanosensors are in great demand owing to their good sensitivity and cost effectiveness. Applications of nanosensors is not limited to a particular field only, they are seen in various areas like health care, electronics, agriculture, food and drink packaging, genome analysis, security, etc. to name a few. Nanosensors work on the principles of transducers i.e they sense the physicochemical changes in the surroundings and convert them into a measurable parameter. The sensing material used in nanosize that is highly sensitive. The physical, chemical and mechanical strength of carbon based NPs make them very much helpful in developing nanosensors. [110]. Various aspects related to the crop development like moisture, water availability, soil fertility, presence of pest, fungus and bacteria, status of macro and micro nutrients in the soil can be sensed with the help of nanosensors. All these help a lot in making optimal use of resources and increase the yield. Water cultivation can be improved with biosensors, so as to conserve it. New technological instruments that can detect the contaminants and pollutants present in the water over the field will be developed in near future [111].

Carbon based NPs find greater space in the nanosensor technology because of their properties like mechanical strength, larger surface area for sensing the molecules, etc. They are highly sensitive hence are useful in numerous agricultural and environmental applications[112]. Wu et al developed a graphene based sensor to detect the presence of cadmium in water to a concentration level of 0.25 -1 $\mu\text{g}/\text{L}$ [113]. In a similar manner, Taher et al. developed a nickel sensor that detects the presence of nickel in food as well as environment [114]. Ammonia gas sensor was developed using CNTs[115]. Pesticide, fungi and micro organism detector were developed by the slight modification of MWCNTs [116, 117]. Remote monitoring of the crop, presence of pest, moisture level can be sensed by nanosensors.

There are number of research papers that shows how carbon based Nanosensors are helpful in checking the overall growth and development of the crop remotely [118-121] .

There are NPs that can detect the contamination of the water and help us in a way to keep the water bodies clean and free from pollutants [122-124].

IV. Conclusions:

ENPs are proving to be very beneficial to the mankind and the society because of their unique physical, mechanical and chemical properties. Advancement in the technology and the merger of different disciplines of science has opened a new frontier in the form of nanotechnology. This field is capturing the market very fast and shaping the economy of a nation. Still, a major challenge with this technology is a matter of concern for the research world. All the advantageous and benefits of ENPs are studied in the laboratory conditions in a controlled manner, very little is known about the behavior and impact NPs in natural or environmental conditions. Impact of NPs on non-targeted organisms require extensive studies and research before their commercialization.

Large scale production with costly equipment and raw materials will be a challenge for the industries and commercial world [125 126]. Reduced size is an advantage, at the same time it also a drawback of NPs from health and safety point of view of the human and environment both. Impact of NPs to the various biotic and abiotic ecosystems is a matter of concern as very less is known about it. Studies are to be carried out about the potential environmental risks of NPs. Risk assessment of the product (NP) right from production to degradation should be carried out in order to see its environmental impact. There should rules and protocols laid by the competent authority for the production, fabrication and degradation of the NPs and should be seriously followed so that one can encash only the benefits and minimize the hazards of novel materials called NANOPARTICLES.

A ray of hope is seen in the form of green synthesis where NPs are synthesized in ecofriendly way with minimal side effects or byproducts.

V. Final References

[1]Mansha, M., Qurashi, A., Ullah, N., Bakare, F.O., Khan, I., Yamani, Z.H., 2016. Synthesis of In₂O₃/graphene heterostructure and their hydrogen gas sensing properties. *Ceramics International* 42, 11490–11495. <http://dx.doi.org/10.1016/j.ceramint.2016.04.035>

- [2] Ullah, H., Khan, I., Yamani, Z.H., Qurashi, A., 2017. Sonochemical driven ultrafast facile synthesis of SnO₂ nanoparticles: growth mechanism structural electrical and hydrogen gas sensing properties. *Ultrasonics Sonochemistry* 34, 484–490. <http://dx.doi.org/10.1016/j.ultsonch.2016.06.025>
- [3] Barrak, H., Saied, T., Chevallier, P., Laroche, G., M'nif, A., Hamzaoui, A.H., 2016. Synthesis, characterization, and functionalization of ZnO nanoparticles by N-(trimethoxysilylpropyl) Nanoparticles 927 ethylenediamine triacetic acid (TMSEDTA): investigation of the interactions between phloroglucinol and ZnO@TMSEDTA. *Arabian Journal of Chemistry*. <http://dx.doi.org/10.1016/j.arabjc.2016.04.019>
- [4] Lee, J.E., Lee, N., Kim, T., Kim, J., Hyeon, T., 2011. Multifunctional mesoporous silica nanocomposite nanoparticles for theranostic applications. *Accounts of Chemical Research* 44, 893–902. <http://dx.doi.org/10.1021/ar2000259>.
- [5] Shaalan, M., Saleh, M., El-Mahdy, M., El-Matbouli, M., 2016. Recent progress in applications of nanoparticles in fish medicine: a review. *Nanomed. Nanotechnol. Biol. Med.* 12, 701–710. <http://dx.doi.org/10.1016/j.nano.2015.11.005>
- [6] Hoek E M V and Ghosh A K 2009 Nanotechnology-based membranes for water purification Nanotechnology Applications for Clean Watered N Savage, M Diallo, J Duncan, A Street and R Sustich (Norwich, NY: William Andrew Inc.) chapter 4, p 47
- [7] P. Podsiadlo, A. K. Kaushik, E. M. Arruda et al., “Ultrastrong and stiff layered polymer nanocomposites,” *Science*, vol. 318, no. 5847, pp. 80–83, 2007.
- [8] Y. Vasquez, A. E. Henkes, J. Chris Bauer, and R. E. Schaak, “Nanocrystal conversion chemistry: a unified and materials general strategy for the template-based synthesis of nanocrystalline solids,” *Journal of Solid State Chemistry*, vol. 181, no. 7, pp. 1509–1523, 2008
- [8] Gahlawat G, Choudhury AR. A review on the biosynthesis of metal and metal salt nanoparticles by microbes. *RSC Adv.* 2019;9(23):12944–67.
- [9] Soni M, Mehta P, Soni A, Goswami GK. Green nanoparticles: Synthesis and applications. *IOSR J Biotechnol Biochem.* 2018;4:78–83.

- [10] Pal G, Rai P, Pandey A. Green synthesis of nanoparticles: A greener approach for a cleaner future. In: Green synthesis, characterization and applications of nanoparticles: Elsevier; 2019. p. 1–26. Bahrulolum et al. Journal of Nanobiotechnology (2021) 19:86 Page 22 of 26
- [11] Roychoudhury A. Yeast-mediated green synthesis of nanoparticles for biological applications. Indian Journal of Pharmacology and Biological Research 2020;8(03):26–31
- [12] Prasad, R. (2014). Synthesis of silver nanoparticles in photosynthetic plants. Journal of Nanoparticles. 2014:963961. doi: 10.1155/2014/963961
- [13] Prasad, R., Kumar, V., and Prasad, K. S. (2014). Nanotechnology in sustainable agriculture: present concerns and future aspects. African Journal of Biotechnology. 13, 705–713. doi: 10.5897/AJBX2013.13554
- [14] Prasad, R., Pandey, R., and Barman, I. (2016). Engineering tailored nanoparticles with microbes: quo vadis. WIREs Nanomedicine and Nanobiotechnology. 8, 316–330. doi: 10.1002/wnan.1363
- [15] Kato Y, Suzuki M. Synthesis of metal nanoparticles by microorganisms. Crystals. 2020;10(7):589
- [16] Khan T, Abbas S, Fariq A, Yasmin A. Microbes: Nature’s cell factories of nanoparticles synthesis. In: Prasad R, Jha AK, Prasad K, editors. Exploring the Realms of Nature for Nanosynthesis. Cham: Springer; 2018. p. 25–50
- [17] Velasco-Santos C. Naturally produced carbon nanotubes. Chemistry and Physics Letters. 2003;373:272–276.
- [18] MacKenzie KJ, See CH, Dunens OM, Harris AT. Do single-walled carbon nanotubes occur naturally? Nature Nanotechnology. 2008;3:310.
- [19] Su DS, Chen X. Natural lavas as catalysts for efficient production of carbon nanotubes and nanofibers. Angewandte Chemie International Edition Engl. 2007;46:1823–4.
- [20] Mracek J, D. Fagan R, M. Stengelin R, Hesjedal T. Are carbon nanotubes a naturally occurring material? Hints from methane CVD using lava as a catalyst. CNANO. 2011;7:294–6.
- [21] Buseck PR, Tsipursky SJ, Hettich R. Fullerenes from the geological environment. Science. 1992;257:215–7.

- [22] Parthasarathy G, Srinivasan R, Vairamani M, Ravikumar K, Kunwar AC. Occurrence of natural fullerenes in low grade metamorphosed Proterozoic shungite from Karelia, Russia. *Geochimica et Cosmochimica Acta*. 1998;62:3541–4.
- [23] Misra KS, Hammond MR, Phadke AV, Plows F, Reddy US, Reddy IV, Parthasarathy G, Rao CRM, Gohain BN, Gupta D. Occurrence of fullerene bearing shungite suite rock in Mangampeta area, Cuddapah District, Andhra Pradesh. *Journal of Geological Society of India*. 2007;69:25–8.
- [24] Reznikov VA, Polekhovskii YS. Amorphous shungite carbon: a natural medium for the formation of fullerenes. *Technical Physics Letters*. 2000;26:689–93.
25. Becker L, Bada JL, Winans RE, Bunch TE. Fullerenes in Allende meteorite. *Nature*. 1994;372:507.
- [26] Andrade K, Guerra S, Debut A, Andrade K, Guerra S, Debut A. Fullerene-based symmetry in *Hibiscus rosa-sinensis* pollen. *PLoS One*. 2014;9:e10212328.
- [27] Begum P, Fugetsu B. Phytotoxicity of multi-walled carbon nanotubes on red spinach (*Amaranthus tricolor* L) and the role of ascorbic acid as an antioxidant. *Journal of Hazardous Materials*. 2012;243:212–22.
- [28] Begum P, Ikhtiar R, Fugetsu B. Graphene phytotoxicity in the seedling stage of cabbage, tomato, red spinach, and lettuce. *Carbon*. 2011;49:3907–19.
- [29] Pouratashi, M., and Iravani, H. (2012). Farmers' knowledge of integrated pest management and learning style preferences: implications for information delivery. *Int. J. Pest Manage.* 58, 347–353. doi: 10.1080/09670874.2012.724468
- [30] Usman, M., Farooq, M., Wakeel, A., Nawaz, A., Cheema, S.A., ur Rehman, H., Ashraf I. and Sanaullah M. (2020) Nanotechnology in Agriculture: Current Status, Challenges and Future Opportunities. *Science of the Total Environment*, 721, Article No. 137778. <https://doi.org/10.1016/j.scitotenv.2020.137778>
- [31] Ojeda-Barrios, D.L., Morales, I., Juárez-Maldonado, A., Sandoval-Rangel, A., Fuentes-Lara, L.O. and Benavides-Mendoza, A. (2020) Chapter 35—Importance of Nanofertilizers in Fruit Nutrition. In: Srivastava, A.K. and Hu, C., Eds., *Fruit Crops: Diagnosis and Management of Nutrient Constraints*, Elsevier, Amsterdam, 497-508. <https://doi.org/10.1016/B978-0-12-818732-6.00035-6>

- [32] Pérez-de-Luque, A. (2017). Interaction of nanomaterials with plants: what do we need for real applications in agriculture. *Frontiers in Environmental science*. 5:12. doi: 10.3389/fenvs.2017.00012
- [33] Deepti Mittal, Gurjeet Kaur, Parul Singh, Karmveer Yadav and Syed Azmal Ali (2020). Nanoparticles- Based Sustainable Agriculture and Food Science: Recent Advances and Future Outlook. *Frontiers in Nanotechnology*.2,1-38.doi:10.3389/fnano.2020.579954.
- [34] Monica RC, Cremonini R. Nanoparticles and higherplants. *Caryologia*. 2009;62(2):161–165.
- [35] Zhu ZJ, Wang H, Yan B, et al. Effect of surface charge on the uptake and distribution of gold nanoparticles in four plant species. *Environmental Science Technology*. 2012;46(22):12391–12398.
- [36] Wang, X., Yang, X., Chen, S., Li, Q., Wang, W., Hou, C., et al. (2016). Zinc oxide nanoparticles affect biomass accumulation and photosynthesis in *Arabidopsis*. *Frontiers in Plant Science*. 6:1243. doi: 10.3389/fpls.2015.01243
- [37] Wang, P., Lombi, E., Zhao, F. J., and Kopittke, P. M. (2016). Nanotechnology: a new opportunity in plant sciences. *Trends in Plant Science*. 21, 699–712. doi: 10.1016/j.tplants.2016.04.005
- [38] Carlson, C., Hussain, S. M., Schrand, A. M., K., Braydich-Stolle, L., Hess, K. L., Jones, R. L., et al. (2008). Unique cellular interaction of silver nanoparticles: size-dependent generation of reactive oxygen species. *Journal of Physical Chemistry. B* 112, 13608–13619. doi: 10.1021/jp712087m
- [39] Hotze, E. M., Phenrat, T., and Lowry, G. V. (2010). Nanoparticle aggregation: challenges to understanding transport and reactivity in the environment. *Journal of Environmental Quality*. 39, 1909–1924. doi: 10.2134/jeq2009.0462
- [40] Santiago, M., Pagay, V., and Stroock, A. D. (2013). Impact of electroviscosity on the hydraulic conductance of the bordered pit membrane: a theoretical investigation. *Plant Physiol*. 163, 999–1011. doi: 10.1104/pp.113.219774
- [41] Zeng, Y., Himmel, M. E., and Ding, S. Y. (2017). Visualizing chemical functionality in plant cell walls. *Biotechnology and Biofuel*. 10, 1–16. doi: 10.1186/s13068-017-0953-3

- [42]Zhu, Z. J., Wang, H., Yan, B., Zheng, H., Jiang, Y., Miranda, O. R., et al. (2012). Effect of surface charge on the uptake and distribution of gold nanoparticles in four plant species. *Environmental Science Technology*. 46, 12391–12398. doi: 10.1021/es301977w
- [43]Meychik, N. R., Nikolaeva, J. I., and Yermakov, I. P. (2005). Ion exchange properties of the root cell walls isolated from the halophyte plants (*Suaeda altissima* L.) grown under conditions of different salinity. *Plant Soil* 277:163. doi: 10.1007/s11104-005-6806-z
- [44]Milewska-Hendel, A., Zubko, M., Stróz, D., and Kurczynska, E. U. (2019). Effect of nanoparticles surface charge on the *Arabidopsis thaliana* (L.) roots development and their movement into the root cells and protoplasts. *International Journal of Molecular Science*. 20:1650. doi: 10.3390/ijms20071650
- [45] Khodakovskaya, M. V., De Silva, K., Biris, A. S., Dervishi, E., and Villagarcia, H. (2012). Carbon nanotubes induce growth enhancement of tobacco cells. *ACS Nanotechnology*. 6, 2128–2135. doi: 10.1021/nn204643g
- [46] Lahiani, M. H., Dervishi, E., Chen, J., Nima, Z., Gaume, A., Biris, A. S., et al. (2013). Impact of carbon nanotube exposure to seeds of valuable crops. *ACS Applied Materials Interfaces*. 5, 7965–7973. doi: 10.1021/am402052x
- [47] Pyrzynska, K. (2011). Carbon nanotubes as sorbents in the analysis of pesticides. *Chemosphere* 83, 1407–1413. doi: 10.1016/j.chemosphere.2011.01.057
- [48] Chahine, N. O., Collette, N. M., Thomas, B. C., Genetos, D. C., and Loots, G. G. (2014). Nanocomposite scaffold for chondrocyte growth and cartilage tissue engineering: effects of carbon nanotube surface functionalization. *Tissue Engineering. Part A*. 20, 2305–2315. doi: 10.1089/ten.TEA.2013.0328
- [49] Acharya, P., Jayaprakasha, G. K., Crosby, K. M., Jifon, J. L., and Patil, B. S. (2020). Nanoparticle-mediated seed priming improves germination, growth, yield, and quality of watermelons (*Citrullus lanatus*) at multi-locations in texas. *Science Report*. 10:5037. doi: 10.1038/s41598-020-61696-7
- [50] Giraldo JP, Landry MP, Faltermeier SM, McNicholas TP, Iverson MN, Boghossian AA, Reuel NF, Hilmer AJ, Sen F, Brew J, Strano MS. Plant nanobionics approach to augment 136

New Visions in Plant Science photosynthesis and biochemical sensing. *Nature Materials*. 2014;13:400-408. DOI: 10.1038/nmat3890

[51] Ahmed, B., Rizvi, A., Zaidi, A., Khan, M. S., and Musarrat, J. (2019). Understanding the phyto-interaction of heavy metal oxide bulk and nanoparticles: evaluation of seed germination, growth, bioaccumulation, and metallothionein production. *RSC Advances*. 9, 4210–4225. doi: 10.1039/C8RA09305A

[52] Rastogi, A., Tripathi, D. K., Yadav, S., Chauhan, D. K., and Živcák, M., Ghobanpour, M. et al. (2019). Application of silicon nanoparticles in agriculture. *3Biotech* 9:90. doi: 10.1007/s13205-019-1626-7

[53] Suriyaprabha, R., Karunakaran, G., Yuvakkumar, R., Rajendran, V., and Kannan, N. (2012). Silica nanoparticles for increased silica availability in maize (*Zea mays*. L) seeds under hydroponic conditions. *Current Nanoscience*. 8, 902–908. doi: 10.2174/157341312803989033

[54] Boykov, I. N., Shuford, E., and Zhang, B. (2019). Nanoparticle titanium dioxide affects the growth and microRNA expression of switchgrass (*Panicum virgatum*). *Genomics* 111, 450–456. doi: 10.1016/j.ygeno.2018.03.002

[55] Mohammadi, R., Maali-Amiri, R., and Abbasi, A. (2013). Effect of TiO₂ nanoparticles on chickpea response to cold stress. *Biological Trace Element Research*. 152, 403–410. doi: 10.1007/s12011-013-9631-x

[56] Larue, C., Castillo-Michel, H., Sobanska, S., Trcera, N., Sorieul, S., Cécillon, L., et al. (2014). Fate of pristine TiO₂ nanoparticles and aged paint-containing TiO₂ nanoparticles in lettuce crop after foliar exposure. *Journal Hazardous Management* 273, 17–26. doi: 10.1016/j.jhazmat.2014.03.014

[57] Tarafdar, J. C., Xiong, Y., Wang, W. N., Quinl, D., and Biswas, P. (2012). Standardization of size, shape and concentration of nanoparticle for plant application. *Applied Biology Research*. 14, 138–144.

[58] Dimkpa, C. O., Bindraban, P. S., Fugice, J., Agyin-Birikorang, S., Singh, U., and Hellums, D. (2017a). Composite micronutrient nanoparticles and salts decrease drought stress in soybean. *Agricultural Sustainable Development*. 37:5. doi: 10.1007/s13593-016-0412-8

- [59] Sun, D., Hussain, H. I., Yi, Z., Rookes, J. E., Kong, L., and Cahill, D. M. (2018). Delivery of abscisic acid to plants using glutathione responsive mesoporous silica nanoparticles. *Journal Nanoscience and Nanotechnology*. 18, 1615–1625. doi: 10.1166/jnn.2018.14262
- [60] Verma, V., Ravindran, P., and Kumar, P. P. (2016). Plant hormone mediated regulation of stress responses. *BMC Plant Biology*. 16:86. doi: 10.1186/s12870-016-0771-y
- [61] Raza, A., Mehmood, S. S., Tabassum, J., and Batool, R. (2019). “Targeting plant hormones to develop abiotic stress resistance in wheat,” in *Wheat Production in Changing Environments* (Singapore: Springer), 557–577. doi: 10.1007/978-981-13-6883-7_22
- [62] Sharifi, M., Faryabi, K., Talaei, A. J., Shekha, M. S., Ale-Ebrahim, M., and Salihi, A. (2020). Antioxidant properties of gold nanozyme: a review. *Journal of Molecular Liquids*. 297:112004. doi: 10.1016/j.molliq.2019.112004
- [63] Siddiqui, M. H., Al-Whaibi, M. H., Faisal, M., and Al Sahli, A. A. (2014). Nanosilicon dioxide mitigates the adverse effects of salt stress on *Cucurbita pepo* L. *Environmental Toxicological Chemistry*. 33, 2429–2437. doi: 10.1002/etc.2697
- [64] Mingyu, S., Chao, L., Chunxiang, Q., Lei, Z., Liang, C., and Hao, H. (2008). Nano-anatase relieves the inhibition of electron transport caused by linolenic acid in chloroplasts of spinach. *Biological Trace Element Research* 122, 73–81. doi: 10.1007/s12011-007-8055-x
- [65] Wu, H., Shabala, L., Shabala, S., and Giraldo, J. P. (2018). Hydroxyl radical scavenging by cerium oxide nanoparticles improves arabidopsis salinity tolerance by enhancing leaf mesophyll potassium retention. *Environmental Science and Nanotechnology*. 5, 1567–1583. doi: 10.1039/C8EN00323H
- [66] Wu, H., Tito, N., and Giraldo, J. P. (2017b). Anionic cerium oxide nanoparticles protect plant photosynthesis from abiotic stress by scavenging reactive oxygen species. *ACS Nanotechnology* 11, 11283–11297. doi: 10.1021/acsnano.7b05723
- [67] Marshner H. *Mineral Nutrition of Higher Plants*. 3rd ed. London: Elsevier/Academic Press; 2012. p. 672. DOI: 10.1016/B978-0-12-384905-2.00030-3
- [68] Stewart WM, Dibb DW, Johnston AE, Smyth TJ. The contribution of commercial fertilizer nutrients to food production. *Agronomy Journal*. 2005;7(1):1-6. DOI: 10.2134/agronj2005.0001

- [70] Welch RM, Shuman L. Micronutrient nutrition of plants. *Critical Reviews in Plant Sciences*. 1995;14(1):49-82. DOI: 10.1080/07352689509701922
- [71] Alloway BJ. Heavy metals and metalloids as micronutrients for plants and animals. In: Alloway B, editor. *Heavy Metals in Soils. Environmental Pollution*. Vol. 2013, 22. Dordrecht: Springer; 2013. pp. 195-209. DOI: 10.1007/978-94-007-4470-7_7
- [72] Dwivedi, S., Saquib, Q., Al-Khedhairi, A. A., and Musarrat, J. (2016). "Understanding the role of nanomaterials in agriculture," in *Microbial Inoculants in Sustainable Agricultural Productivity* (New Delhi: Springer), 271–288. doi: 10.1007/978-81-322-2644-4_17
- [73] Sarlak N, Taherifar A, Salehi F. Synthesis of nanopesticides by encapsulating pesticide nanoparticles using functionalized carbon nanotubes and application of new nanocomposite for plant disease treatment. *Journal of Agricultural Food Chemistry*. 2014;62:4833–8
- [74] Rameshaiah, G. N., Pallavi, J., and Shabnam, S. (2015). Nano fertilizers and nano sensors—an attempt for developing smart agriculture. *International Journal of Engineering Research and General Science*. 3, 314–320
- [75] [44] de França Bettencourt, G.M., Degenhardt, J., Zevallos Torres, L.A., de Andrade, Tanobe, V.O. and Soccol, C.R. (2020) Green Biosynthesis of Single and Bimetallic Nanoparticles of Iron and Manganese Using Bacterial Auxin Complex to Act as Plant Bio-Fertilizer. *Biocatalysis and Agricultural Biotechnology*, 30, Article ID: 101822. <https://doi.org/10.1016/j.bcab.2020.101822>
- [76] Abd El-Azeim, M.M., Sherif, M.A., Hussien, M.S., Tantawy, I.A.A. and Bashandy, S.O. (2020) Impacts of Nano- and Non-Nanofertilizers on Potato Quality and Productivity. *Acta Ecologica Sinica*, 40, 388-397. <https://doi.org/10.1016/j.chnaes.2019.12.007>
- [77] Liu Q, Chen B, Wang Q, Shi X, Xiao Z, Lin J, Fang X. Carbon nanotubes as molecular transporters for walled plant cells. *Nanotechnology Letters*. 2009;9:1007–10.
- [78] Liu, X., Zhang, F., Zhang, S., He, X., Wang, R., Fei, Z., et al. (2005). Responses of peanut to nano-calcium carbonate. *Plant Nutrition and Fertilizer Science* 11, 385–389.
- [79] Liu, R., and Lal, R. (2015). Synthetic apatite nanoparticles as a phosphorus fertilizer for soybean (*Glycine max*). *Science. Reports*. 4:5686. doi: 10.1038/srep 05686
- [80] Ozdemir, M., and Kemerli, T. (2016). "Innovative applications of micro and nanoencapsulation in food packaging," in *Encapsulation and Controlled Release Technologies in Food Systems*, ed. J. M. Lakkis (Chichester: John Wiley & Sons, Ltd).
- [81] DeRosa, M.C., Monreal, C., Schnitzer, M., Walsh, R., et al. (2010) Nanotechnology in Fertilizers. *Nature Nanotechnology*, 5, 91. <https://doi.org/10.1038/nnano.2010.2>

- [82] Naderi, M.R. and Abedi, A. (2012) Application of Nanotechnology in Agriculture and Refinement of Environmental Pollutants. *Journal of Nanotechnology*, 11, 18-26.
- [83] Moaveni, P. and Kheiri, T. (2011) TiO₂ Nano Particles Affected on Maize (*Zea mays* L). 2nd International Conference on Agricultural and Animal Science, Maldives, 25-27 November 2011, Vol. 22, IACSIT Press, Singapore, 160-163.
- [84]. Zhang M, Gao B, Chen J, Li Y, Creamer AE, Chen H. Slow-release fertilizer encapsulated by graphene oxide films. *Chemical Engineering Journal*. 2014;255:107–13.
- [85]Khota, L. R., Sankarana, S., Majaa, J. M., Ehsania, R., and Schuster, E.W.(2012). Applications of nanomaterials in agricultural production and crop protection:a review. *Crop Prot.* 35, 64–70. doi: 10.1016/j.cropro.2012.01.00
- [86] Kah M, Machinski P, Koerner P, et al. Analysing the fate of nanopesticides in soil and the applicability of regulatory protocols using a polymer-based nano formulation of atrazine. *Environmental Science Pollution Research*. 2014;21
- [87] Lhomme L, Brosillon S and Wolbert D 2008 *Chemosphere* **70** 381
- [88]. Hui L, Piao J, Auletta J, Hu K, Zhu Y, Meyer T, Liu H, Yang L. Availability of the basal planes of graphene oxide determines whether it is antibacterial. *ACS Application Materials & Interfaces*. 2014;6:13183–90.
- [89] Mangadlao JD, Santos CM, Felipe MJL, De Leon ACC, Rodrigues DF, Advincula RC. On the antibacterial mechanism of graphene oxide (GO) Langmuir-Blodgett films. *Chemical Communication*. 2015;51: 2886–9.
- [90] Akhavan O, Ghaderi E. Toxicity of graphene and graphene oxide nanowalls against bacteria. *ACS Nano*. 2010;4:5731–6.
- [91] Liu S, Zeng TH, Hofmann M, Burcombe E, Wei J, Jiang R, Kong J, Chen Y. Antibacterial activity of graphite, graphite oxide, graphene oxide, and reduced graphene oxide: membrane and oxidative stress. *ACS Nanotechnology*. 2011;5:6971–80.
- [92] Li J, Wang G, Zhu H, Zhang M, Zheng X, Di Z, Liu X, Wang X. Antibacterial activity of large-area monolayer graphene film manipulated by charge transfer. *Science Reports*. 2014;4:4359.
- [93] Bhattacharyya, A., Duraisamy, P., Govindarajan, M., Buhroo, A. A., and Prasad, R.(2016). “Nano-biofungicides: emerging trend in insect pest control,” in *Advances and Applications through Fungal Nanobiotechnology*, ed. R. Prasad (Cham: Springer International Publishing), 307–319. doi: 10.1007/978-3-319-42990-8_15

- [94] Nuruzzaman, M., Rahman, M. M., Liu, Y., and Naidu, R. (2016). Nano encapsulation, nano-guard for pesticides: a new window for safe application. *Journal of Agricultural Food Chemistry* 64, 1447–1483. doi: 10.1021/acs.jafc.5b05214
- [95] de Oliveira, J. L., Campos, E. V., Bakshi, M., Abhilash, P. C., and Fraceto, L. F. (2014). Application of nanotechnology for the encapsulation of botanical insecticides for sustainable agriculture: prospects and promises. *Biotechnology Advances*. 32, 1550–1561. doi: 10.1016/j.biotechadv.2014.10.010
- [96] Kah, M., and Hofmann, T. (2014). Nanopesticides research: current trends and future priorities. *Environment International* 63, 224–235. doi: 10.1016/j.envint.2013.11.015
- [97] Grillo, R., Abhilash, P. C., and Fraceto, L. F. (2016). Nanotechnology applied to bio-encapsulation of pesticides. *Journal of Nanoscience and Nanotechnology* 16, 1231–1234. doi: 10.1016/j.tifs.2003.10.005
- [98] Gouin, S. (2004). Microencapsulation: industrial appraisal of existing technologies and trends. *Trends in Food Science and Technology*. 15, 330–347. doi: 10.1038/nature.2015.17987
- [99] Murphy K (ed) 2008 *Nanotechnology: Agriculture's Next "Industrial" Revolution* (Williston, VT: Financial Partner, Yankee Farm Credit, ACA) Spring, pp 3–5
- [100] Debnath N, Mitra S, Das S, et al. Synthesis of surface functionalized silica nanoparticles and their use as entomotoxic nanocides. *Powder Tech.*2012;221:252–256.
- [101] Barik T, Sahu B, Swain V. Nano silica—from medicine to pest control. *Parasitol Research*. 2008;103(2):253.
- [102] Chormule KA. Synthesis and evaluation of antimicrobial potential of copper nanoparticles on bacterial blight of pomegranate. Parbhani: Vasant Rao Naik Marathwada Krishi Vidyapeeth; 2017.
- [103] Baker, C., Pradhan, A., Pakstis, L., Pochan, D. J., and Shah, S. I. (2005). Synthesis and antibacterial properties of silver nanoparticles. *Journal of Nanoscience and Nanotechnology*. 5, 244–249. doi: 10.1166/jnn.2005.034
- [104] Anjali, C. H., Sharma, Y., Mukherjee, A., and Chandrasekaran, N. (2012). Neem oil (*Azadirachta indica*) nanoemulsion—a potent larvicidal agent against *Culex quinquefasciatus*. *Pest Management. Sci.* 68, 158–163. doi: 10.1002/ps.2233
- [105] Fan, P., Gu, Z., Xu, D., Xu, X., and Xu, G. (2010). Action analysis of drops of emamectin-benzoate microemulsion on rice leaf. *Chine. J. Rice Sci.* 24, 503–508. doi: 10.3969/j.issn.1001-7216.2010.05.010

- [106] Kumar, R. S., Shiny, P. J., Anjali, C. H., Jerobin, J., Goshen, K. M., and Magdassi, S. (2013). Distinctive effects of nano-sized permethrin in the environment. *Environment Science and Pollution Research Int.* 20, 2593–2602. doi: 10.1007/s11356-012-1161-0
- [107] Li Q, Wu P and Shang J K 2009 Nanostructured visible-light photocatalysts for water purification *Nanotechnology Applications for Clean Water* ed N Savage, M Diallo, J Duncan, A Street and R Sustich (Norwich, NY: William Andrew Inc.) chapter 2, p 17.
- [108] Patel, N., Desai, P., Patel, N., Jha, A., and Gautam, H. K. (2014). Agro nanotechnology for plant fungal disease management: a review. *International Journal of Current Microbiological Application Science.* 3, 71–84.
- [109] Pérez-de-Luque, A. (2017). Interaction of nanomaterials with plants: what do we need for real applications in agriculture. *Environmental Science-Frontier.* 5:12. doi: 10.3389/fenvs.2017.00012
- [110] Ion I, Culetua A, Gherase D, Sirbu F, Ion AC. Environmental applications of carbon-based nanomaterials. Acetylcholinesterase biosensors for organophosphate pesticide analysis. In: Ion A, Dascalu D, Carja G, Cirea M, editors. *New Applications of Nanomaterials.* Bucharest: Academiei Române; 2014. p. 33–51.
- [111] Chen H and Yada R 2011 *Trends Food Sci. Technol.* **22** 585 <http://www.nseafs.cornell.edu/web.roadmap.pdf>
- [112] Diallo M 2009 Water treatment by dendrimer-enhanced filtration: principles and applications in *Nanotechnology Applications for Clean Water* ed N Savage, M Diallo, J Duncan, A Street and R Sustich (Norwich, NY: William Andrew Inc.) chapter 11, p 143
- [113]. Wu L, Fu X, Liu H, Li J, Song Y. Comparative study of graphene nanosheet and multiwall carbon nanotube-based electrochemical sensor for the sensitive detection of cadmium. *Analytica Chimica Acta.* 2014;851:43–8.
- [114]. Taher MA, Mazaheri L, Ashkenani H, Mohadesi A, Afzali D. Determination of nickel in water, food, and biological samples by electrothermal atomic absorption spectrometry after preconcentration on modified carbon nanotubes. *Journal of AOAC International.* 2014;97:225–31.
- [115] Guerin H, Le Poche H, Pohle R, Syavoch Bernard L, Buitrago E, Ramos R, Dijon J, Ionescu AM. High-yield, in situ fabrication and integration of horizontal carbon nanotube arrays at the wafer scale for robust ammonia sensors. *Carbon.* 2014;78:326–38.
- [116]. Luo M, Liu D, Zhao L, Han J, Liang Y, Wang P, Zhou Z. A novel magnetic ionic liquid modified carbon nanotube for the simultaneous determination of aryloxyphenoxy-propionate herbicides and their metabolites in water. *Analytica Chimica Acta* 2014;852:88–96.

- [117] Ma G, Chen L. Development of magnetic molecularly imprinted polymers based on carbon nanotubes – Application for trace analysis of pyrethroids in fruit matrices. *Journal of Chromatography A*. 2014;1329:1–9.
- [118] Tabani H, Fakhari AR, Shahsavani A, Behbahani M, Salarian M, Bagheri A, Nojavani S. Combination of graphene oxide-based solid phase extraction and electro membrane extraction for the preconcentration of chlorophenoxy acid herbicides in environmental samples. *Journal of Chromatography A*. 2013;1300:227–35.
- [119] Jackson T, Mansfield K, Saafi M, Colman T, Romine P. Measuring soil temperature and moisture using wireless MEMS sensors. *Meas: Journal of the International Measurement Confederation*. 2008;41:381–90.
- [120] Ren Q, Yuan X, Huang X, Wen W, Zhao Y, Chen W. In vivo monitoring of oxidative burst on aloe under salinity stress using hemoglobin and single-walled carbon nanotubes modified carbon fiber ultramicroelectrode. *Biosensors and Bioelectronics*. 2013;50:318–24.
- [121] Lee K, Park J, Lee M, Kim J, Hyun BG, Kang DJ, Na K, Lee CY, Bien F, Park J. In-situ synthesis of carbon nanotube-graphite electronic devices and their integrations onto surfaces of live plants and insects. *Nanotechnology Letters*. 2014;14:2647–54.
- [122] Cross K M, Lu Y, Zheng T, Zhan J, McPherson G and John V 2009 Water decontamination using iron and iron oxide nanoparticles *Nanotechnology Applications for Clean Water* ed N Savage, M Diallo, J Duncan, A Street and R Sustich (Norwich, NY: William Andrew Inc.) chapter 24, p 347.
- [123] Nangmenyi G and Economy J 2009 Nonmetallic particles for oligo dynamic microbial disinfection in *Nanotechnology Applications for Clean Water* ed N Savage, M Diallo, J Duncan, A Street and R Sustich (Norwich, NY: William Andrew Inc.) chapter 1, p 3
- [124] Farnen L 2009 Commercialization of nanotechnology for removal of heavy metals in drinking water in *Nanotechnology Applications for Clean Water* ed N Savage, M Diallo, J Duncan, A Street and R Sustich (Norwich, NY: William Andrew Inc.) chapter 9, p 115
- [125] Swierczewska M, Liu G, Lee S, Chen X. High-sensitivity nanosensors for biomarker detection. *Chemical Society Reviews*. 2012;41:2641–55.
- [126]. Sarkar T, Gao Y, Mulchandani A. Carbon nanotubes-based label-free affinity sensors for environmental monitoring. *Applied Biochemistry and Biotechnology*. 2013; 170:1011–25.

A Short Review on Effect of Nanosizing on Biological Activities of Some Herbal Medicinal Plants based Nanoparticles.

Vaishali S. Raut*

Department of Chemistry

K.V.N. Naik College, Nashik, Maharashtra, India.

Abstract:

Modern medicine has brought improvement in the fight against many diseases but since these medicines have large number of large number of side effects scientist have turned their attention again towards natural herbal medicines which are human friendly with lesser side effects. Herbal medicines are used from ancient times to cure many diseases. But, there are many hurdles in their practical uses due to their lower bioavailability and solubility. Nanoparticles of plant materials have demonstrated more effective activity, increase in the bioavailability and solubility of the herbal medicines for their effective use The objective of this review is to highlight the use of nanotechnology systems as an innovative drug delivery system in herbal medicines to enhance the therapeutic effects and bioavailability of naturally occurring drugs. It can be presumed that this detailed review will be beneficial for subsequent applications in biomedical science and create the latest research opportunities. Data was collected from PubMed, Google scholar and Med line.

Keywords: Nanosizing, herbal medicines, bioavailability, therapeutic effect.

Introduction:

From ancient times plants have been considered to be source of medicines According to World Health Organization (WHO) 80% of the world population depends on drugs from natural origins [1]. Human body can accept anything that occurs naturally therefore phytopharmaceuticles that is drugs from plant origin have very few or no side effects whereas synthetically prepared drugs have numerous side effects [2]. Many synthetic medicines are used on regular basis but many medicines are reported to have severe side effects. The common medicines like Aspirin, Clopidogrel,

Diclofenac [3], Enoxaparin [4], Ibuprofen, Naproxen [5] and Warfarin [6] are sold over the counter and found to have minor side effects like back pain to headaches if not administered properly can have serious side effects like excessive bleeding, hemorrhage and difficulty in breathing There are many side effects of medicines used for several major diseases like cancer [7] diabetes [8]. Therefore, natural compounds are screened for treatment of several major diseases like cancer [9], diabetes, [10] microbial, inflammatory, and cardiovascular diseases [11]. The herbal medicines are source of these natural compounds. The use of a plant 's seeds, roots, leaves, bark, or flowers for medicinal purposes is done by civilization since many years The recorded herbal medicines is about 5000 years ago when the Sumerian's used plants such as thyme and laurel were used as a remedy for diseases. The root of marshmallow grass was chewed thoroughly to get relief from stomach upsets [12]. The herb may be used in many forms e.g. fresh, dried, ointment, tincture, or oil extract or made into liquid by infusion or decoction [13]. Herbal medicines, boosts immune system of the human body and also enhance detoxification process [14]. Herbal medicines are derived from plant material hence they are easily digestible. They are easy to consume and can be taken frequently [15] One of important advantage of herbal medicine is their cost They are quiet cheap as compared to synthetically prepared drugs and comparatively less toxic [16]. Thus herbal medicines are cost effective, comparatively less toxic Growing antimicrobial resistance is a serious threat to human health. The development of new antibiotics is limited and slow. Herbal medicine can be used for this purposes [17].

One of greater risk in consumption of these herbal medicines is over dosage of these medicines during self-medication. In addition to this if correct plant is not identified then there is risk of poisoning. It is quite possible that medicine producer uses low quality starting material, standardization of ready product is not done. All these issues can be handled by proper care. There

use also has additional limitation of bioavailability of active phytochemical constituents [18]. They have problems like vivo instability, and poor solubility, poor absorption in the body, difficulty in target-specific delivery, and tonic effectiveness [19].

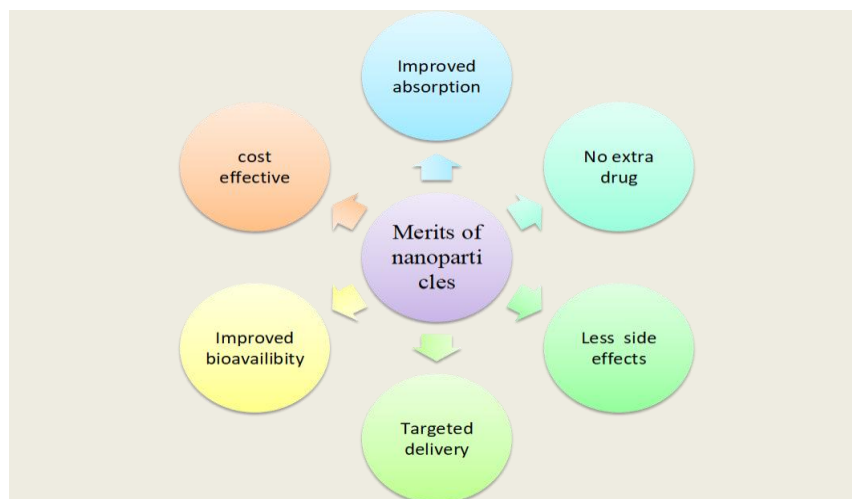
Herbal medicines have to be manufactured so that they should be stable for long duration and safe for self-utilization of patient generally when drug is administered in body only finite amount of drug centers in targeted site and remaining gets dispersed in body depending upon physicochemical and biochemical properties resulting in low therapeutic effect [20]. There is more than one active ingredient in herbal medicine so its stability effected therefore, stable phytoformulation is important [21]. Medicinal plant extracts contain lot of tannins flavonoids, and terpenoids which are soluble in water but are unable to pass the lipid membranes of the cells so show low absorption [22]. These extracts also have components of extremely large molecular size, so have low bioavailability and effectiveness. Because difficulty associated with their biocompatibility, toxicity for using them as medicine as a result many naturally occurring compounds do not clear clinical trial phases [23]. In order to overcome these difficulties innovative herbal drug delivery is formulated. These systems include vesicular delivery systems and particulate delivery system. The vesicular delivery systems such as liposomes, ethosomes, phytosomes, transferosomes [24] and particulate delivery systems such as micropellets, microspheres, nanoparticles, and micro and nano emulsions [25]. These drug delivery systems enhance the stability, bioavailability and depletion of toxicity, many natural drugs have been assimilated into these systems. Nanoparticles are considered to be an efficient drug delivery system among all the drug delivery systems [26].

Application of Nanotechniques is able to enhance the efficiency of herbal extracts, it also minimizes the required dose and lower side effects and enhance activity of drug Nano technology

can supply the active ingredients at an adequate concentration to the required site of action throughout the duration of treatment [19]. Many efforts are made in this direction for this purpose Australia-India Science Research Funding Programme is provided funds of 20 million dollars are donated by Indian and Australian governments. The global nanomedical market was valued at \$134.4 billion in 2016. This market is projected to grow at a compound annual growth rate (CAGR) of 14.0% from 2017-2022, and should reach \$293.1 billion by 2022 from \$151.9 billion in 2017 [27]. Nanoparticles can be prepared by biological processes but if we prepare nanoparticles from parts of medicinal plants the whole process becomes environmental friendly [28]. The large size of material in drug delivery faces challenges like vivo instability, poor bioavailability, and poor solubility, poor absorption in the body, also have problems like with target-specific delivery and adverse effects of drugs

Therefore, according to herbal drug researchers nanosized material is preferable These materials have advantages like enhancement of bioavailability, stability and solubility, impeding toxicity, improving biological activity and tissue macrophages dispensation, controlled delivery, inhibit the physical and chemical changes and disintegration [26]. Nano dosage is the best choice owing to their distinctive size and elevated carrying capabilities as they have more power to distribute the high amounts of drugs to the required sites [29].

Therefore, nanosized particles of these medicinal plants can be used to overcome them Nanosized particles are found to be potentially effective in improving the bioavailability and bioactivity of phytomedicines [30]. There are several methods in which nanotechnology can be used like nano particles are prepared and they can be utilized directly [31] or nanocarriers are prepared from harmless materials such as synthetic bio-decomposable polymers, polysaccharides and lipids [32]



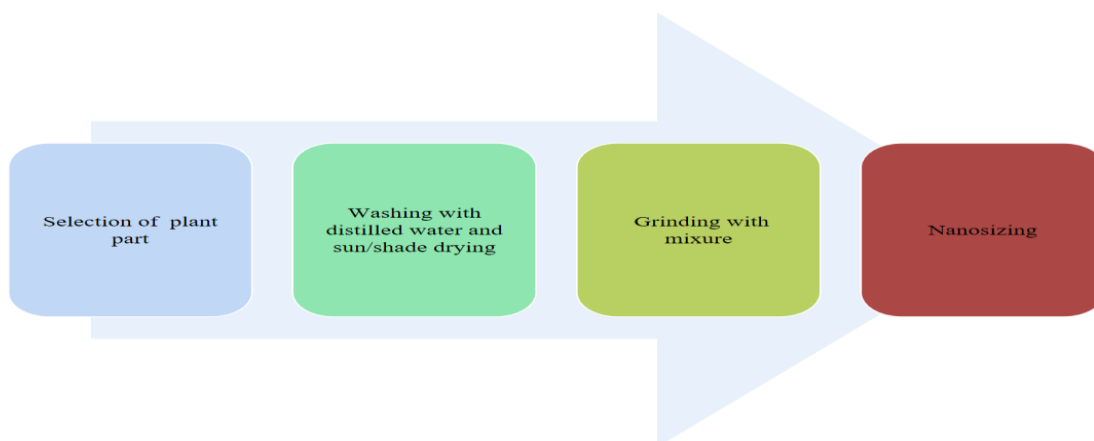
But in this study the main focus is on synthesis and comparison of biological activity of nanosized particles with bulk material from which they are synthesized

Techniques for preparation of nanosized particles: Nanoparticles can be synthesized by top down approach or bottom - up synthesis method [33]. In Top-down methods bulk material is physically broken down to make smaller molecules using milling, laser ablation, and spark ablation method Bottom-up synthesis methods are generally called as “wet” methods as they involve lot of solvents and other chemicals [34].

In this short review we are going to discuss about synthesis and determination of biological activities of nanoparticles made from medicinal plants prepared by top-down methods Milling is a top-down approach in producing nanoparticles it uses energy to break the bigger particles and produce smaller particles. In this process either the milling medium is moved by an agitator, or complete container is moved in a complex movement leading to an acceleration of the milling media [35] In the ball milling process are milling duration, ratio between sample and beads and mill speed are important parameters [36]. These parameters have great influence on physicochemical properties of milling materials

In a ball milling process, a powder mixture placed in the ball mill and then it is subjected to high-energy collision from the balls.

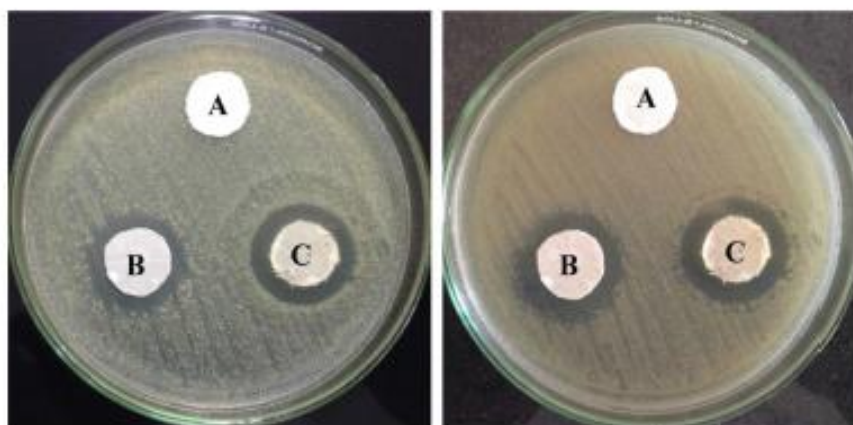
Nanomaterial synthesis using Milling method



1] **Acalypha indica**: It is a common weed that belongs to the Euphorbiaceae family. It grows in common farmlands, gardens and uncultivated lands. It is used in treatment of pneumoniae, asthma, rheumatism. The dried leaves of *Acalypha indica* are used for treatment of Bedsores and wounds are reported to be treated by poultice made by its dry leaves[37] All parts of this plant include constituents like acalyphine, triacetoneamine, cyanogenic glucosides, and alkaloids, are highly valuable for medicinal applications, due to their anti-inflammatory and antimicrobial properties [38]. Karthik S et al have prepared 50nm amorphous particles of this plants from their dried leaves The dried leaves were ground using ball mill for 15 h at 300 rpm. 10 mm diameter Zirconium balls were used for milling. The milling with a ball ratio of 20: 1 was used for 10 g of leaves The

observed antimicrobial activities of the synthesized herbal nanoparticles are found to be higher than the antimicrobial activities of organic extracts of the particles. This is due to the existence of intact reactive organic compounds such as alicyclophane, triacetoneamine, cyanogenic glucosides, and alkaloids remain intact while nanosizing and are responsible for biochemical and cell wall reactions to inhibit bacterial growth [39].

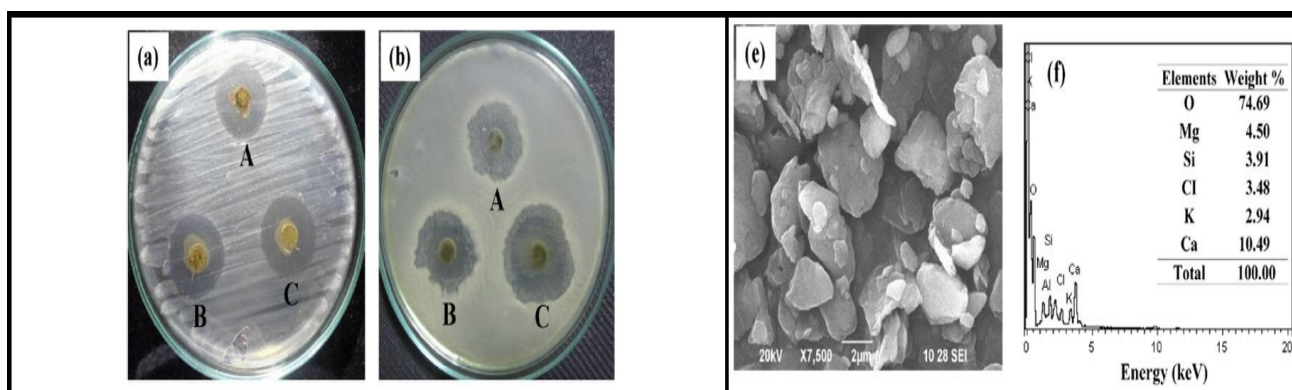
2]Aloe-Vera: It is succulent plant of genus Aloe. It is used as medicinal plant since ancient times Aloe vera gel is an ingredient in skin lotions, sun blocks and cosmetics. The gel of the inner leaf can be applied directly to the minor burns immediately after the injury The inner leaf lining of the plant is used as a potent natural laxative [40]The terpenoids, flavonoids, tannins and saponins, anthraquinone derivatives, barbaloin, aloe-emodin-9-anthrone, isobarbaloin, and anthrone-C-glycosides are chemical constituents of this plant[41] Karthik Subramani et al have proved that nanoparticles prepared from leaves of this plant have better antimicrobial properties. They used gel from leaves to prepare nanoparticles of size 40 ± 2 nm The particles were synthesized using top to down approach The gel was ground using a mixer grinder to make coarse powder. The coarse powder was then milled for 1 h using 20 mm sized Zirconia balls using Ball mill at 300 rpm to get fine powder. The obtained fine powder was again milled using 10 mm balls with speed of 300 rpm, 20:1 ball ratio for 15 h The amorphous herbal A. vera nanoparticles possess an average particle size of 40 ± 2 nm Synthesized nanoparticles used to with chitosan to prepare nanocomposite. This composite is found to have advanced antimicrobial activity [42].



Ref no 42 Antimicrobial activity

3] **Selected Mangroves:** Mangroves are halophytic plants [43]. They grow along the coastline in the areas where river water mixes with sea water under extreme environmental conditions such as high salinity, temperature and radiation [44]. Mangroves synthesize number of secondary metabolites adjust to change in environment. [45]. Mangroves have lot of medicinal properties Many species of mangroves produce bioactive compounds with anti-microbial activity against pathogenic strains. [46] They contain secondary metabolites like alkaloids, phenolics, steroids and terpenoids [47]. Mangroves are plants that have antibacterial, antioxidant, and antifungal, anti-cancer properties [48]. K. Vijaya Kumar et al synthesized nanoparticles of some mangrove plants like *Rhizophora apiculata*, *Avicennia marina*, *Excoecaria agallocha*. The average crystal size of *Rhizophora apiculata* was found to be 14.38 nm that of *Avicennia marina* 26.38 nm and *Excoecaria agallocha* nanoparticles are of 28.70 nm. The herbal nanoparticles prepared through ball milling technique have excellent antimicrobial activity. Due to smaller size of homogeneous nanoparticles, there is enhancement in the antimicrobial activity. This study confirms that smaller nanoparticles with high surface area showed the maximum zone of inhibition than higher particle size with smaller surface area. [49]

. 4] **Azadirachta indica** : It is commonly known as Neem, it belongs to Meliaceae family [50]. Nimbin, nimbanene, 6-desacetylnimbinene, nimbandiol, nimbolide, ascorbic acid, n-hexacosanol and amino acid, 7-desacetyl-7-benzoylazadiradione, 7-desacetyl-7-benzoylgedunin, 17-hydroxyazadiradione and nimbiol are chemical constituents of neem leaves extract [51]. Because of these compounds. its extracts have antiviral, antibacterial, antifungal, anthelmintic, antiallergic, anti-dermatic and anti-inflammatory properties Neem seeds oil is used in medicines, pest control and cosmetics etc. Neem leaves are used in the treatment of chicken pox. Neem is also used as pesticide [52]. Karthik Subramani et al prepared nanoparticles of various sizes from shade dried neem leaves using ball mill without using any additive by keeping the processing parameters such as diameter of ball as 10 mm, 300 rpm speed and a milling time of 15 h These nanoparticles were coated on cotton fabrics. The presence of nanoparticles on the fabric electron microscopy and spectroscopic studies were used for confirmation of presence of nanoparticles. The elemental composition of the herbal nanoparticles was analyzed using EDX and XRF. Nanoparticles on fabric shows antimicrobial activity This proves that the natural phytochemical constituents of *A. indica* nanopowder retain their medicinal property even after nanosizing [53].



Antimicrobial activity and image of nanoparticles [53]

5]Cordia myxa : Cordia myxa is a plant from Boraginaceae family [54] The fruits of this plant have carbohydrates, proteins, glycosides, alkaloids, flavonoids, phenolic compounds and tannins. In addition to these they found to contain phytol, linoleic acid, olealdehyde, stigmastanol, γ -sitosterol, several esters and phosphate ester-derivatives, and a fat-soluble form of ascorbic acid [55]. The extract of this fruit is found to have antitussive, analgesic, acute and chronic anti-inflammatory effects. An attempt has been made by Shokooh Salimimoghadam et al to

compare the pharmacological efficacy of Cordia myxa hydro-alcoholic extract and nanoparticles of hydro-alcoholic extract (NPE) for hypoglycemic, antitussive, anti-inflammatory and analgesic activity. They synthesized nanoparticles by using hydro-alcoholic extract powders which were cryomilled in the liquid nitrogen using the zirconia balls at -50°C using a home-made attritor. The ball to powder ratio was 25:1 and the attrition speed was 250 rpm. The resulting mixture has been dried in an oven at 50°C for 12 hr. SEM imaging was used for particle size determination. It was observed that nanoparticles of extract had better anti-inflammatory and analgesic activity compared to bulk extract [56].

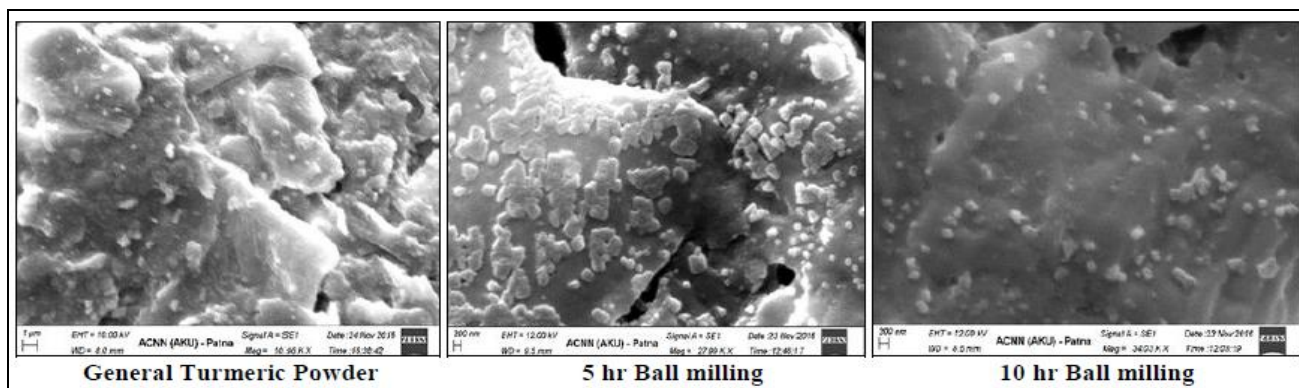
6]Curcuma longa: Curcuma longa L. (turmeric) belongs to ginger family (Zingiberaceae). It is the oldest cultivated spice plant in the south-east Asian countries. [57] For many years rhizome of this plant were used as a safe and active drug for the treatment of various chronic diseases, especially of diabetes mellitus [58]. The active components of turmeric are the volatile oil and curcuminoids and both the constituents are present in oleoresin extracted from the turmeric root. The essential oils are composed mainly of sesquiterpenes, many of which are specific for the Curcuma genus [59]. Abhay Kumar Aman et al in 2018 prepared curcuma longa nanopowder using ballmilling method. In these experiments, High energy ball-mill equipped with an insulation cover and cooling machine was used for this purpose. The weight ratio of powder to ball was taken as

1:20 in the 50 mL stainless steel jar. Each container was filled to approximately one third of their capacity. During milling, the jars were rotated at a constant milling speed of 500 rpm for up to 5 h and 10 h respectively. The ball-milling rotational direction was changed every 30 min. The ballmilling process was carried out at 27 °C and the temperature was maintained by the air cooling system to prevent overheating Particle size determination was done by X-ray diffractometer Thus XRD study proved that particle size, crystallinity and peak intensity height changes as the milling hour change As milling hours change from 5 hrs to 10 hrs colour of the material changes from yellow to light

red deep red. Fluorescence peak intensity was found to change with change in size Changed sized [nanosized] materials possess luminescence hence can be usedfor biomedical applications and inpharmaceutical industry. Therefore, superfine particle canbe potential for drug delivery system. [60].



Continous colour change [60]



SEM images for prepared Nanoparticles[60]

7]Jatropha curcas: *Jatropha curcas* belongs to Euforbiaceae family is a multipurpose tree, an alternative source for biodiesel production, food, feed, fertilizers and in traditional medicine [61]. All parts of this plant are useful *Jatropha curcas* is traditionally used as anti- bacterial and anti-fungal infections and for muscle pain or jaundice [62]. Shells of fruit have 34%, 10% and 12% cellulose, hemicellulose and lignin, respectively. Volatile matter, ash and fixed carbon content of the shell have been shown to be 69%, 15% and 16%, respectively [63]. An innovative effort was made by Ramamoorthy KOKILA et al to make nanoparticles from shells of fruit They used high energy milling using 20 mm sized ball (Zirconia) in a Planetary Ball mill for 1 h. fine powders were obtained which was divided equally into four parts. The separated fine powders were again milled using 10 mm balls at speed of 300 rpm for 1 h. TEM images were used to obtain particle size and SAED patterns were used determination of crystallinity Effect of nanosizing was noticing changes on biological activity of the shell nanoparticles in terms of their antibacterial activity against gram positive and gram negative organisms, antioxidant property against DPPH reagent at different concentrations of particle treatment. The particles were in size range of 80-96 nm exhibited considerable broad spectrum antibacterial activity against gram positive and gram

negativemicroorganismsThe evaluation of antioxidant property of shell powders showed the good response against DPPH. This shows that nanosized shell particles can be used for biological and cosmetic applications [64].

7] **Melinjo:**The scientific name of melinjo is *Gnetum gnemon*. It is a species of *Gnetum*. It is native to southeast Asia and the western Pacific Ocean islands, from Mizoram and Assam in India. The melinjo seeds contain dimeric stilbenoids gnetin C and its glucosides (gnemonosides A, C, and D), with trans-piceid glucoside as a minor constituent, including negligible amount (0.1%) of trans-resveratrol (tRV)[65]. Its seed powder extract exhibited antioxidant and tyrosinase inhibitory activity, thus can be used as a dietary supplement or can act as nutraceutical to prevent aging or hyperpigmentation[66]. Particle size plays an important role in extraction of bioactive compounds and influences their bioactivity therefore VIENNA SARASWATY et al in 2019 made an attempt to transform melinjo seed micropowders into nanopowders by nanomilling using a high-energy ball mill. The dried and powdered melinjo seeds and 10 stainless beads of 50 g of 0.5 cm diameter were used in the milling chamber. Milling durations of 30, 60, 90 and 120 min were applied. The effects of particle size of melinjo seed powder on its physicochemical characteristics, extraction efficiency and release of phenolic compounds, and its tyrosinase inhibitory activity was observed. Particle size analysis proved that melinjo seed nanopowders were with a mean particle diameter of ~675 nm (PI 0.270). SEM images of the nanopowders showed a smaller particle size, a smooth surface, amorphous shapes and irregular edges. The melinjo seed nanopowders at mean particle diameter of ~675 nm exhibited the highest extraction yield and phenolic compounds release. The tyrosinase inhibitory activity of nanopowders was 4.5 times greater than that of the melinjo seed micropowders. From these observations it can be proved that transformation of

melinjo seed micropowders into nanopowders is good method for improving the efficacy of melinjo seed as tyrosinase inhibitor [67].

8] 9] **Loranthus micranthus**: *Loranthus micranthus* (L. *micranthus*) as member of the Loranthaceae family It is called as “an all-purpose herb” due as it is traditionaly and widely used in ethnomedicine for various purposes like antihypertensive, anticancer, antispasmodic, and antidiabetic herb, It is also used for treatment of epilepsy, headache, infertility, menopausal syndrome and rheumatism[68]. It is found to possess terpenoids, steroids, oils, proteins, resins, flavonoids, tannins, saponins, alkaloids, reducing sugar, acidic compounds, glycosides, and carbohydrates [69]. Muhammad Sarfraz et al in 2018 synthesized nanoparticles from dried leaves and stems of *Loranthus micranthus* with the ball-milling, high speed stirring, and high-pressure homogenization techniques. The nanoparticles were characterized using laser diffraction analysis, photon correlation spectroscopy analysis, and light microscopy.

The average size of nanoparticles was around 245 nm and that of stem nanoparticles was around 180 nm. The nanoparticles were tested for their antimicrobial and nematicidal properties against a Gram-negative bacterium *Escherichia coli*, a Gram-positive bacterium *Staphylococcus carnosus*, fungi *Candida albicans* and *Saccharomyces cerevisiae*, and a nematode *Steinernema feltiae* The research showed that nanosuspensions can be prepared easily and which shows pronounced antimicrobial and nematicidal activities, These suspensions shows higher particle concentrations of 0.1% (w/w), compete well with those of established antibiotics and fungicides [70].

9] **Tridax procumbens**: It is commonly known as coatbuttons or tridax daisy, it belongs to the daisy family. e flavonoid procumbenetin has been isolated from the aerial parts of *Tridax procumbens*. Other chemical compounds isolated from the plant include alkyl esters, sterols, pentacyclic triterpenes fatty acids_ and polysaccharides [71]. Subramani

Karthik et al in 2018 prepared from shade dried *Tridax procumbens* plant leaves using ball milling technique using different process parameters, like ball ratio/size and milling time. The obtained nanoparticles were characterised using X-ray diffraction, Fourier transform infrared spectroscopy, UV-visible spectroscopy, dynamic light scattering, scanning electron microscopy and antimicrobial analysis techniques. The antibacterial activities of the prepared herbal nanoparticles against *Staphylococcus aureus* and *Escherichia coli* were found. It showed the influence of particle size on antimicrobial activities and their functional properties. They proved that with the increase in ball ratio and milling time periods leads to a decrease in nanoparticle size from 114 to 45 nm which increases the antimicrobial activities [72].

10] **Zingiber officinale** :It is commonly known as ginger. It is a flowering plant of which rhizomes are used as spice or herbal medicine. Ginger contains compounds such as gingerols, shogaols and their derivatives [73]. Its major constituents are inefficiently absorbed because of their complex structure and insolubility in water. A. Norhidayah et al prepared its nanoparticles using a planetary ball milling process and investigated the effect of prolonged milling time up to 8 hours on the physical and antioxidant properties. The particle size was reduced to 222.3 nm after 4 hours of milling process. Sample milled for 4 hours showed higher Total Phenolic Content and Total Flavonoid Content (TFC) but their amount reached lowest value when sample was milled for 8 hours. The inhibition of DPPH reached up to 60% for the tested nanostructured ginger except very low percent of inhibitory shown by sample milled for 6 hours. The sample milled for 8 hours showed significantly greater Ferric Reducing Antioxidant Power (FRAP) among all other samples [74]. They also investigated effect of nanosizing ginger rhizome by dry and wet milling and compared activity of nanoparticles with micron and submicron size particles and they found ABTS free radical scavenging activity and FRAP compared to the other samples tested. The antioxidant

activity was maximum for nanoparticles prepared by dry milling and least in micron size particles. It emphasizes the fact nanosizing by dry grinding improves activity of ginger [75].

Conclusion:

It can be proved that particle size reduction especially nanosizing particles can improve solubility and increase the dissolution rate of poorly water soluble active pharmaceutical ingredients. There are many researches going on in the world on the herbal medicines and remedies. The drawbacks of herbal drugs have been studied. Many other methods are suggested to overcome these issues but nanotechnology gives promising results. Nanosizing these herbal medicines improve their bioavailability, stability and water solubility. All of the nano-herbal medicines discussed above have demonstrated the significantly enhanced efficacies. Also due to nanosizing side effects of large dosages are also minimized.

References

1. Saudagar, Ravindranath B., and Shivani Saokar. "Anti-inflammatory natural compounds from herbal and marine origin." *Journal of Drug Delivery and Therapeutics* 9.3 (2019): 669-672.
2. Almatroodi, Saleh A., et al. "Ocimum sanctum: role in diseases management through modulating various biological activity." *Pharmacognosy Journal* 12.5 (2020).
3. Baraf, Herbert SB, et al. "Gastrointestinal side effects of etoricoxib in patients with osteoarthritis: results of the Etoricoxib versus Diclofenac Sodium Gastrointestinal Tolerability and Effectiveness (EDGE) trial." *The Journal of rheumatology* 34.2 (2007): 408-420.

4. Maniar, Kevin H., et al. "Lowering side effects of NSAID usage in osteoarthritis: recent attempts at minimizing dosage." *Expert opinion on pharmacotherapy* 19.2 (2018): 93-102.
5. Vodnar, Dan Cristian, et al. "Removal of bacteria, viruses, and other microbial entities by means of nanoparticles." *Advanced Nanostructures for Environmental Health*. Elsevier, 2020. 465-491.
6. Karimi, Mahdi, et al. "pH-Sensitive stimulus-responsive nanocarriers for targeted delivery of therapeutic agents." *Wiley Interdisciplinary Reviews: Nanomedicine and Nanobiotechnology* 8.5 (2016): 696-716.
7. Häuser, Winfried, et al. "Efficacy, tolerability and safety of cannabis-based medicines for cancer pain." *Der Schmerz* 33.5 (2019): 424-436.
8. Taylor, Jeff. "Over-the-counter medicines and diabetes care." *Canadian journal of diabetes* 41.6 (2017): 551-557.
9. Etheridge, Michael L., et al. "The big picture on nanomedicine: the state of investigational and approved nanomedicine products." *Nanomedicine: nanotechnology, biology and medicine* 9.1 (2013): 1-14.
10. Bonifácio, Bruna Vidal, et al. "Nanotechnology-based drug delivery systems and herbal medicines: a review." *International journal of nanomedicine* 9 (2014):
11. Taylor, Jeff. "Over-the-counter medicines and diabetes care." *Canadian journal of diabetes* 41.6 (2017): 551-557.
12. Maqbool, Mudasir, et al. "Herbal medicines as an alternative source of therapy: a review." *World Journal of Pharmacy and Pharmaceutical Sciences* 3.2 (2019): 374-380.

13. Kumadoh, D. O. R. I. S., and K. W. A. B. E. N. A. Ofori-Kwakye. "Dosage forms of herbal medicinal products and their stability considerations-an overview." *J Crit Rev* 4.4 (2017): 1-8.
14. Sahoo, Jyoti Prakash, et al. "Turmeric (Haldi)-A strapping strategy for enhancing the immune system to reduce the effect of SARS-CoV-2." *Food and Scientific Reports* 1.8 (2020):
15. Kafle, Gandhiv, et al. "Why do patients choose to consume Ayurvedic Medicines in Nepal? An exploratory study." *International Journal of Ayurvedic Medicine*. 9.4 (2018): 250-7.
16. Qadir, Sami Ullah, and Vaseem Raja. "Herbal medicine: Old practice and modern perspectives." *Phytomedicine*. Academic Press, 2021. 149-180.
17. Mundy, Lorna, Barbara Pendry, and Mukhlesur Rahman. "Antimicrobial resistance and synergy in herbal medicine." *Journal of Herbal Medicine* 6.2 (2016): 53-58.
18. Khogta, Saloni, et al. "Herbal nano-formulations for topical delivery." *Journal of Herbal Medicine* 20 (2020): 100300.
19. Patra, Jayanta Kumar, et al. "Nano based drug delivery systems: recent developments and future prospects." *Journal of nanobiotechnology* 16.1 (2018): 1-33.
20. Carmona, Fabio, and Ana Maria Soares Pereira. "Herbal medicines: old and new concepts, truths and misunderstandings." *Revista Brasileira de Farmacognosia* 23 (2013): 379-385.
21. Sarangi, Manoj Kumar, and Sasmita Padhi. "Novel herbal drug delivery system: An overview." *Archives of Medicine and Health Sciences* 6.1 (2018): 171.
22. Garg, Ashish. "Herbal Nanotherapeutics: A noval approach for herbal drug delivery system." *Journal of Medical Pharmaceutical and Allied Sciences (March_2016)* 1.10 (2016): 1.

23. Arai, Ichiro. "Clinical studies of traditional Japanese herbal medicines (Kampo): Need for evidence by the modern scientific methodology." *Integrative medicine research* (2021): 100722.
24. Dongare, Prajakta N., et al. "Recent development in novel drug delivery systems for delivery of herbal drugs: An updates." *GSC Advanced Research and Reviews* 8.2 (2021): 008-018.
25. Shah, Syed Muhammad Ali, et al. "Nanobiomedicine: A New Approach of Medicinal Plants and Their Therapeutic Modalities." *Journal of Materials and Environ* 12.1 (2021): 1-14.
26. Sur, Srija, et al. "Recent developments in functionalized polymer nanoparticles for efficient drug delivery system." *Nano-Structures & Nano-Objects* 20 (2019): 100397
27. Sahu, Alakh N. "Nanotechnology in herbal medicines and cosmetics." *International Journal of Research in Ayurveda and Pharmacy (IJRAP)* 4.3 (2013): 472-474.
28. Goga, Michal, et al. "Biological activity of selected lichens and lichen-based Ag nanoparticles prepared by a green solid-state mechanochemical approach." *Materials Science and Engineering: C* 119 (2021): 111640.
29. Silva Adaya, Daniela, et al. "Nanobiomaterials' applications in neurodegenerative diseases." *Journal of biomaterials applications* 31.7 (2017): 953-984.
30. Elkordy, Amal Ali, et al. "An overview on natural product drug formulations from conventional medicines to nanomedicines: Past, present and future." *Journal of Drug Delivery Science and Technology* (2021): 102459
31. Qidwai, Afifa, et al. "Advances in biogenic nanoparticles and the mechanisms of antimicrobial effects." *Indian Journal of Pharmaceutical Sciences* 80.4 (2018): 592-603.

- 32.** Vodnar, Dan Cristian, et al. "Removal of bacteria, viruses, and other microbial entities by means of nanoparticles." *Advanced Nanostructures for Environmental Health*. Elsevier, 2020. 465-491.
- 33.** Illath, Kavitha, et al. "Metallic Nanoparticles for Biomedical Applications." *Nanomaterials and Their Biomedical Applications* 16 (2021): 29.
- 34.** Arora, Anil. "Nanomaterials: Methods of Generation." *Nanotechnology*. CRC Press, 2020. 11-22.
- 35.** Nilssen, Benedicte Eikeland, and Rolf Arne Kleiv. "Silicon Powder Properties Produced in a Planetary Ball Mill as a Function of Grinding Time, Grinding Bead Size and Rotational Speed." *Silicon* (2020): 1-11.
- 36.** Akkaya, Barış, İhsan Toroğlu, and Mehmet Bilen. "Studying the effect of different operation parameters on the grinding energy efficiency in laboratory stirred mill." *Advanced Powder Technology* 31.11 (2020): 4517-4525.
- 37.** Mondal, Rimi, Arvind Negi, and Manish Mishra. "ACALYPHA INDICA—A BOON TO MANKIND." (2021).
- 38.** Marwah, Ruchi G., et al. "Antioxidant capacity of some edible and wound healing plants in Oman." *Food chemistry* 101.2 (2007): 465-470.
- 39.** Karthik, S., et al. "Larvicidal, super hydrophobic and antibacterial properties of herbal nanoparticles from *Acalypha indica* for biomedical applications." *RSC advances* 7.66 (2017): 41763-41770.
- 40.** Raad, Bibi, et al. "3. Phytochemical screening and biological activities of *Aloe vera* (L.) Burm. F." *Pure and Applied Biology (PAB)* 10.2 (2020): 360-367.

41. Bhattacharya, Mamta, Suman Malik, and Archana Singh. "Aloe vera *Barbedensis*: A review on its Ethanopharmacological value." *J. Pharm. Res* 4 (2011): 4507-4510
42. Subramani, Karthik, et al. "Screening the UV-blocking and antimicrobial properties of herbal nanoparticles prepared from Aloe vera leaves for textile applications." *IET nanobiotechnology* 12.4 (2018): 459-465.
43. Vanegas, Javier, et al. "Effect of salinity on fungal diversity in the rhizosphere of the halophyte *Avicennia germinans* from a semi-arid mangrove." *Fungal Ecology* 42 (2019): 100855.
44. Cavanaugh, Kyle C., et al. "Climate-driven regime shifts in a mangrove–salt marsh ecotone over the past 250 years." *Proceedings of the National Academy of Sciences* 116.43 (2019): 21602-21608.
45. Gouda, Sushanto, et al. "Synthesis of nanoparticles utilizing sources from the mangrove environment and their potential applications: an overview." *Nanomaterials in plants, algae and microorganisms* (2019): 219-235.
46. Hodhod, Mohamed Salah El-Din, et al. "Molecular characterization and bioactive potential of newly identified strains of the extremophilic black yeast *Hortaea werneckii* isolated from Red Sea mangrove." *Biotechnology & Biotechnological Equipment* 34.1 (2020): 1288-1298.
47. Khalil, A. M. A., et al. "Fungal endophytes from leaves of *Avicennia marina* growing in semi-arid environment as a promising source for bioactive compounds." *Letters in Applied Microbiology* 72.3 (2021): 263-274.
48. Rahaman, Md Sohanur, et al. "Molecular phylogenetics and biological potential of fungal endophytes from plants of the sundarbans Mangrove." *Frontiers in microbiology* 11 (2020).

49. Kumar, Kovvada Vijaya, et al. "A STUDY ON ANTIMICROBIAL PROPERTIES OF HERBAL NANOPARTICLES OF SELECTED MANGROVE PLANTS." (2018).
50. Chakraborty, Krishnasis, Arun Shivakumar, and Sundaram Ramachandran. "Nano-technology in herbal medicines: a review." *Int J Herb Med* 4.3 (2016): 21-27.
51. Rangiah, Kannan, and Malali Gowda. "Method to quantify plant secondary metabolites: quantification of neem metabolites from leaf, bark, and seed extracts as an example." *The Neem Genome*. Springer, Cham, 2019. 21-30.
52. Sharma, Vikash. "A review on medicinal properties of neem (*Azadirachta indica*)." (2018).
53. Subramani, Karthik, et al. "An ecofriendly route to enhance the antibacterial and textural properties of cotton fabrics using herbal nanoparticles from *Azadirachta indica* (neem)." *Journal of Alloys and Compounds* 723 (2017): 698-707.
54. Guz, Nurper, et al. "Detection of *Wolbachia* (Rickettsiales: Anaplasmataceae) and *Candidatus Liberibacter asiaticus* (Rhizobiales: Rhizobiaceae) Associated With *Diaphorina citri* (Hemiptera: Liviidae) Collected From *Citrus reticulata* (Sapindales: Rutaceae) and Alternate Host, *Cordia myxa* (Boraginales: Boraginaceae)." *Journal of economic entomology* 113.3 (2020): 1486-1492.
55. Sahib, Ahmed Hadi Abdal, Ekhlal Al-Shareefi, and Imad Hadi Hameed. "Harpagophytum procumbens and *Cordia myxa*: In vitro Antibacterial Activity and Bioactive Compounds of Methanolic Fruit Extract Using Fourier-Transform Infrared Spectroscopic Technique." *Indian Journal of Public Health Research & Development* 10.1 (2019): 981-987.

- 56.** Salimimoghadam, Shokooh, et al. "Hypoglycemic, antitussive and analgesic effects of nanoparticles of *Cordia myxa* fruits extract." *International Journal of Pharmaceutical Investigation* 9.4 (2019): 205-209.
- 57.** Nair, Kodoth Prabhakaran. *Turmeric (Curcuma Longa L.) and Ginger (Zingiber Officinale Rosc.)-World's Invaluable Medicinal Spices: The Agronomy and Economy of Turmeric and Ginger*. Springer Nature, 2019.
- 58.** Arlı, Merve, and Hülya Çelik. "The Biological Importance of Curcumin." (2020).
- 59.** Dosoky, Noura S., and William N. Setzer. "Chemical composition and biological activities of essential oils of *Curcuma* species." *Nutrients* 10.9 (2018): 1196.
- 60.** Aman, Abhay Kumar, et al. "Effect of high energy ball milling grinding on physico-chemical, morphological and optical properties of *Curcuma longa* nanoparticles powders." *Int J Pharm Sci Res* (2018): 672-77.
- 61.** Kancharla, Nagesh, et al. "De novo sequencing and hybrid assembly of the biofuel crop *Jatropha curcas* L.: identification of quantitative trait loci for geminivirus resistance." *Genes* 10.1 (2019): 69.
- 62.** Susaya-Garcia, Janice, et al. "An Ethnobotanical Study of Medicinal Plants and Perceptions on Plant Biodiversity Conservation in Leyte, Philippines." *Journal of Human Ecology* 7.1 (2018).
- 63.** Piloto-Rodríguez, Ramón, et al. "An approach to the use of *Jatropha curcas* by-products as energy source in agroindustry." *Energy Sources, Part A: Recovery, Utilization, and Environmental Effects* (2020): 1-21.

- 64.** Kokila, Ramamoorthy, et al. "Antibacterial and antioxidant potential of herbal nanoparticles produced from the shells of *Jatropha Curcas*." *Adv. Nano-Bio-Mater. Dev* 1 (2017): 39-47.
- 65.** Narayanan, Narayanan K., et al. "Antitumor activity of melinjo (*Gnetum gnemon* L.) seed extract in human and murine tumor models in vitro and in a colon-26 tumor-bearing mouse model in vivo." *Cancer medicine* 4.11 (2015): 1767-1780.
- 66.** Espinoza, J. Luis, et al. "Stilbene derivatives from melinjo extract have antioxidant and immune modulatory effects in healthy individuals." *Integrative Molecular Medicine* 2.6 (2015): 405-413.
- 67.** Saraswaty, Vienna, Ni Wayan Wulan Prawerti Suparta, and Henry Setiyanto. "Transformation of Melinjo Seed Micropowders into Nanopowders Enhances Extractability of Phenolic Compounds and Tyrosinase Inhibitory Activity." *Sains Malaysiana* 48.5 (2019): 983-990.
- 68.** Zorofchian Moghadamtousi, Soheil, et al. "Loranthus micranthus Linn.: biological activities and phytochemistry." *Evidence-Based Complementary and Alternative Medicine* 2013 (2013).
- 69.** Osadebe, P. O. "An Investigation into The Seasonal Variation of The Phytochemical and Anti-Diabetic Properties of The Eastern Nigerian Specie of African Mistletoe (*Loranthus Micranthus*) Sourced from *Kola Acuminata*. *Diabetes Complications*. 2021; 5 (2); 1-5. Correspondence: Johnson-Ajinwo, OR, Department of Pharmaceutical." *Medicinal Chemistry, Faculty of Pharmaceutical Sciences, University of Port Harcourt, Choba*. Received 2 (2021).

- 70.** Sarfraz, Muhammad, et al. "Milling the mistletoe: Nanotechnological conversion of african mistletoe (*Loranthus micranthus*) into antimicrobial materials." *Antioxidants* 7.4 (2018): 60.
- 71.** Jaiswal, Rushika, Yash Jaiswal, and Aakash Gajbhaye. "A Review Study of Various Pharmacological Activity of *Tridax Procumbens* Linn Plant."
- 72.** Mao, Qian-Qian, et al. "Bioactive compounds and bioactivities of ginger (*Zingiber officinale* Roscoe)." *Foods* 8.6 (2019): 185.
- 73.** Norhidayah, A., A. Noriham, and Mohamad Rusop. "Changes in physical and antioxidant properties of nanostructured zingiber officinale (ginger) rhizome as affected by milling time." *Advanced Materials Research*. Vol. 667. Trans Tech Publications Ltd, 2013.
- 74.** van der Wall, Sake J., et al. "Higher adherence to treatment with low-molecular-weight-heparin nadroparin than enoxaparin because of side effects in cancer-associated venous thromboembolism." *HemaSphere* 2.1 (2018).
- 75.** A. Norhidayah 1 & 2, A. Noriham 1 and M. Rusop "Antioxidant Property of Dry and Wet Mill Nanostructured *Zingiber Officinale* Rosc. (Ginger) Rhizome: A Comparative Study ." *International Conference on Food and Agricultural Sciences IPCBEE* vol.55 (2013).

Paper-28

Optimization of Gamma Ray Spectroscopy Technique for Measurement of Nuclear Pollution of Water samples due to Uranium and Thorium salts.

Swarali Hinge, Digvijay Gore, G. R. Pansare

Department of Physics, Haribhai V. Desai College, Pune

ABSTRACT

Uranium and Thorium are naturally occurring radioactive elements in the earth crust, which emits alpha particles, gamma and beta radiations with long half life of 10^{10} years. Though Uranium and Thorium are used as nuclear fuel in thermal and fast neutron reactor technology for the nuclear power generation, but it is hazardous for living life due to its harmful nuclear radiations. Salts of Uranium and Thorium are water soluble, therefore, they make the nuclear water pollution mostly at coastal areas where Uranium and Thorium storage in the earth crust are found. In view of this, efforts are made to optimize gamma ray spectroscopy technique to determine the concentration level of these radioactive material in water samples. In present work, it has been found that Uranium salt emits gamma radiation of energies **590 KeV, 750 KeV, 980 KeV, 1450 KeV**, and Thorium salt emits gamma radiation of energies **340KeV, 570KeV, 910KeV**. Concentrations of Uranium and Thorium in water samples are measured using NaI(Tl) gamma ray scintillation detector. Solutions of water samples are prepared with different concentration of Uranium and Thorium salt in the range **5% to 1.25% of Uranium and 1% to 0.125%of Thorium**. The minimum detectable levels of concentration of Uranium and Thorium in water samples are found to be **0.058 gm and 0.005gm** respectively. Estimated gamma ray activities of this minimum detectable level of the samples are found to be **0.0078Bq** and **0.046Bq** respectively for Uranium and Thorium. This gives the specific gamma ray activities of **0.1327 Bq/gm** and **9.2Bq/gm** of Uranium and Thorium in water samples respectively.

Keywords: NaI(Tl) , Gamma Ray Spectrometer, Activity, Uranyl Nitrate, Thorium Nitrate, Nuclear pollution

INTRODUCTION :

Salts of Uranium and Thorium are naturally radioactive and decays with their own series resulting into many radioactive nuclides such as Radium-228, Actinium-228, Radium-224, Radon-220, Polonium-216, Lead-212, Bismuth-212, Polonium-212. Many of them are having long half lives. These radioactive products emits alpha, beta and gamma radiations. These radiations are harmful to the living organisms. Uranium and Thorium are available in the form of salts. These salts dissolve into water and make soil and water pollution. Finally, these salts are taken up by the various crops through the water. This results into nuclear pollution in vegetables and food. Its radioactivity possesses increased risks of lung cancer and bone cancer. Uranium and Thorium are also chemically toxic at high concentrations and can cause damage to internal organs, notably the kidneys. Animal studies suggest that Uranium and Thorium may affect reproduction, increase the risk of soft tissue cancer, and drinking massive amounts of it can cause death from metal poisoning. Literature survey shows that the water of the coastal areas of India is naturally contaminated with Uranium and Thorium salts. In view of this, present research work is carried out to estimate trace concentration of Uranium and Thorium salt in water samples.

EXPERIMENTAL DETAILS :

NaI(Tl) gamma ray Spectrometer is calibrated using standard gamma ray sources provided by the B.A.R.C, Mumbai. This Spectrometer is coupled to 8K Multi-Channel Analyzer and computer. Water samples are prepared using Uranium and Thorium salts with different concentration levels in the range of 5% to 1.25% and 1% to 0.125% respectively. For this, standard Thorium nitrate $[\text{Th}(\text{NO}_3)_4 \cdot 5\text{H}_2\text{O}]$ and Uranyl Nitrate $[\text{UO}_2(\text{NO}_3)_2 \cdot 6\text{H}_2\text{O}]$ are used. Gamma ray activity of each water sample with different concentrations of Uranium and Thorium salt is measured for the gamma ray photo peak of gamma energies 750KeV and 570 KeV respectively. Measured gamma ray activity of each sample is used to estimate the activity of Uranium and Thorium using the efficiency of detector and geometrical factor. From this data, specific activity of the Uranium and Thorium sample are estimated using standard relations.

Table-1 represents gamma ray activities of water samples with different concentration of Uranium and Thorium salts.

Table 1: Measured Gamma Ray Activity of Thorium and Uranium in water samples.

Percentage of Thorium Nitrate in water	Amount of Thorium Nitrate (gm)	Amount of Thorium (gm)	Measured counts for 3600 sec. under photo peak	Estimated Activity (Bq)
100%	1.000	0.400	20786	0.607
1.000%	0.100	0.040	4326	0.126
0.500%	0.050	0.020	2464	0.072
0.250%	0.025	0.010	2213	0.066
0.125%	0.012	0.005	1536	0.046

Percentage of Uranyl Nitrate in water	Amount of Uranyl Nitrate (gm)	Amount of Uranium (gm)	Measured counts for 3600 sec. under photo peak	Estimated Activity (Bq)
100%	1.000	0.4670	2021	0.1180
5.00%	0.500	0.2350	666	0.0370
2.50%	0.250	0.1175	505	0.0290
1.25%	0.125	0.05875	143	0.0078

Figure-1: Gamma ray spectrum of pure Thorium Nitrate [Th(NO₃)₄.5H₂O] recorded by NaI(Tl) gamma ray detector

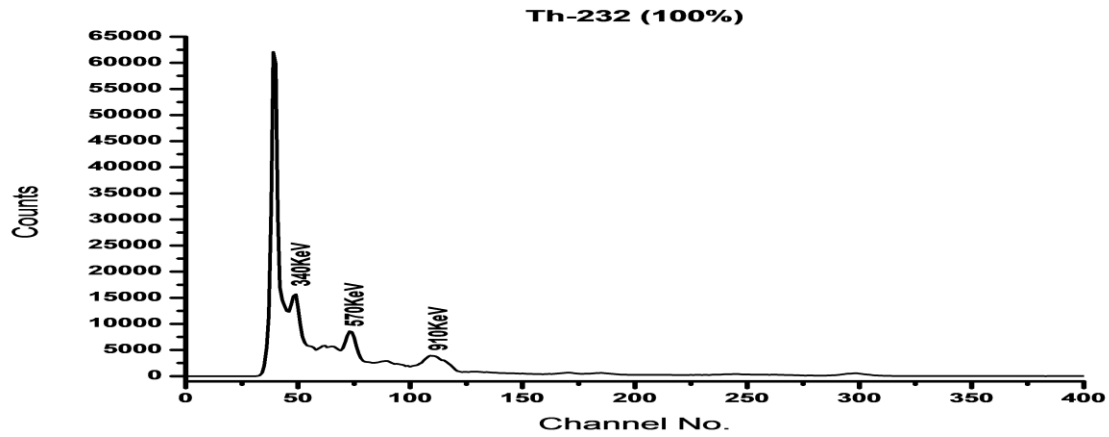


Figure-2: Gamma ray spectrum of 1% and 0.125% Thorium Nitrate in water sample

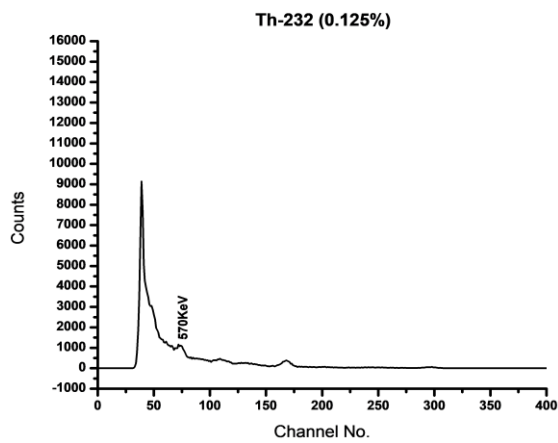
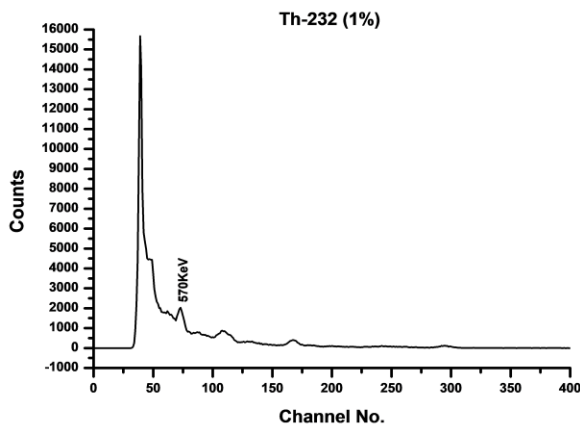


Figure-3: Gamma ray spectrum of pure Uranyl Nitrate $[UO_2(NO_3)_2 \cdot 6H_2O]$ recorded by NaI(Tl) gamma ray detector

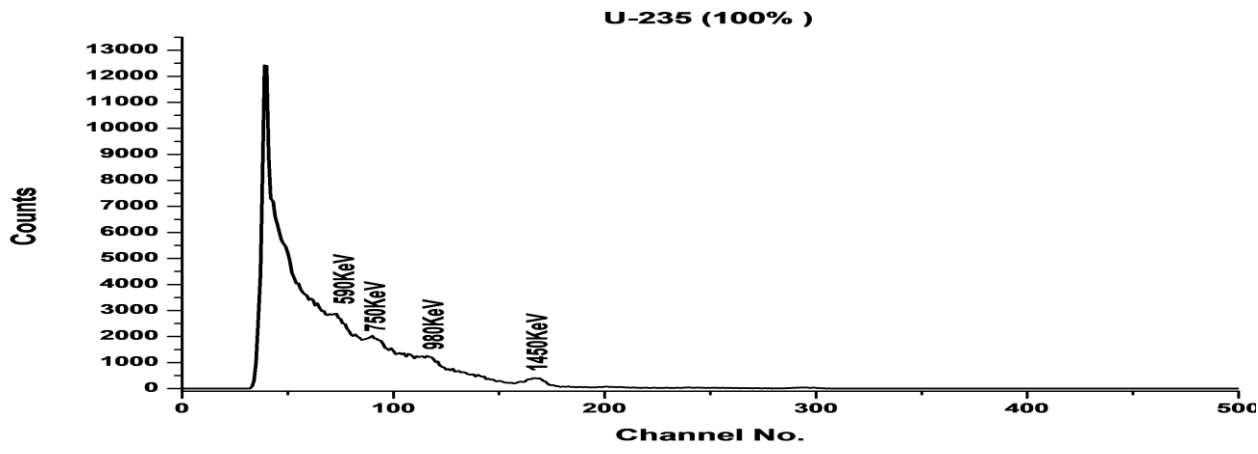
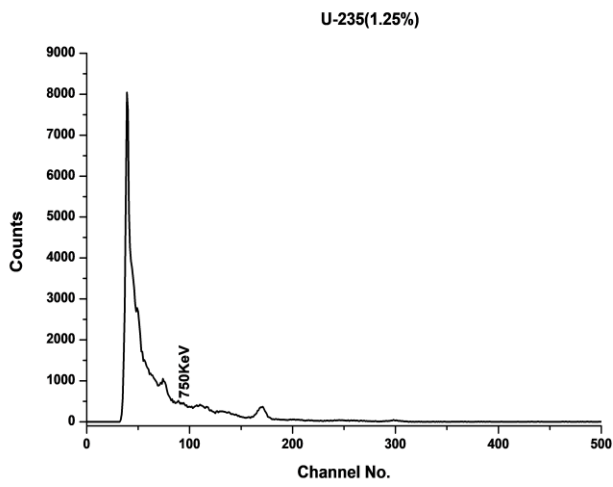
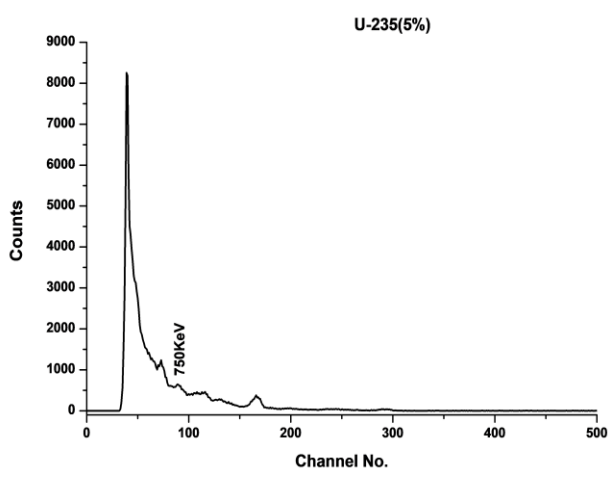


Figure-4: Gamma ray spectrum of 5% and 1.25% Uranyl Nitrate in water sample



RESULTS AND CONCLUSIONS :

Gamma ray spectrum of Thorium and Uranium salts given in figure-1 indicates that the Thorium salt [$\text{Th}(\text{NO}_3)_4 \cdot 5\text{H}_2\text{O}$] emits gamma ray of energies 340 KeV, 570 KeV, 910 KeV and figure-3 indicate that Uranyl Nitrate [$\text{UO}_2(\text{NO}_3)_2 \cdot 6\text{H}_2\text{O}$] emits gamma ray of energies 590 KeV, 750 KeV, 980 KeV, 1450 KeV.

The intensities of gamma energy 570KeV and 750KeV are found to be more as compared to the other gamma radiations of Thorium and Uranium respectively. These gamma photo peaks are used for analysis in the present work. Gamma ray spectrum of water samples of 1% and 0.125% concentration of Thorium and similarly Gamma ray spectra of water samples of 5% and 1.25% concentration of Uranium are given in fig-2 and fig-4 respectively. This indicate that intensity of gamma radiations has decreased rapidly with decreasing concentration of solution. The results obtained in present work shows that the gamma ray activity of Thorium and Uranium salt in water of minimum level are found to be **0.046 Bq and 0.0078 Bq** respectively. These minimum level of detection gives the specific activity of Thorium **9.2 Bq/gm** and of Uranium **0.1327 Bq/gm**. Results in the current work indicate that the present method can be used to estimate the trace concentration of Uranium and Thorium in water samples and hence can be used to determine the nuclear pollution in water.

ACKNOWLEDGEMENT :

Authors are thankful to the P.G.K. Mandal, Pune and the Principal Dr. G.R. Pathade, Haribhai V. Desai College, Pune for laboratory equipments and financial support.

REFERENCE :

- [1] S. S. Kapoor and V. S. Rmanurthy, "Nuclear Radiation Detectors New Age" International publications, 1986.
- [2] V. N. Manokhin, A. B. Pashchenko and V. I. Plyaskin, Handbook on Nuclear Activation Data, Technical Series Report No. 273, IAEA, Vienna (1987).
- [3] H. S. Hans, "Experimental and theoretical Nuclear Physics" New Age International publications, 2001.
- [4] D. C. Tayal, "Nuclear Physics" Himalaya Publishing House, 2008.
- [5] R. K. Singal, "Nuclear Reactor" New Age International publications, 2014

Paper-29

Theoretical drying time from drying characteristics

S.R. Navale, S. K. Thorat and S.N. Dalvi

¹S.R. Navale, Assistant Professor, Department of Physics, S.N. Arts, D.J.M.Commerce and B.N. Sarda Science College, , Sangamner, Maharashtra, India.

³Assistant Professor, Department of Physics, Adoc. M. N. Deshmukh College, Rajur Maharashtra, India

² Assistant Professor, Department of Physics, .N. Arts, D.J.M.Commerce and B.N. Sarda Science College, Sangamner, Maharashtra, India

Abstract:

Dehydration of fruits and vegetables means elimination of moisture from the internal part of the material to the surface and further to remove the moisture from the surface of the drying material in to the atmosphere. It is composite process of heat and mass transfer which depends on constraints such as humidity, temperature, air flow velocity, shape and size of the material. It also depends on properties of drying material such as physical structure (density and porosity), surface characteristics (smooth or rough) and chemical composition (starches and sugar). In present research work we trying to calculate the drying time of vegetables theoretically by using Newton's law of cooling in falling rate period

Key Words: Dehydration, Constant rate period, Falling rate period

Introduction

The solar drying systems are classified in number of ways such as: natural convection solar dryers or direct type solar dryers, indirect type solar dryers and forced circulation solar dryers (**Leon et al., 2002; Tripathy and Kumar, 2009**). In case of direct type of solar dryers, the foodstuff is directly exposed into solar radiations through transparent glass or sheet covering and hence solar radiations are directly absorbed by the product. It is called natural convection dryers because the heated air flow is induced by temperature gradient. The effect of natural convection may be improved by the addition of chimney to the cabinet in which existing air is heated still more.

The indirect types of solar dryers are the dryers in which air is heated separately in solar air heater by utilizing solar radiations and then passed to the foodstuff. In these types of solar dryers, the drying chambers are insulated from all sides to decrease the rate of heat loss by conduction and convection through the sides. In case of forced convection solar dryers, the air is forced through a solar collector and perforated trays by fan or a blower normally used to as

active dryer. The advantages of these dryers are usually higher air flow rates, faster drying rate and superior control of hot air temperature. The comparative tests on these basic designs advised that, the mixed mode natural convection solar dryer is potentially the most effective and it shows to be particularly promising in tropical humid areas where climatic conditions favour to the sun drying of agricultural products. (Zaman and Bala, 1989, Navale et al,2015). For the dehydration of different agricultural products at a farm level, natural convection solar dryers are more preferred over forced convection solar dryers due to non- accessibility of or irregular electric power supply in rural communities. For comprehensive drying applications, numerous of direct, indirect and natural circulation solar dryers have been build up.

Material and Method

Characteristics of Drying

The amount of moisture transfer from the foodstuffs is varies from one material to another. It is greatly depends on wheather the material is hygroscopic or non-hygroscopic. In case of non hygroscopic materials, this can be dried to zero moisture level. For the hygroscopic materials like most of fuits and vegetables, it will constantly have a residual moisture. In hygroscopic material, the possible moisture is bound moisture (surface forces or closed capillaries) or unbound moisture due to surface tension of water as shown in figure 1. As the hygroscopic material is exposed to air, it will either desorb moisture or absorb moisture depending upon relative humidity of air. When the vapour pressure of water in the material becomes equal to the partial pressure of water in the surrounding air then equilibrium moisture content (EMC) will be reached (Srarma et al, 1995, Garg and Prakash, 2002). Therefore the equilibrium moisture content is important in the drying process as this is the minimum moisture to which the material can be dried under a given position of drying conditions

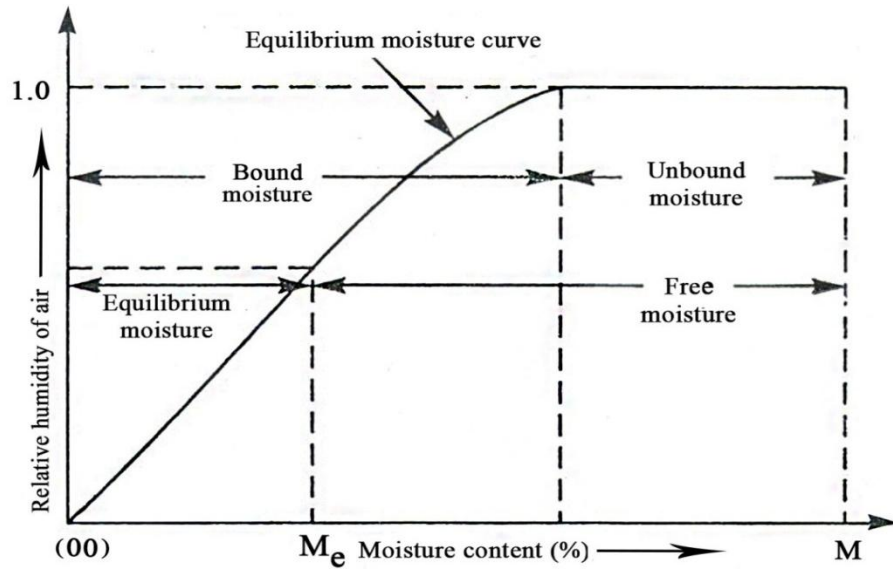


Figure:1 Moisture in the drying material

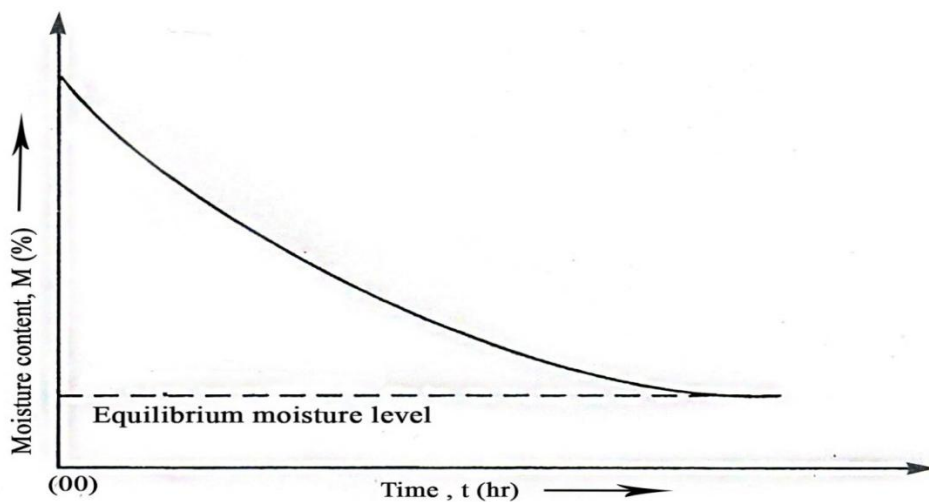


Figure: 2. Rate of moisture loss

A chain of drying curves can be plotted. The moisture content M of the material is plotted versus time as shown in figure 2. This characteristic indicates that, as time increases moisture content in the product is gradually decreases and attains the lowest position called as equilibrium moisture content. Moreover, another curve can be plotted between drying rate i.e. dM / dt versus moisture content M as shown in figure 3. which gives more information.

From this figure, it is observed that, constant drying rate terminating at the critical moisture content followed by falling drying rate for both hygroscopic & non hygroscopic material

For hygroscopic and non-hygroscopic materials the constant drying rate period is same whereas a falling rate period is little different. In case of non hygroscopic materials, the drying rate, the period of falling rate goes on decreasing till the moisture content becomes minimum

that is zero. But for the hygroscopic materials, the falling rate period is similar until the unbound moisture is entirely removed, then it is further decreases and a few bound moisture is removed. This process is continuous till the vapor pressure of drying air becomes equal to the vapor pressure of material (Garg and Prakash, 2002). As the equilibrium attains, then the drying rate becomes zero. The total heat content of the air remains constant therefore the constant drying rate is called as an adiabatic drying and depends on exterior factors such as thermodynamic state, transport properties of air, air flow rate and state of aggregation of material.

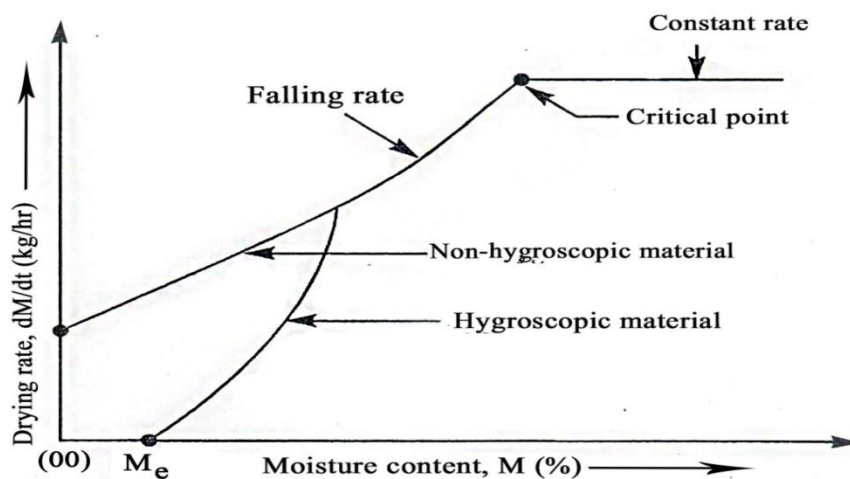


Figure 3: Drying rate Vs moisture content

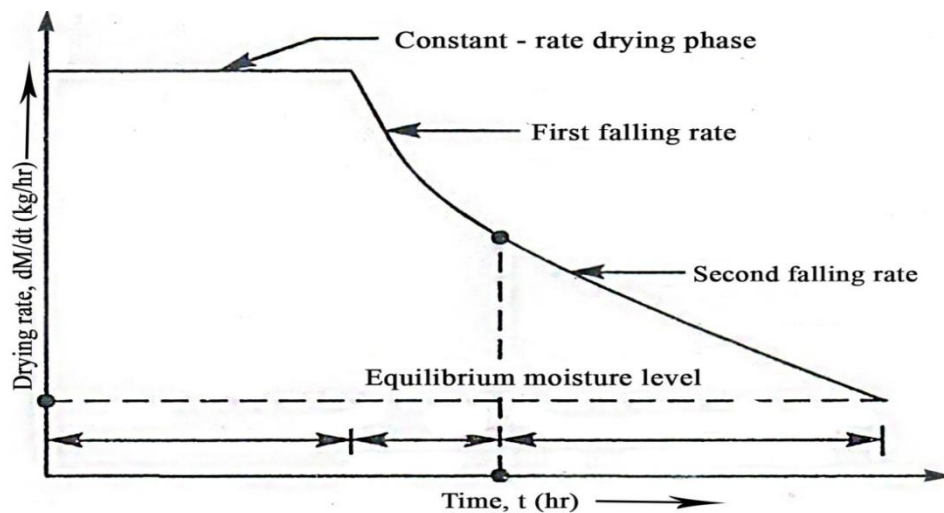


Figure 4: Drying rate Vs moisture content

For the dynamic equilibrium conditions, the rate of heat transfer to the surface is equal to the rate of water evaporated (Garg and Prakash, 2002).

$$\frac{dM}{dt} = \frac{Ah_D}{R_v T_{abs}} (P_{vwb} - P_\infty)$$

$$\frac{dM}{dt} = \frac{Ah_c}{L} (T_\infty - T_{wb}) \quad 2$$

Where,

A is surface area of drying material

h_D is mass transfer coefficient

h_c is convective heat transfer coefficient

L is latent heat of vaporisation

P_{vwb} is the vapour pressure of water in air at temperature T_∞

$P_{v\infty}$ is the vapour pressure of water at the surface of material and

T_{wb} is the wet bulb temperature.

For the constant rate period, the drying time, t_c is given by

$$t_c = \int_{M_e}^{M_0} \frac{R_v T_{abs} dM}{Ah_D (P_{vwb} - P_{v\infty})} = \int_{M_e}^{M_0} \frac{LdM}{Ah_c (T_\infty - T_{wb})} \quad 3$$

In case of constant rate period, the driving forces ($P_{vwb} - P_{v\infty}$) and ($T_\infty - T_{wb}$) are constant and above equation 3 becomes

$$t_c = \frac{(M_0 - M_e)R_v T_{abs}}{Ah_D (P_{vwb} - P_{v\infty})} = \frac{L(M_0 - M_e)}{Ah_c (T_\infty - T_{wb})}$$

4

From equations 1 and 2 it is observed that by increasing the surface area, initial air temperature, heat transfer coefficient, mass transfer coefficient, vapour pressure difference between drying material and drying air, the drying rate in the constant rate period can be increased.

For the falling rate period, the transport properties of material become important when the effects of external factors start declining. In this step, the temperature of material starts increasing and suitable drying can be finished by appropriately controlling the humidity and temperature of the air. Therefore, in falling rate period, it is difficult to obtain an expression of drying rate for predicting the drying time. A number of mechanisms are given to explain the movement of moisture in the drying material such as liquid diffusion or vapour due to concentration gradients, liquid movement due to capillary forces are given but no existing

theory can properly explain the drying process. (**Ekechukwu and Norton, 1999, Ahmad et al, 2015**)

The constant drying period for most of the organic materials like vegetables, fruits and timbres is small and particularly falling rate period. The falling rate period in fruits and vegetables are depends on the rate at which the moisture is removed and migration of moisture is particularly by diffusion. The diffusion of moisture content is comparatively slow due to affected cells and jammed interstices in high moisture content materials (**Garg and Prakash, 2002**). In most of fruits and vegetables, there is starch and sugar in the liquid phase which also migrates to surface. This increases the viscosity and hence reduces the surface vapour pressure moisture evaporation. Drying of agricultural products is done either in thin layer drying or deep layer drying.

Thin layer drying is done for the most of fruits and vegetables in which the product is spread in thin layers with whole surface exposed to air moving through the product. Here the Newton's law of cooling is applicable in the falling rate regime (**Garg and Prakash, 2002**). The rate of moisture loss of a food product surrounded by medium at constant temperature is directly proportional to the difference between the food product moisture and its equilibrium moisture content

$$\frac{dm}{dt} = k (m - m_{\text{equ}}) \quad 5$$

Solving this equation we get

$$t = \frac{1}{K} \ln \left(\frac{m_{(t)} - m_{\text{equ}}}{m_{(0)} - m_{\text{equ}}} \right) \quad 6$$

The value of equilibrium moisture content is very small as compared to initial moisture content and therefore it is neglected. Then the moisture content at any time 't' is given by

$$t = \frac{1}{K} \ln \left(\frac{m_{(t)}}{m_{(0)}} \right) \quad 7$$

$$\text{But, } \left(\frac{m_{(t)}}{m_{(0)}} \right) = \text{MR} \quad 8$$

$$t = \frac{1}{K} \ln(\text{MR}) \quad 9$$

From equation 9, we can obtain the time required for drying of the material

Where K is drying constant (1/sec)

m_{equ} = Equilibrium moisture content

m_0 = initial moisture content

m_t = moisture content at any time

Conclusion

Drying characteristics inform us that dehydration of vegetables are also depends on nature of drying material, surface tension and viscosity of liquid in the drying vegetables. The classification distinctly indicates that, the designs of solar dryer can be grouped systematically according to their modes of operation, heating sources and operating temperature. The Newton's law of cooling is applicable in falling rate period.

References

- 1) Leon, M.A., Kumar, S., Bhattacharya, S. C. (2002), Renewable sustainable energy review, A comprehensive procedure for performance evaluation of solar food dryers, 6(4), pp. 367-393
- 2) Tripathy, P.P. and Kumar, S. (2009), International journal of green energy, Influence of sample geometry and rehydration temperature on quality attributes of potato dried under open sun and mixed mode solar drying, 6(2) pp. 143-156
- 3) Zaman, M.A. and Bala, B.K. (1989), Solar energy, Thin layer solar drying of rough rice, 42(2) pp. 167-171
- 4) S.R. Navale, V.M. Harpale and K.C. Mohite*, "Comparative study of open sun and cabinet solar drying for fenugreek leaves", International journal of renewable energy technology research 4(2), 2015.
- 5) Sharma, V.K, A. Colangelo and G. Spagna (1995), Renewable energy, "Experimental investigation of different solar dryers suitable for fruit and vegetable drying", vol. 6(4) pp.413-424
- 6) Garg, H.P. (2002), Solar energy, 1st Reprint, Tata McGraw hill publications, New Delhi. Pp.191-200.
- 7) Ekechukwu L. And Norton S.D (1999), Nigerian journal of solar energy, Development and use of solar drying technologies, 89, pp. 133-164.
- 8) Ahmad, F., Sopian, K., Bakhtyar, B., Mohamed Gabbasa, Mohd Yusof Othman and Ruslan, M.H. (2015), Renewable and sustainable energy, Review of solar drying systems with air based solar collectors in Malaysia, 51, 1191-1200

Paper-30

DIELECTRIC PROPERTIES OF ALLYL AMINE AND 2- BUTOXYETHANOL USING MICROWAVE FREQUENCY 9.85 GHz AT ROOM TEMPERATURE

Sangita S. Meshram 1, U. B. Tumberphale 2, P. G. Gawali 3

1. Department of Physics, B. N. Bandodkar Science College, Thane, Maharashtra. India
2. Department of Physics, N.E.S. Science College, Nanded-, Maharashtra. India
3. Head of Department of Physics, B.S. College, Basmath, Dist. Hingoli, Maharashtra. India.

ABSTRACT:

The study of liquid mixtures is gaining popularity due to the production of hydrogen bonding in the system as a result of solute-solvent interaction. (G. Nath, S. Sahu, and R. Paikaray 2009) [1] The existence of hydrogen bonds alters the dielectric characteristics of liquid mixtures significantly. (R. J. Sengwa, V. Khatri, S. Sankhla 2009) [2] Surber's technique is used to determine the dielectric constant (ϵ') of Allyl amine (AA)+2- Butoxyethanol (2-BE) for various mole fractions of Allyl amine (AA) at a single microwave frequency of 9.85 GHz using an X-band microwave bench at 303 K. AA+2-BE viscosity and refractive index are also measured. The dielectric parameters that were derived, dielectric loss (ϵ''), molar polarisation (P_{12}) and the tangent of loss ($\tan \delta$) These evaluated dielectric properties. explain the formation of system's complexes.

In a binary combination of Allyl amine (AA)+ Butoxyethanol (2-BE), the dielectric constant (ϵ'), dielectric loss (ϵ''), and loss tangent ($\tan \delta$) all vary non-linearly, whereas molar polarisation (P_{12}), activation energy (E_a), viscosity (η), and density (ρ) all drop exponentially with increasing mole fraction (2-BE). Data offer information on the interaction of solutes and solvents with wobbling nature. The types and intensities of intermolecular interactions in the binary mixtures of the solvent systems analysed were evaluated using excess data from binary mixture densities obtained at 303 K encompassing the whole spectrum of solvent compositions.

Keywords: Allyl amine, 2- Butoxyethanol (2-BE), dielectric constant, dielectric loss, molar polarization, activation energy, Molecular interaction.

INTRODUCTION

The study of dielectric properties of binary liquid mixtures has gained popularity in recent years, as the heating characteristics of a given substance via microwave radiation are influenced by its dielectric properties. Microwave heating has been extensively acknowledged by scientists for facilitating organic chemical reactions. Knowledge of the properties of binary liquid mixtures is essential in chemical industry designs including chemical separations heat transfer (Rathnam, Mohite, and Kumar, 2010; Rana, 2010), and other processes.[3] [4]

Dielectric properties are created when a binary mixture is formed. Excess parameters stray from linearity and dielectric parameters do not vary linearly. The, dielectric properties of binary liquid

mixtures are useful in understanding the nature of bonding between the liquids. It is critical to investigate the dielectric behaviour of the AA and 2-EE binary systems at 30°C and 9.85 GHz.

In many biological systems observes, the neutral (NH₂) or charged (-NH₃⁺) group, which is the basic building block of amines. The presence of an NH₂ group in an amine is important for intermolecular hydrogen bonding (Deshmukh, Ingole and Shinde, 2019) [5]. Alcohols and amines are known for their self-association through intermolecular hydrogen bonding.

Allylamine is a colourless liquid that is made up of an organic component and a main aliphatic amine group. Allylamine is a monoalkylamine, also known as 3-aminopropylene or prop-2-en-1-amine. It's an antifungal drug that's used to create antibiotics, diuretics, and sedatives (Pawar, Swami and Patil, 2014) [6]. V. P. Pawar uses Time Domain Reflectometry to study the dielectric relaxation of allylamine-1,2,6-hexanetriol.

Ethylene glycol monobutyl ether (2-butoxyethanol)2-butoxyethanol is a main alcohol made comprised of ethanol with a butoxy group replacing one of the methyl hydrogens. It's a colourless, high-boiling liquid (171°C) that's used as a solvent for paints and inks, as well as in some drycleaning solutions. 2-Butoxyethanol is used in many industries. It is used as a solvent and is found in paint strippers, thinners, and household cleaners. It performs the function of a protic solvent. It's a glycol ether and a primary alcohol. We explore their binary combinations and examined for intermolecular interactions among mixture molecules.

MATERIALS AND METHODS:

Materials: A.R. grade 2-butoxyethanol (EE) and allyl amine (AA) were obtained from EMerck Pvt. Ltd., Mumbai, and Spectrochem Ltd., Mumbai, respectively. To maintain good thermal equilibrium, the two polar liquids were mixed according to their molar proportions and held for six hours in well-sealed bottles.

Measurements: At room temperature (303 ±0.01) K, the densities of pure solvents and binary mixtures were determined using a 10 mL capacity single stem capillary pycnometer. At atmospheric pressure and room temperature, the pycnometer was calibrated with doubly distilled water. The density readings were estimated to be ±1 × 10⁻⁵ gcm⁻³ accurate. The viscosities of the binary mixture were determined using Oswald's viscometer and a Digital stopwatch model W3 (Vitronics, Pune) of least count 0.1 Sec. Abbe's Refractometer, model No. AR-204, was used to determine the refractive indices of sodium D lines with accuracy up to the five places of decimal. Surber's technique (Jogdand, 2019) [7] of measuring reflection coefficient from the air dielectric boundary of the liquid was used to test the dielectric constant (ε') and dielectric loss (ε'') using an X-Band Microwave Bench with a Klystron power supply model no-MITKP503. For various mole fractions of AA, all measurements were carried out at 30°C.

The values of ε' and ε'' have been used to evaluate the loss tangent (tan δ), molar polarization (P₁₂) activation energy (E_a) and density, viscosity, square of the refractive index are reported in table 1.

Table-1.

Mole fraction of AA X_A	ρ Density gm/cm^3	η Viscosity cp	ϵ'	ϵ''	$\tan\delta$	P12	E_a	n^2D Sq. Refractive
0	0.9056	3.0099	4.3894	0.8607	0.1961	69.2261	3.8169	2.026381
0.2007	0.889	3.1510	4.2323	0.7999	0.8190	61.7924	3.8445	2.032136
0.3694	0.872	2.5651	4.4325	0.8505	0.1919	58.5101	3.7206	2.020691
0.5133	0.855	2.0582	4.6131	0.8943	0.1939	55.4805	3.5880	2.023535
0.6374	0.838	1.5682	5.4716	1.0658	0.1948	56.5922	3.4243	2.020776
0.7455	0.821	1.1726	5.0663	0.9948	0.1964	50.9125	3.2492	2.035016
0.8406	0.804	0.9253	5.6098	0.9872	0.1760	50.3512	3.1070	2.029257
0.9248	0.787	0.7623	5.3502	0.9971	0.1864	56.6932	2.9899	2.032136
1	0.7699	0.4115	6.1500	0.9777	0.1590	46.8571	2.6186	2.017877

Excess permittivity (ϵ'), excess dielectric loss ($\Delta\epsilon''$), excess molar polarization (ΔP_{12}), excess activation energy (ΔE_a) and excess viscosity ($\Delta\eta$) are reported in table 2.

Table-2.

Mole Fraction of AA	$\Delta\epsilon'$	$\Delta\epsilon''$	$\Delta\tan\delta$	ΔP_{12}	ΔE_a	$\Delta\eta$
0	0	0	0	0	0	0
0.2007	-0.6847	-0.2979	-0.0344	-5.1994	0.2681	0.662599
0.3694	-0.7639	-0.3065	-0.0310	-5.3625	0.3464	0.515049
0.5133	-0.8216	-0.1557	0.0056	-3.3029	0.3862	0.382059
0.6374	-0.5739	-0.1654	-0.0078	-1.4289	0.3712	0.214520
0.7455	-0.3476	-0.0861	-0.0018	-0.2866	0.3256	0.099807
0.8406	-0.6265	-0.1875	-0.0092	-1.7711	0.2970	0.099615
0.9248	-0.5063	-0.0532	0.0105	-1.4382	0.2812	0.155400
1	0	0	0	0	0	0

Results and Discussion:

The density of binary mixtures drops as a result of hydrogen bonding with AA and 2-BE molecules, meaning that the binary solution's molar volume decreases. Figure (1) depicts the density measurement curve. As the mole fraction of AA in a binary liquid mixture grows, the density of the binary liquid mixture drops at 30 °C. Similar density patterns were discovered by Chandra Mohan Saxena et al, P. Jeevanandham et al, and Seyed Hesammirfakhar et al [8-10].

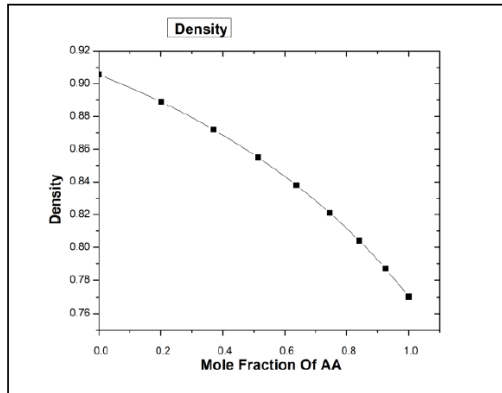


Fig. No. (1): Plot of Density with Mole Fraction of AA.

The viscosity (η) of the amine and 2-BE mixture reduces as a result of ion interaction in the mixture. According to Huyskens et al [11], the growth of dissociated ions produces an increase in viscosity in the acid amine and 2-ME combination.

Plotting the dielectric constant (ϵ') versus the mole fraction of AA [Fig. (2)] reveals two discrete zones in the range $0 < X_A < 0.7$ and $0.7 < X_A < 1$. In the $0 < X_A < 0.7$ (2-BE rich region) range, the values (ϵ') change nonlinearly with X , while in the $0.7 < X_A < 1$ (AA rich region) range, random nonlinear behaviour is observed. The nonlinear mixing range of $0 < X_A < 0.7$ indicates that the molecular structures of AA and 2-BE differ from those of pure liquid and fluctuating nonlinear region shows that the chemical structures have changed significantly.

The graph's minima is found at $X_A = 0.8$ mole fraction of Allyl amine, and the complex forms at this mole fraction of Allyl amine. According to B. S. Narwade et al and N. P. Pawar et al [12], complex formation is caused by a non-linear connection between the dielectric constant and the mole fraction of the mixture. Curve minima between two maxima in this study indicate the greatest change in slope at roughly $X_A=0.8$, which is where the complex formation occurs. This effect is caused by the presence of molecular association (homogeneous interaction) even at low concentrations of the solute and Solvent [13].

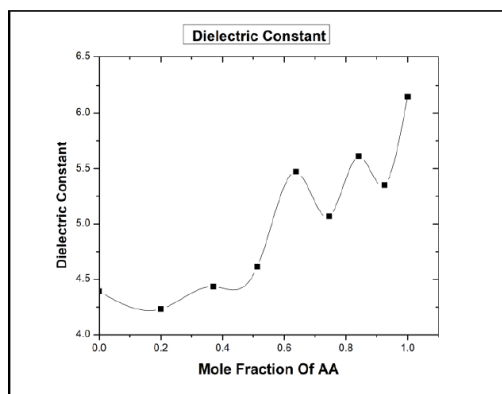


Fig. No. (2): Plot of Dielectric constant with Mole Fraction of AA.

The values of dielectric loss (ϵ'') are non-linear with increasing concentration of AA in this case of the AA+2-BE combination, with maximum absorption recorded at a different concentration of AA at $X_A=0.8406$. U. Tumberphale et al. [14] found the same pattern for dielectric loss. In figure (3), the Loss tangent ($\tan \delta$) varies with the molar concentration (X) of AA in the mixture. The graph shows that the minima occur at $X_A=0.8406$, which signifies the occurrence of a complex with a microwave energy absorption smaller than pure 2-BE but greater than pure AA. Microwave energy absorption increases with increasing mole fraction of AA after $X_A=0.2007$, with the maximum microwave energy absorption. Microwave energy absorption decreases, increases, and decreases as the mole fraction of AA increases. The formation of complexes due to H-bond interaction causes the curve to wobble.

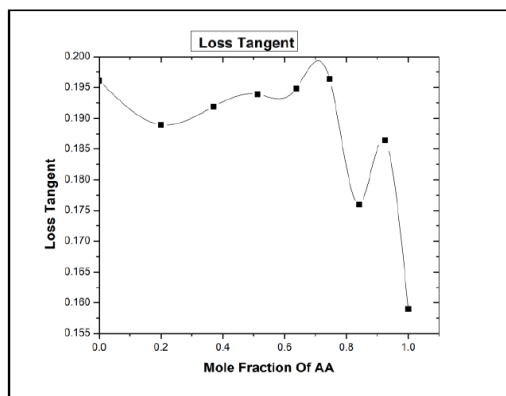


Fig. No. (3): Plot of Loss Tangent with Mole Fraction of AA

The occurrence of complex formation at $X_A=0.8406$ supports our earlier conclusion and the decrease in the effect of hydrogen bonding in the binary mixture (Kalmase G. M et al 2004) [15]. An increase in the binary system's molecular polarizability indicates the presence of a hydrogen connection between the two separate systems (Vishwama T et al 2016)[16].

E_a is the energy required to produce a hole electron volt, which serves as the "activation energy" for individual molecules to pass from one equilibrium site to the next. The activation energy vs the mole fraction of AA in the device is shown in Figure (4). We discovered that the activation energy reduces as the molar concentration of AA in the binary mixture increases. [17] (Kh. Abdul Maleque 2013) yields the same graph nature. At $X_A=0.8406$ the slope deviation reaches its maximum.

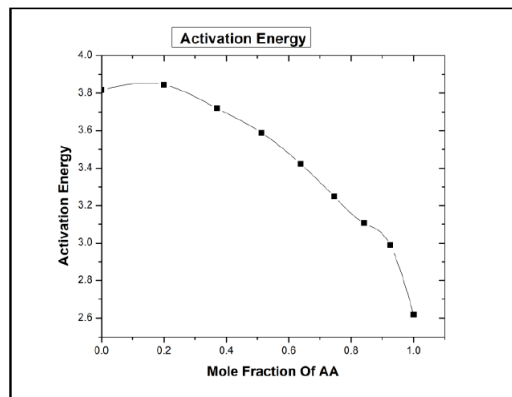


Fig. No. (4): Activation Energy with Mole Fraction of AA.

Excess Parameters:

Excess permittivity ($\Delta\epsilon$) has been connected to polarisation and loss in molecular movements governed by complicated intermolecular forces (Subramanian V et al 1993) [18].

The frequency of intermolecular interactions between dissimilar molecules (heterogeneous interaction) and the intermolecular contact between solute and solvent molecules in a mixture can be calculated using the excess permittivity ($\Delta\epsilon$). Multimers can arise when the total number of effective dipoles in the two liquid mixtures is lowered. The ($\Delta\epsilon$) values of the AA+2-BE mixtures are negative over the entire concentration range due to dipolar interaction between the components in the mixture or dipolar self-association of the more polar component (Sengwa R.J., Sankhla Sonu 2007) [19]. As seen in figure (5), the values reached a minimum at a particular mole fraction of the AA. This illustrates the hetero connection between the $-OH$ groups of the 2-BE and the $-NH_2$ groups of the AA. Negative values indicate that when the overall number of dipoles in the mixture declines, closed multimers develop with the dipoles oriented anti-parallel (Aswathaman H et al 2018) [20]. This negative number indicates that due to hydrogen bonding, the molecules in the mixture form multimers, lowering the effective dipole moment value. At $X_A = 0.7$ mole fraction of AA, the excess dielectric constant is at its highest.

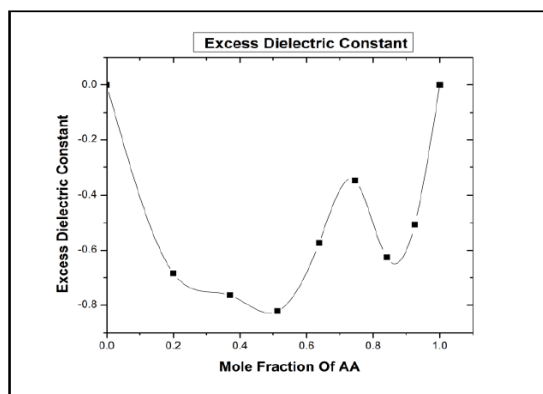


Fig. No. (5): Plot of Excess Dielectric Constant with Mole Fraction of AA.

Excess dielectric loss ($\Delta\epsilon''$)

When the concentration of AA in the combination is increased, the system shifts from minima to maxima and back to minima negatively [Fig. (6)], which could be due to parallel alignment being the main factor in the 2-BE and AA mixture.

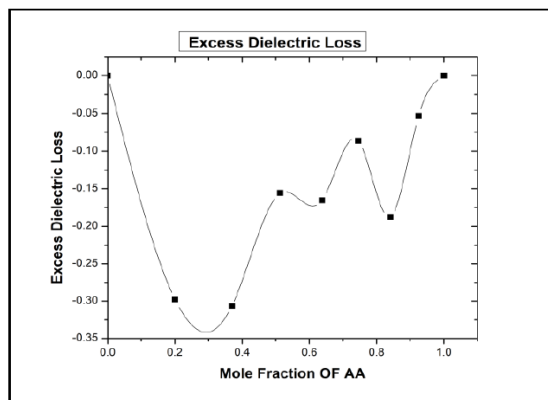


Fig. No. (6): Plot of Excess Dielectric Loss with Mole Fraction of AA

Excess molar polarization (P_{12})

In this analysis, the value of excess molar polarisation is negative in the region indicated in Figure (7). Negative variance is indicated by dipole association, dipole mediated dipole contact, or a decrease in hydrogen bonding with dilution. S. Tripathy et al. [21] discovered the similar effect in dimethylaniline and p-Xylene. The Excess molar polarisation (P_{12}) vs Mole fraction of AA curve has a negative trend, comparable to that of methyl methacrylate MMA and 1-Heptanol (1-HtOH) (Sastry N.V et al) [22].

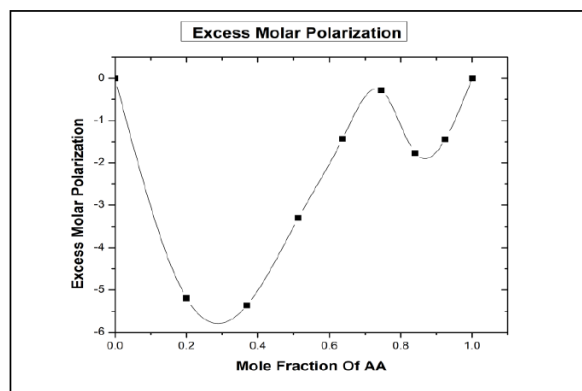


Fig. No. (7): Plot of Excess Molar Polarization with Mole Fraction of AA

Excess activation energy (ΔE_a):

The excess activation energy (E_a) of the binary mixes studied was all positive over the whole range of solvent compositions at 303 K. A positive excess activation energy value indicates significant

intersections between the AA and 2-BE molecules. The overall variance of extra activation energy points to an increase in the internal energy of the viscous flow.

Excess viscosity ($\Delta\eta$):

Positive values of excess viscosity due to strong specific contacts produce complex development in systems of various molecular sizes when dispersion forces are dominating, while negative values of excess viscosity cause complex formation. In our situation, the excess viscosity is positive, as illustrated in Figure (8). for the complete composition spectrum of the binary mixture under inquiry According to Ford and Moor, positive values of cause complex development due to strong specific interaction. The largest excess viscosity is found at $X_A = 0.8406$ minima between two maxima, indicating a significant interaction between the system's dissimilar molecules. Over the whole mole fraction range, the systems show positive departures of excess viscosities by G. Moumouzas from ideal. The molecular size of the binary mixture increases as $X_A = 0.8406$ is reached. At 298.15K, Hulya YILMAZ discovered a similar tendency in the water-methanol, ethanol, and n-propanol systems [23].

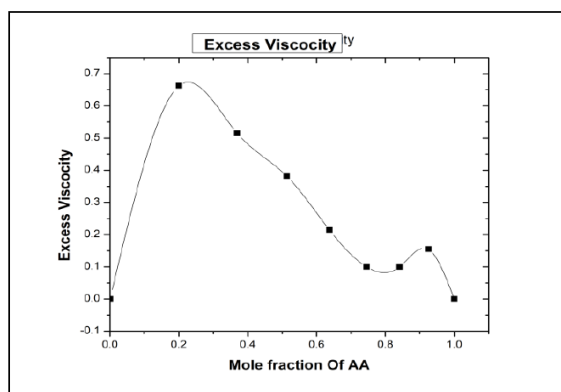


Fig. No. (8): Plot of Excess Viscosity with Mole Fraction of AA.

Conclusions:

The dielectric parameters dielectric constant (ϵ'), dielectric loss (ϵ''), Loss tangent ($\tan\delta$), molar polarization (P12), activation energy (Ea) and excess dielectric parameters Excess permittivity ($\Delta\epsilon'$), Excess dielectric loss ($\Delta\epsilon''$), Excess molar polarization (P12) and Excess activation energy are computed for the binary mixtures of the systems Allyl amine with 2-Butoxyethanol for various mole fractions at 303 K temperature. The formation of hydrogen bonding between the mixture system is identified by studying the variations in the parameters determined. The complex formation is favored by linkage between $N^{-\delta}$ of amine with $H^{+\delta}$ of alcohol through hydrogen bonding. The study of dielectric properties of the binary mixture reveals the existence of the solute-solute type of molecular associations.

References:

- [1] G. Nath, S. Sahu, and R. Paikaray, "Study of acoustic parameters of binary mixtures of a non-polar liquid with polar liquid at different frequencies," *Indian Journal of Physics*, vol. 83, no. 4, pp. 429-436, 2009.
- [2] R. J. Sengwa, V. Khatri, S. Sankhla, "Static dielectric constants and Krikwood correlation factor of the binary mixtures of N-methylformamide with formamide, N,N-dimethylformamide and N,N-dimethylacetamide," *Journal of Solution Chemistry*, vol. 38, no. 6, pp. 763-769, 2009.
- [3] Rathnam, M.; Mohite, S, and Kumar, M. (2010). Density, Excess Volume, and Viscosity of Vinyl Acetate or Benzyl Acetate with (o-, m-, p-) Xylenes and Ethylbenzene at T=(303.15 and 313.15) K. *Journal of Solution Chemistry*, 39:1735-1748.
- [4] Rana, V.; Chaube, H, and Gadani, D. (2011). Dielectric permittivity, density, viscosity and refractive index of binary mixtures of anisole with methanol and 1-propanol at different temperatures. *Journal of Molecular Liquids*, 164(3): 191-196.
- [5] Deshmukh, A.; Ingole, S, and Shinde, R. (2019). Dielectric relaxation properties of aqueous dimethylamine, trimethylamine and ethylamine using time domain reflectometry technique. *Indian Journal of Pure & Applied Physics*, 57: 406-410.
- [6] Pawar, V.; Swami, M, and Patil, A. (2014). Dielectric Relaxation Study of 1,2,6-hexanetriol+Allylamine Mixture Using Pico-second Time Domain Reflectometry Technique. *International Journal of ChemTech Research CODEN (USA): IJCRGG* , 6(3): 1817-1820.
- [7] Jogdand A. (2019). Dielectric behavior of acetonitrile + n-Butyl alcohol binary mixtures at microwave frequency. *IOSR Journal of Applied Physics (IOSR-JAP)*, 11(2): 40-49.
- [8] Saxena Chandramohan, Saxena Archana, Srivastava Ashok Kumar and Shukla Noveen Kumar, *American chemical science journal* 3 (4), 468-478(2013).
- [9] Jeevanandham P., Kumar S., Periyasamy P., *Journal of Molecular Liquids*, 188, 203-209(2013).
- [10] Hesammirfakhar Seyed, Rezaei Davood - Teimourbagloo, *Journal of science and Today's world*, 2(4),344-357(2013).
- [11] Huyskens P., Fellx N., Janssens N., Broeck F. V. and Kapuku F., *J. Phys. Chem.* 84,1387(1980).
- [12] Pawar N. P., Tumberphale U. B., Kawle R. S., Kalamse V. G. and Chavan A. G., *Bionanofrontier*, 8(3), (2015).
- [13] Gilani A. Ghanadzadeh, Ghanadzadeh H., Bahrpaima Kh., Ranjkesh A. *J. Chem. Thermodynamics* 42, 967-972(2010).
- [14] Tumberphale U., Kawle R., Karhale G., Pawar N., and Kalamse G, *International journal of physics and mathematical sciences*, 2(4), 1-4(2012).
- [15] Kalmase G. M., Nimkar M. J., *Asian journal of chemistry*, 14(3-4),1487-93(2004).
- [16] Vishwama T, Parvateesam K, Shaik Babu, Sastry S Sreehari & Murthy V R K, *Indian Journal of Pure & Applied Physics*, 54, 597-611(2016).

- [17] Kh. Abdul Maleque Hindawi publishing corporation ISRN Thermodynamics Volume 1-9(2013).
- [18] Subramanian V., Bellubbi V. S., Shobhanadri J. Pramana journal of physics, 41(01,09-20(1993).
- [19] Sengwa R.J., Sankhla Sonu, Journal of Non-Crystalline Solids, 353, 4570–4574(2007).
- [20] Aswathaman H., Parthipan G., Thenappan T., Shoba A. & Shreedevi S. International Journal of Advanced Trends in Engineering and Technology (IJATET), 3(1), 126(2018).
- [21] TRIPATHY S. and SWAIN B. B. Chem. Papers 45 (3) 321- 329(1991).
- [22] Sastry N.V., Patel S.R. and George J. and Prasad D.H.L. Indian journal of Chemistry, 39(A), 1270-1279(2000).
- [23] H`ulya YILMAZ, Turk J Phys 26, 243 - 246(2002).